SAPIENZA
UNIVERSITÀ DI ROMA

Radiation Pressure and Nonlinear Wave-Body Interaction in Acoustics

DIMA - Dipartimento di Ingegneria Meccanica e Aerospaziale

Dottorato di Ricerca in Meccanica Teorica e Applicata – XXXVII Ciclo

Candidate

Tiziano Tini
ID number 305192

Thesis Advisor

Prof. Antonio Carcaterra

Co-Advisor

Prof. Sergey Sorokin

December 2024

Thesis defended on 23 January 2025
in front of a Board of Examiners composed by:

Prof. Roberto Brighenti - Università di Firenze
Prof. Marco Lauricella - IAC, Consiglio Nazionale delle Ricerche, Roma
Prof. Erika Ottaviano - Università degli studi di Cassino e del Lazio meridionale

---

Radiation Pressure and Nonlinear Wave-Body Interaction in Acoustics
Ph.D. thesis. Sapienza – University of Rome

This thesis has been typeset by LaTeX and the Sapthesis class.

Author's email: tiziano.tini@uniroma1.it

Dedicata
alla mia famiglia, ai miei nonni e a Francesca
il mio bene più prezioso.

Acknowledgments

Innanzitutto, vorrei ringraziare i miei genitori, senza i quali tutto questo percorso non avrebbe avuto né un inizio, con la Laurea Triennale, né una fine, culminata con il Dottorato. Mi avete sempre appoggiato in ogni mia scelta, più di quanto abbia fatto io verso me stesso, e non vi siete mai tirati indietro di fronte alle mille difficoltà della vita per permettermi di conseguire questo obiettivo. Non era scontato, e questo vale più di ogni altro sostegno al mondo. Siete i migliori.
Ringrazio i miei nonni, delle vere rocce al mio fianco, che mi hanno fatto capire che lo studio, alla fine, paga sempre. Non tanto da un punto di vista materiale, ma d'animo. Infatti, ogni volta che guardavo i vostri occhi, vedevo la soddisfazione di avere un nipote arrivato fino alla fine di un lunghissimo percorso di studi, che quasi sembrava non finire mai. Invece, eccoci qua: io ho concluso questo percorso e voi siete ancora al mio fianco. Non potevo chiedere di meglio.
Ringrazio mio fratello Leonardo, che mi ha sostenuto in ogni momento difficile e che, per buona parte del tempo, ha condiviso anche le mie preoccupazioni emotive. Mentre mi disperavo nel tentativo di conseguire risultati utili ai fini della ricerca, mi sei sempre stato accanto con il tuo aplomb inglese, che ammiro e che ho tentato, invano, di fare mio per concludere al meglio questo percorso. Ti invidio.
Ringrazio il Prof. Antonio Carcaterra, colui che ha reso operativamente possibile questo percorso e che ha alimentato in me la passione per la ricerca e per l'ingegneria sin da quando ci siamo incontrati per la prima volta a Marina Velka, in spiaggia. Grazie per questa bellissima opportunità nell'affascinante mondo della ricerca.
Ringrazio tutti i miei parenti, zii, cugini e amici, che mi hanno seguito durante questi tre anni, dando ognuno il proprio prezioso contributo.
Un ringraziamento particolare e doveroso lo rivolgo a Gianni e Roberta, che mi hanno supportato come un secondo figlio.
Last but not least, ringrazio Francesca. Sono stati tosti, questi tre anni, e lo sappiamo entrambi, così come sappiamo che, senza di te, non ce l'avrei mai fatta a concludere questo viaggio. Guardando indietro, è stato un percorso che ci ha messo a dura prova (Danimarca docet), ma, sapendo di averti sempre al mio fianco, ho potuto contare su quella spinta decisiva che mi ha portato fino al massimo traguardo possibile. Alla fine, ne è valsa la pena e ora raccogliamo insieme i frutti di questa avventura, guardando al futuro insieme. Sei, e sarai, il mio faro nella notte.

Abstract

The aim of the research is to investigate the effect of the radiation pressure phenomenon on light-weight bodies and controlling their movement in space. The application of this novel technology could support several interesting applications, including contact-less actuators, contact less manipulators, powering micro-vehicles that lack their own on-board motors, and acoustic recharging power for batteries of wireless devices.

The actuation mechanism, specifically the non-linear acoustic field, is clarified and theoretically described. The conventional linear acoustic theory is insufficient in this context. In the linear regime, only small oscillations of the body under the influence of an impinging wave are expected, without any potential for producing long stroke motion. Non-linear effects are essential to generate a drift motion of the body, namely the net effect of radiation pressure. To this end, a very general and rigorous formulation of the acoustic problem based on Hamilton's principle has been developed. The resulting equations are highly non-linear, and numerical finite difference simulations of such an acoustic field interacting with a moving body present considerable challenges. The nature of radiation pressure has been examined to clarify its nature. The historical debate between tensorial and scalar form is analyzed in detail, providing an additional contribution in terms of clarity regarding the various hypotheses presented historically. This exploration emphasizes the distinctions and implications of each perspective, enhancing understanding of the foundational principles. The analysis aims to clarify misconceptions and consolidate knowledge surrounding these concepts, contributing to ongoing discussions in the field.

On the other hand, based on the mechanism of wave-body interaction supported by Hamilton's principle, the radiation force phenomenon is treated as an "actuator" that connects electronically controlled loudspeaker acoustic emissions with the net force acting on the body. In this context, the objective is to move a light-weight body along a specified trajectory in one-dimensional space by varying the pressure level emitted by a piston using non-linear control theory. Achieving real-time control necessitates establishing a relationship through a semi-analytical method capable of providing instantaneous values for the radiation pressure on the body. For this purpose, a perturbative approach was employed to find an approximate solution to the problem with second-order accuracy.

Initially, the case of a rigid body was analyzed; subsequently, a body represented by an impedance was studied in detail. Once the physical model was established, it became possible to implement a predictive control strategy that modifies amplitude and frequency parameters to consistently achieve optimal force required for guiding the object along a defined trajectory.

To compare the semi-analytical results with the exact expressions, a finite difference (FD) scheme was implemented using one of the most robust methods for compressible flows, the Rusanov method. This method proved to be decisive in conducting a validation and comparison campaign among the results obtained for different cases. This treatment is unique because, in

addition to deriving and formalizing a new method to find the expression of radiation pressure on a perfect reflective body, a numerical validation was first conducted, comparing results with formulas present in the literature (including models by Rayleigh, King, Westervelt, Beyer, and Hasegawa). Following this, an engineering application was developed based on these concepts, implementing a controller capable of moving a small object at will under the influence of the acoustic wave.

Contents

Chapter 1

Historical introduction to the pressure radiation concept

Three phenomena associated with the passage of a sound beam are radiation pressure, streaming and cavitation, and some remarks on the history of each are in order [1]. The subject of the proposed research points the investigation of the actuation of light bodies through radiation pressure. The objective is control the motion of a body in space by using acoustic waves, a more ambitious goal with respect to the existing acoustic levitation effects or acoustic tweezers. Use of this novel technology could support several interesting applications: contactless actuators, contactless manipulators, powering of micro-vehicles not equipped with their own on-board motors, acoustic power recharge for batteries of wireless devices. The present study analyze two different steps and related technologies.

On one hand, the actuation mechanism that allows a wave to exert a force on a body requires better theoretical description, as conventional acoustic linear theory is inadequate in this context. In the linear regime, one can only anticipate small oscillations of the body due to the influence of an impinging wave, which precludes the possibility of generating a relatively long stroke motion. To achieve a drift motion of the body, it is essential to utilize nonlinear effects, particularly radiation pressure. Despite the extensive investigation into the problem of wave radiation pressure, various theories exist, each based on different mathematical and physical assumptions to derive the pressure expression. Consequently, comparing these theories is challenging, especially when seeking a credible and robust model to underpin acoustic control. To address this issue, a comprehensive and rigorous formulation of the acoustic problem based on Hamilton's principle has been developed. The resulting equations are highly nonlinear, making numerical simulations using finite difference methods of such an acoustic field interacting with a moving body quite challenging.

On the other hand, based on the mechanism of wave-body interaction supported by the Hamilton's principle, the radiation force phenomenon as an "actuator" can be used. This mechanism permits to connect a loudspeaker acoustic emission, electronically controlled, with the body

force. In this context, the body is required to describe a given trajectory in space, driving the loudspeaker's frequency using optimal control theory.

1.1 Early Theoretical Foundations: Lord Rayleigh's Contributions

When one attempts to determine the time average of the pressure at a fixed point in a medium traversed by a sound wave, one finds that an asymmetry has been produced by the fact that the hypothetical particle of the medium is itself displaced from its rest position. For equal displacements from the rest position, the first order density changes are the same, but the second order changes differ. The following quotation from Poynting [2] gives an account of the situation:

> In sound waves there is at a reflecting surface a node-a point of no motion but of varying pressure. If the variations of pressure from the undisturbed value were exactly proportional to the displacements of a parallel layer near the surface, and if the displacements were exactly harmonic, then the average pressure would be equal to the normal undisturbed value. But consider a layer of air quite close to the surface. If it moves up a distance y towards the surface, the pressure is increased. If it moves an equal distance away from the surface, the pressure is decreased, but by a slightly smaller quantity. To illustrate this, take an extreme case and, for simplicity, suppose that Boyle's law holds. If the layer advances half-way towards the reflecting surface the pressure is doubled. If it moves an equal distance outwards from its original position the pressure falls, but only by one-third of its original value; and if we could suppose the layer to be moving harmonically, it is obvious that the mean of the increased and diminished pressures would be largely in excess of the normal value. Though we are not entitled to assume the existence of the harmonic vibrations when we take into account the second order of small quantities, yet this illustration gives the right idea. The excess of pressure in the compressed half is greater than its defect in the extension halt, and the net result is an average excess of pressure-a quantity itself of second order on the reflecting surface. This excess in the compression half of a wave train is connected with the extra speed which exists in that half, and makes the crests of intense sound waves gain on the troughs.

It is not surprising to learn that Lord Rayleigh made substantial contributions to the theory of radiation pressure, defining a particular form that bears his name. After him, Brillouin pointed out the tensor character of the pressure in the sound wave, and various aspects of the phenomenon have been studied in detail by Borgnis and Westervelt [3].

Lord Rayleigh's Studies

The concept of radiation pressure has a long history. Everything started when Lord Rayleigh was thrilled by the exciting results achieved in the late nineteenth century in the field of radiation pressure. From the outset, Lord Rayleigh was fascinated by the important consequences

of Boltzmann and Wien on the radiation pressure of the waves. As Maxwell's deduction of vibration phenomena that exert pressure on bodies proved to be correct, the same then was confirmed experimentally by Lebedew [4], of net pressure exerted by beams of light on bodies. For this reason, he questioned, in a well-known publication dating back to 1902 [5], the possibility that other types of wave phenomena, such as acoustic waves, could also exert pressure on the surfaces they hit.

In this foundational paper, Lord Rayleigh examines the pressure exerted by sound waves on surfaces from the example of a pendulum with a spring-suspended mass capable of moving along the vertical line. From this he derived the analogy for pressure waves in the case of air contained within a vibrating cylinder using Boyle's law as the state law.

Rayleigh first solved the problem of a vibrating pendulum, the length of which is constrained by a ring that can move only vertically (figure 1.1).

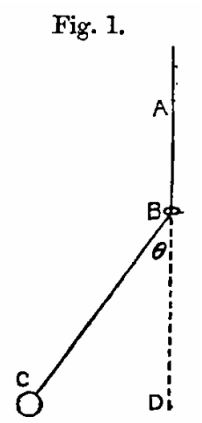

Figure 1.1. Rayleigh Pendulum

The work explores how sound waves, as mechanical vibrations, impart momentum to objects, resulting in a steady force known as radiation pressure. Rayleigh provides a quantitative analysis of this phenomenon, establishing the relationship between the properties of sound waves and the resultant pressure on different surfaces. This paper lays the groundwork for the theoretical understanding of acoustic radiation pressure and influences subsequent research in acoustics.

This paper is considered one of the most important concerning the acoustic radiation pressure because:

- It was the first quantitative analysis of acoustic radiation pressure;
- It explores of the relationship between sound wave properties (intensity and frequency) and pressure;
- It defined the fundamental principles governing acoustic radiation pressure;
- It states the basis for subsequent theoretical and experimental research in acoustics.

Following three years of research and inspired by the previous paper by Prof. Poynting, Rayleigh presented a first discussion on the sound radiation pressure [6] where he considered for the first time the question of the moment associated with the propagation of progressive waves. From there he wrote a more complete and general result, as he stated himself, considering a pipe containing a gas whose pressure P is a density function of the type $P{=}f(\rho)$. This effectively guaranteed a much higher generality of the physical model than the case of gas obedient to Boyle's law alone.
From this initial hypothesis and from Bernoulli's theorem for non-stationary flows, Rayleigh defined and found the sound radiation pressure as the increase of the mean pressure within the tube, compared to the pressure P_0, defined by the formula:

$$P_{Ray} = \frac{\gamma + 1}{2} \langle \mathcal{E} \rangle \tag{1.1}$$

Where $\mathcal{E}$ is the energy density of the sound beam in the cylinder, γ is the ratio between the specific calories c_v and c_p and p_r is the increase in the average pressure within the tube with reference pressure P_0. Note that these studies were performed using the linear equation of acoustic waves within a L-long closed tube as a solution, which is:

$$\varphi(x,t) = \cos\left(\frac{k\pi x}{L}\right) \cdot \cos\left(\frac{k\pi c_0 t}{L}\right) \tag{1.2}$$

Equation 1.1 can be defined as the first ever analytical formula for radiation pressure in acoustics.

1.2 Mid-20th Century Advancements: Langevin, King, Brillouin and Westervelt

Langevin's Studies in an open vessel

The formulation developed by Langevin is proposed, which is commonly contrasted in the literature with Rayleigh's theory. Although Langevin derived one of the two formulations generally accepted and recognized by the scientific literature, he reported his theory on radiation pressure exclusively on the boards of the Collège de France in Paris. It is thanks to the work of one of his students, Pierre Biquard, that his contribution on the subject reached us, through the pages of the Revue d'Acoustique (1932) [7].
Like Rayleigh, Langevin coined his own definition of sound radiation pressure. He first considered a totally different case study, in fact he was interested in the propagation of perfectly collimated acoustic beams in a duct no longer closed and limited, but open.
The fluid in the duct, under these conditions, is free to expand or compress freely to ensure the continuity of the average pressure over the entire acoustic beam domain.

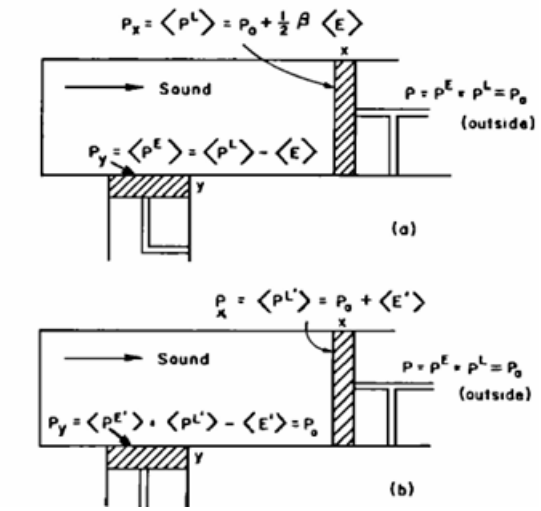

Figure 1.2. Rayleigh vs Langevin Pressure

When a sound wave encounters an obstacle, Langevin's radiation pressure P_l is defined as the force per unit area exerted on the body due to the action of the sound beam. Conventionally, as illustrated in the figure 1.2, Langevin radiation pressure is measured by determining the reaction force F_c that must be applied externally (through mechanisms such as springs or electromagnetic fields) to maintain the obstacle in its equilibrium position. Langevin radiation pressure is distinct from Rayleigh's, and it has been explored in various contexts. The relationship between these two forms of radiation pressure has been a subject of investigation, particularly in understanding how they differ in their underlying assumptions and implications for acoustic systems. By analyzing the reaction force required to keep the obstacle stationary, one can derive meaningful insights into the dynamics of acoustic radiation pressure.
The preservation of the momentum of the material system contained in the hatched volume, associated with the continuity condition of the average pressure at the acoustic beam boundary, allows the following expression of the sound radiation pressure to be derived:

$$P_{Lang} = < \mathcal{E} > \tag{1.3}$$

Unlike Rayleigh, Langevin's formulation therefore led to the equality between the sound radiation pressure and the mean energy density associated with the wave.

King's studies on rigid spheres

King's seminal work on the radiation pressure on spheres provides a detailed mathematical framework for understanding how spherical objects interact with sound fields [8]. It includes comprehensive equations and models that describe the forces experienced by spheres in an acoustic environment, with practical implications for various scientific and engineering applications. King's motivation for this study stems from the need to understand how sound waves exert forces on objects, a phenomenon observed but not fully explained in prior research. The study

builds on the foundational principles laid by Lord Rayleigh and others, extending the analysis to spherical geometries, which are more complex than the simple planar surfaces initially considered.

King begins by establishing the theoretical framework necessary to analyze the radiation pressure on a rigid sphere. He first introduces the concept of radiation pressure as the net force exerted by a sound field on a spherical object and the primary focus was on deriving the equations that describe this force in terms of the sound wave's properties and the sphere's physical characteristics. One of the key contributions of the paper is the derivation of the radiation pressure formula for a sphere. King first derived the acoustic radiation pressure in terms of velocity potential by making the Lagrangian expression of the acoustic field appear in the treatment. The formula introduced was considered as one of the most credited formulas and it still used today in terms of expression of the acoustic pressure on a body immersed in an acoustic field.

$$< P_{King} > = < \rho_0 \varphi_t - \mathcal{L} > \tag{1.4}$$

Where the Acoustic Lagrangian denstiy is defined as:

$$\mathcal{L} = K - U$$

and:

$$K = \frac{\rho_0 |\nabla \varphi|^2}{2} = \frac{\rho_0 |v^2|}{2},\ U = \frac{\rho (\dot{\varphi_t})^2}{2c_0^2}$$

Where ρ_0 is the air density at equilibrium conditions, and φ_t is the time derivative of the acoustic potential. The paper meticulously details the steps involved in arriving at this formula, providing a clear mathematical derivation. The most striking approximation influencing King's work is the use of the linear acoustic field solution within 1.4 to evaluate the net radiation pressure. In fact, as will be discussed later in Chapter 6, the nonlinearities of the acoustic field, such as those associated with the air, will significantly impact the net pressure calculation. This study will be complemented by further investigations into acoustic radiation pressure on rigid spheres, considering both the viscous effects of the medium [9, 10] and scenarios involving inviscid flow [11–16], particularly in the case of bodies immersed in water [17]. Lord King's work has been so influential in this field that even after many decades, his studies remain a primary benchmark for researchers exploring this area of acoustics.

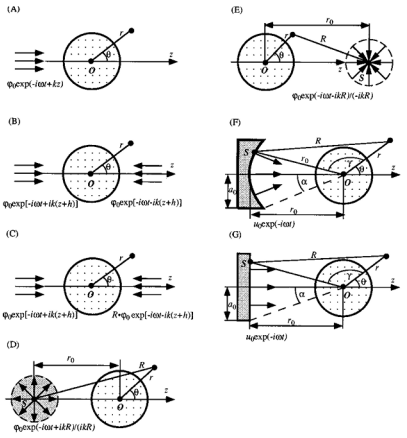

Figure 1.3. Example of Scattered and Incidient Acoustic Wave on a Sphere [13]

Brillouin's Tensor

Up to the first decades of the XX century, the acoustic radiation pressure was always considered as a scalar quantity. Later on, many authors started to write papers about the controversial nature of this ambiguous quantity. The first to introduce the concept of "Radiation Tensor" was Brillouin in his breakthrough paper [18] where he emphasized that radiation pressure could be derived more generally from the Boltzmann–Ehrenfest theory of adiabatic invariance.
Brillouin was sufficiently pleased with this consequence that he summed up his results in the form of a table of components of the mean stress tensor in the interior of a fluid traversed by a plane acoustic wave. One would write this today in the form

$$S_{ij} = -p\delta_{ij} + \rho b_i b_j$$

Where δ_{ij} is the Kronecker delta. Thus, for a sound wave traveling in the x direction, $v_2 = v_3 = 0$ and one obtains:

$$\begin{pmatrix} -(\langle p(x_1)\rangle - \langle \rho v_x^2\rangle) & 0 & 0 \\ 0 & -\langle p(x_1)\rangle & 0 \\ 0 & 0 & -\langle p(x_1)\rangle \end{pmatrix} \tag{1.5}$$

Where, of course, $\langle \rho v_x^2 \rangle$ is equal to the mean energy density of the sound wave $\langle E \rangle$ or double its kinetic energy density. The problem is then the evaluation of the mean pressure at a point x_1. This corresponds to the mean pressure in Eulerian coordinates. Brillouin proved that the quantity $p(x_1)$ can be identified with the term:

$$p(x_1) = \left\langle E\left(\frac{v}{c}\right)\right\rangle \left(\frac{dc}{dv}\right)$$

If the surface is perpendicular to the sound wave, one can easily recover the result of Langevin. Nevertheless, Brillouin was not concerned with the evaluation of the terms involving $\frac{dc}{dv}$ and he didn't observe that he had, in fact, made an error in calculating the terms of the tensor. The correct analysis was made by Fubini, who was a student of Brillouin's, but Brillouin did

not alter this in his book on tensors in 1938. The correct formulation of the principles initially proposed by Brillouin was publicized by Westervelt in 1950. This development is significant in the field of nonlinear acoustics, and the subsequent analysis will now be presented.

Another way in which the tensor nature of radiation pressure appears is proposed by Beissner [19]. In his work, the idea of radiation pressure as a tensor on a generic surface is emphasized and strengthened by drawing attention to the fact that tensor nature may arise in relation to the surface on which it is being integrated to calculate that magnitude. In fact, it can move around and complicate the calculation, requiring the use of a closed surface outside the physical surface. This condition, in the Eulerian coordinate system, introduces tangential components that would also be null in the case of inviscid flow or if it integrates directly onto the contact surface.

In the long run, Brillouin leaves to posterity a new concept of acoustic radiation pressure, giving it a tensor nature and no longer scalar (except for certain special cases). This will be a fundamental step in the history of this topic, as it will be a source of debate and controversy that has lasted for a long time.

Among all, the one of Beyer [7] points out that radiation pressure meant scalar magnitude was actually limited to a few real application cases. To consider radiation pressure as a scalar quantity, there is a need for special boundary conditions. Specifically there has to be the perfect perpendicularity between the acoustic beam and the invested body. When tangential components are born, such as inclined walls, it is assumed that scalar theory is no longer sufficient to describe this phenomenon, and therefore the need to describe it through a tensor arises.

Westervelt's Contribution

Eventually, Westervelt consolidated King and Brillouin's studies of radiation pressure on fluid-immersed bodies with viscosity. In fact, he questioned how viscosity and edge losses could change the value of this pressure, defining this effect as Stokes' forces. Among the most important contributions to radiation pressure, the publication of the correction of the results of Brillouin [20] and the first results obtained in [21] in which a coefficient of pressure loss due to the viscous effect has been introduced for small spheres.

In [20] he does an excellent job in demonstrating the equality of the Lagrangian and Eulerian formulation, going on to consider the solution of the fluid-dynamic field up to the second order. This last step was essential to obtain more accurate solutions than previous models, such as the King step where only linear wave solutions are considered. After that, he extended King's results for the spheres. In the second work, the focus was on the viscous contribution. In addition, he extended the study of this magnitude to different geometries, such as cylinders, also considering their movement under the effect of the acoustic beam.

1.3 Late-20th Century Achievement: Lee, Apfel and Hasegawa

After the first half of the XX century, many works contributed in part to make more complete the picture on the nature and value of radiation pressure on bodies immersed in an acoustic field. Among the most notable are Rooney and Nyborg [22], Chu and Apfel [23], Lee and Wang [24], and the more recent Hasegawa [25]. Each of them brought an element of novelty, but also of further doubts, in reference to how to derive the expression of pressure. Especially, the mere fact that one starts from certain assumptions, rather than others, has historically led to different results for problems of the same kind. This is a consequence of the small order of magnitude of the element sought which makes it very sensitive to the contour hypotheses on which it depends.

Among all the famous cases of different results for the same problem, the one described in the paper by Rooney and Nyborg [26] is worth to be mentioned. The authors commented on the constraining force exerted by an absorbent wall used in the paper of Chu and Apfel [23]. Notably, they suggest an infinite possibility of defining a constraining force for the absorbent wall depending on the physical conditions hypothesized within the system. On the contrary of the definition given by Chu and Apfel, where the fluid movement was considered equal to the case where the target is absent and the tube is infinite, Rooney and Nyborg suggest that one valid alternative to this may be to consider the mass density of the flow as unaltered by the acoustic beam. Their final comment was:

> There are experimental difficulties in satisfying any of the requirements described above. It is probably for this reason that there seem to have been no reported measurements of the radiation force on an absorber in a confined-beam (constant mass) situation in a liquid. Perhaps the lack of experimental ("operational") definitions for the radiation force helps to account for the disarray in the theoretical literature. Until laboratory procedures have been developed for meeting well specified conditions it will probably not be clear what is the best way to define the ("Rayleigh") radiation force on a perfect absorber in a confined beam.

Next, Chu and Apfel [27] responded shortly referring to their definition of perfect absorber claiming that analytical results will be always affected by boundary conditions, leading to this conclusion:

> ... the agreement or disagreement between theoretical and experimental results should be interpreted as how perfect or imperfect does your target approach a 'perfect' absorber.

This, like others, shows how the same problem can lead to profoundly different results due to a very slight difference in physical interpretations of what is happening. This in fact makes the subject worthy of the attention it deserves and highlights the need for a rigorous approach to the problem, as the one proposed in Chapter 4, that can solve most of the problem linked to these uncertainties.

Rooney and Nyborg

Rooney and Nyborg's contribution to the difference between Rayleigh and Langevin's pressure is again enhanced by placing more emphasis on analyzing the impact of conditions at the edge of the problem on the solution [22]. They analyze how the solution for absorbent walls is strongly dependent on considering the system closed or open, marking even more a conceptual difference between the two historically accepted definition of radiation pressure. The treatment is based on planar waves perpendicular to the surface of interest, for this reason considering the integral on that immobile surface, the radiation pressure is a scalar magnitude with modulus equal to that already found by Lord Rayleigh and Langevin in their previous papers.

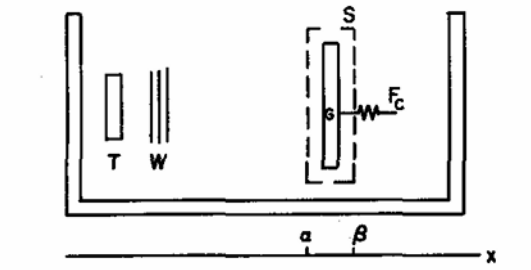

Figure 1.4. Typical Radiation Pressure arrangement by Rooney and Nyborg

Chu and Apfel

A few years later, Chu and Apfel wrote one of the most important papers on the outstanding topic [23], specifying how the controversy and uncertainties over the definition of radiation pressure were not yet concluded. Their research is of extremely importance, because they try to resolve the controversies of previous authors showing the critical points between the different theories and methods. They proposed new studies on different and historical applications, as the case of a tube of both infinite and finite length. At first, they analyzed the case of a progressive planar wave, then the case of acoustic field generated by a sinusoidal external source was considered, with either rigid, absorbent or partially absorbent wall at the end.

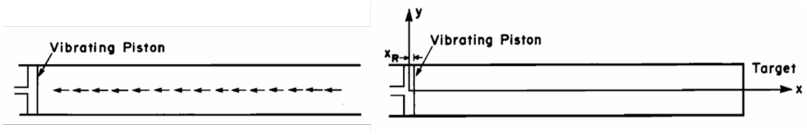

Figure 1.5. Progressive and Externally Induced Plane Wave

In their study, they give space to the search for radiation pressure using corrected acoustic field solutions up to the second order and considering the non-linearity of the medium. They also aim to define the differences between Rayleigh and Langevin pressure based on the geometric constraints of the system and rediscovered how the radiation pressure was related to the total

energy and boundary conditions. In particular, the relationship between absorbent and perfectly reflective walls showed a multiplication factor of 2 in favor of reflective walls and go to confirm Lord Rayleigh's results of nearly a century earlier in the case of reflective walls. In fact their results for pipes of semi-infinite length are:

$$p_{refl} = \frac{\gamma+1}{2}\langle\mathcal{E}\rangle\,, \quad p_{abs} = \frac{\gamma+1}{4}\langle\mathcal{E}\rangle = \frac{p_{refl}}{2} \tag{1.6}$$

Another more than significant result is the solution found in the case of a finished-walled and stressed tube with a sinusoidal oscillating piston. The acoustic field solution for particle displacement was found as:

$$\xi(x) = \epsilon\sin(\omega t)\frac{\sin(k(L-x))}{\sin(kL)} \tag{1.7}$$

Where $k = \frac{\omega}{c_0}$ is the wave number. From 1.7 one can clearly see that the solution is dependent on the geometric constraints of the system, i.e. the length of the tube, driven frequency and speed of sound. Specifically, a finite tube length implies the presence of system resonances that lead to ideally infinite pressure values in absence of any damping. After some mathematical manipulations, the final radiation pressure expression was given:

$$\langle P_{rad}\rangle = K\langle\mathcal{E}\rangle\left[1+\frac{\sin(2kL)}{2kL}\right] \tag{1.8}$$

Nonetheless, equation 1.8 has been arrived at considering the solution to the first order neglecting the second order contributions. They wrote:

> "However, such a procedure is rather tedious, because it is necessary to carry out the perturbation solution to the quadratic order. On the other hand, with a little manipulation of (84) this difficulty can be avoided and the radiation pressure on the target can be computed with the knowledge of the first-order perturbation solution only."

In addition to the purely sinusoidal case, they also found a very interesting expression in the case of generic periodic forces:

$$\langle P_{rad}\rangle = K\sum_{k=1}^{\infty}\langle\mathcal{E}_n\rangle\left[1+\frac{c_0T}{4\pi nL}\sin\left(\frac{(4\pi nL)}{c_0T}\right)\right]$$

Finally, they defined the difference between Rayleigh and Langevin's pressure case by introducing a constant that binds the two pressures. The latter is defined as the uniform hydro-static pressure introduced by the geometric confinement of the system. Specifically:

$$p_{Ray} = < p_{Lang} > +\rho_0 C \tag{1.9}$$

Where the constant C is found from Bernoulli's theorem:

$$C = \left\langle\int_{p_0}^{p_L}\frac{dp}{\rho} - \frac{v_L^2}{2}\right\rangle \tag{1.10}$$

From which you see how for infinite spaces, the value of $p_L \to p_0$ and $v_L \to 0$, for this $C = 0$.

While in confined spaces, variables can no longer be set equal to zero and hydrostatic pressure must be calculated once the type of confinement imposed on the system is known. Chu and Apfel made one of the first analytical approaches to unification between Rayleigh's and Langevin's theory, in fact until that time the considerations made about the difference between the two were never so detailed.

Lee and Wang

Lee and Wang, in their work [24], highlight that radiation pressure is a highly sensitive topic, often prone to confusion and errors. For this reason, they felt the need to piece together the understanding of this phenomenon from fundamental principles, employing a perturbative approach. Specifically, their study focuses on both the one-dimensional and three-dimensional cases, aiming to derive the expression for radiation pressure on perfectly reflecting and absorbing bodies subjected to a plane wave in a semi-infinite domain.
Among the most significant aspects of their work is the use of Bernoulli's theorem to derive the correct second-order equation, which, as noted in their study, leads to the same conclusions reached by Rayleigh and Apfel for a fixed boundary. Moreover, they extended the calculation of net pressure to other points away from the impact surface.
In this treatment, the hydrostatic pressure constant, previously defined as C, reappears. In this context, its value aligns with those found by Nyborg and Beyer [28] in the case of a perfectly reflecting wall.

$$C = \frac{\gamma + 1}{2} \langle E \rangle \tag{1.11}$$

In the case of other geometric constraints, the value is likely to change. An example provided by Lee and Wang is the case of a perforated wall positioned at $x = -h$ within the tube itself. In this scenario, the value of the constant is adjusted to ensure that the fluid can move through the tube, which translates into the following requirement:

$$\left\langle P^E - P_0 \right\rangle_{x=-h} = 0 \tag{1.12}$$

By incorporating this requirement into the equation above, the value of C can be determined:

$$C = -2 \langle E \rangle \cos 2kh \tag{1.13}$$

Additionally, a significant contribution was made by calculating this pressure in the case of an acoustic beam with cylindrical symmetry, incorporating cylindrical Bessel functions into the solution.

Hasegawa et al.

In his paper [25], Hasegawa et al. conducts a detailed analysis of most of the work done on this topic, focusing on aspects that, according to the author, are the most critical and unresolved up to this point. Specifically, his analysis emphasizes that every theory regarding acoustic radiation

pressure has its own peculiarities and underlying assumptions, which vary in rigor. However, these theories often appear ambiguous, lacking logical consistency in some steps, and imposing unnecessary conditions that can potentially alter a result highly sensitive to initial conditions. In fact, radiation pressure is historically known as a second-order effect, and any assumptions or simplifications made during its derivation can lead to significant changes in the outcome.
Starting from the classical equations of nonlinear acoustics, particularly Bernoulli's equation for unsteady flows, he derives the classical second-order corrected pressure-density relationship and the more comprehensive equation of state for inviscid flows, known as the Thompson equation [29], expressed in terms of potential.

$$\frac{\partial^2\varphi}{\partial t^2} - c_0^2\nabla^2\varphi = \frac{\partial}{\partial t}\left|\nabla\varphi\right|^2 - \frac{1}{2}\left(\nabla\varphi\right)\cdot\nabla\left|\nabla\varphi\right|^2 + (\gamma-1)\dot{\varphi}\nabla^2\varphi - \frac{\gamma-1}{2}\left|\nabla\varphi\right|^2\nabla^2\varphi \tag{1.14}$$

Recognizing the importance of nonlinear terms, he divided the problem by considering the terms of the solution up to the second order. To accomplish this, he separated the system of equations by considering:

$$\varphi = \varphi_1 + \varphi_2 \tag{1.15}$$

This led to the formulation of two second-order linearized systems equivalent to 1.14:

$$\begin{cases} \frac{\partial^2\varphi_1}{\partial t^2} - c_0^2\nabla^2\varphi = 0 \\ \frac{\partial^2\varphi_2}{\partial t^2} - c_0^2\frac{\partial^2\varphi_2}{\partial x^2} = \frac{\partial}{\partial t}\left[\left|\nabla\varphi\right|^2 + \frac{\gamma-1}{2c_0^2}\left(\frac{\partial\varphi_1}{\partial t}\right)^2\right] \end{cases} \tag{1.16}$$

Specifically, regarding the pressure, the expansion used is:

$$p = p_0 + p_1 + p_2 \tag{1.17}$$

Where p_0 is the resting pressure, while the other two components are first-order and second-order quantities, respectively.
By using the relationships from linear acoustics to define the Lagrangian of the system, the new expression for the radiation pressure is:

$$p - p_0 = \rho_0(\dot{\varphi}_1 + \dot{\varphi}_2) - \mathcal{L} \tag{1.18}$$

By then utilizing the expression for radiation pressure in the one-dimensional case, one arrives at:

$$P_{rad} = \langle p - p_0\rangle = \langle\rho_0(\dot{\varphi}_1 + \dot{\varphi}_2)\rangle - \langle\mathcal{L}\rangle \tag{1.19}$$

Considering that φ_1 is a solution to the linear wave equation and thus only has zero-mean harmonic components, its contribution can be considered negligible. The contribution of the Lagrangian is certainly non-zero, as it is composed of always positive terms, while nothing is known about the second-order contribution.
Hasegawa, using Bernoulli's theorem, identified this contribution as:

$$\langle\rho_0\dot{\varphi}_2\rangle = \rho_0 C = \left\langle\int_{p_0}^{p_L}\frac{dp}{\rho} + \frac{v_L^2}{2}\right\rangle \tag{1.20}$$

He interpreted this as the factor of change in the static pressure within the considered system, exactly as in previous theories. For integration surfaces different from the body on which the pressure is being evaluated, the first-order contribution of the time-derived velocity potential takes a different, tensorial form, which aligns with the perspective introduced by Brillouin in the early decades of the 1900s. With this consideration, the new expression for the pressure evaluated on a generic closed surface enclosing the body is equivalent to:

$$P_{Ray} = P_{Lang} = \rho_0 C + \langle -\mathcal{L} + \rho v_1 \otimes v_1 \rangle \tag{1.21}$$

As can be seen from the final equation, the disparity between Rayleigh's and Langevin's pressure is addressed in an exemplary manner, showing that both depend exclusively on the system's experimental conditions and that, in fact, both should be treated from the same physical perspective.

1.4 Radiation Pressure: Experimental Studies

The investigation into acoustic radiation pressure initially emerged from a desire to understand the fundamental interactions between sound waves and materials. For instance, standing wave levitation phenomenon was first observed in Kundt's tube experiment [30] in 1866, that small dust particles moved toward the pressure nodes of the standing wave created in a horizontal tube. Kundt was likely one of the first researchers to observe the practical effect of standing acoustic waves on bodies and to intuit the possibility of generating net forces using sound. Then, Bucks and Muller presented an experiment setup for acoustic levitation in 1933 [31] where a small particle was levitated at a position slightly below the pressure nodes of the standing wave between a radiator and a reflector. Following, early theoretical work by King in 1934 provided some of the first insights into how sound waves exert force on objects, particularly on spheres, setting the stage for more detailed studies. This curiosity was driven by both the theoretical implications for physics and the potential practical applications that such understanding could unlock, particularly in fields like materials science, medicine, and manufacturing. The need to experimentally confirm and validate a general formula for radiation pressure led to multiple experimental attempts, both in water and air, on bodies whose interaction with the acoustic field had been previously studied theoretically. Specifically, the simplest shapes were examined, including flat and cylindrical walls, but particularly spherical shapes, owing to the extensive theoretical work developed in the XX century.

Plane Surface

The work conducted by Herrey [32] in 1954 was among the pioneering studies of radiation pressure on flat walls immersed in water. His research demonstrates how the complexity of the experimental setup allowed for various types of tests aimed at validating, based on Brillouin's

work, the tensorial nature of radiation pressure by calculating this quantity as the angle of incidence between the acoustic beam and the wall varied.

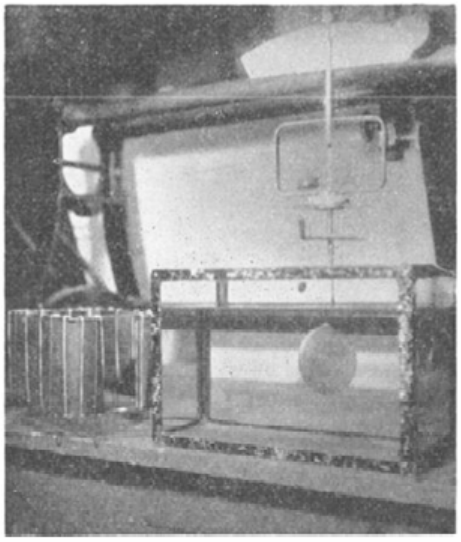

(a) Radiation Balance Apparatus

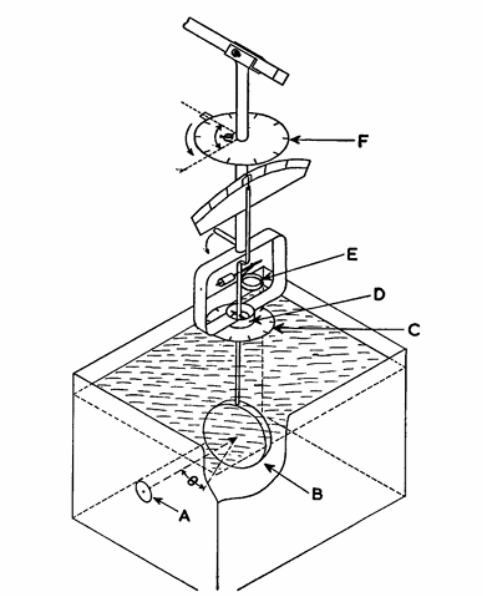

(b) Schematic Drawing of Radiation Balance Apparatus

Figure 1.6. Herry's Experimental Apparatus

Spherical Body

Transitioning from flat to spherical surfaces, numerous studies have been conducted to find a correspondence between King's work and experimental results. Moving from the work of Rudnick [33] to those of Wang [34] and Hasegawa [11, 35, 36], who remains one of the most significant contributors to this field, these studies examine how the nature of the material composing the sphere can affect the results predicted by King for perfectly rigid walls. In fact, the main assumptions of King's work are:

- The sound field is plane progressive;
- The solid sphere is isotropic and elastic;
- The surrounding fluid is nonviscous.

Following the experiments, it is observed that different researchers sometimes reach different conclusions, primarily due to the difficulty of replicating the same experiment under identical physical conditions in this field. Even slight changes in geometry, material, medium, or boundary conditions can cause significant variations in results. This is unfortunately due to the intrinsic nature of the quantity being investigated, as it is very small compared to the typical magnitudes of acoustic fields. Rudnick conducted the experiment in a tube with an amplifier at one end

and a rigid tube at the other, concluding that the pressure observed in the experiments was very similar to that predicted by King.

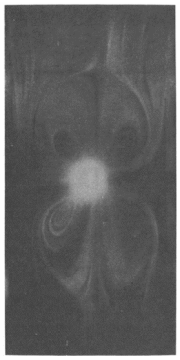

(a) Smoke pattern around a sphere at a pressure node in a standing plane wave field

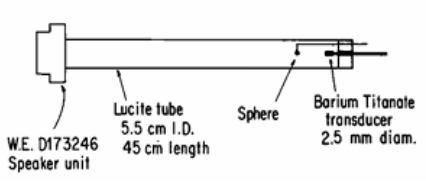

(b) Schematic of Apparatus

Figure 1.7. Rudnik's Experimental Apparatus

Wang measured the acoustic radiation force on a rigid sphere in a resonance chamber for a range of pressures, positions, sizes, and for various gases. Their final remark was that in the low to medium intensity region (< 150 dB) the measured force is consistent with King's theory when analyzed in terms of the fundamental pressure. However, in the high intensity region ($>$ 150 dB), the measured force starts to deviate systematically from King's calculations.

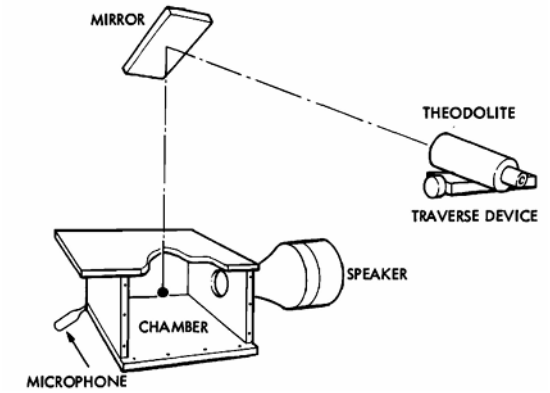

Figure 1.8. Wang's Experimental Apparatus

Hasegawa et al. conducted numerous experiments and different numerical simulations on the

subject. Specifically, the experiments were performed on various spheres, differing in both size and material, and demonstrated the limitations of King's theory. In fact, Hasegawa, unlike others, developed his own formula for radiation pressure, proving it to yield more accurate results than the historically accepted formula by King.

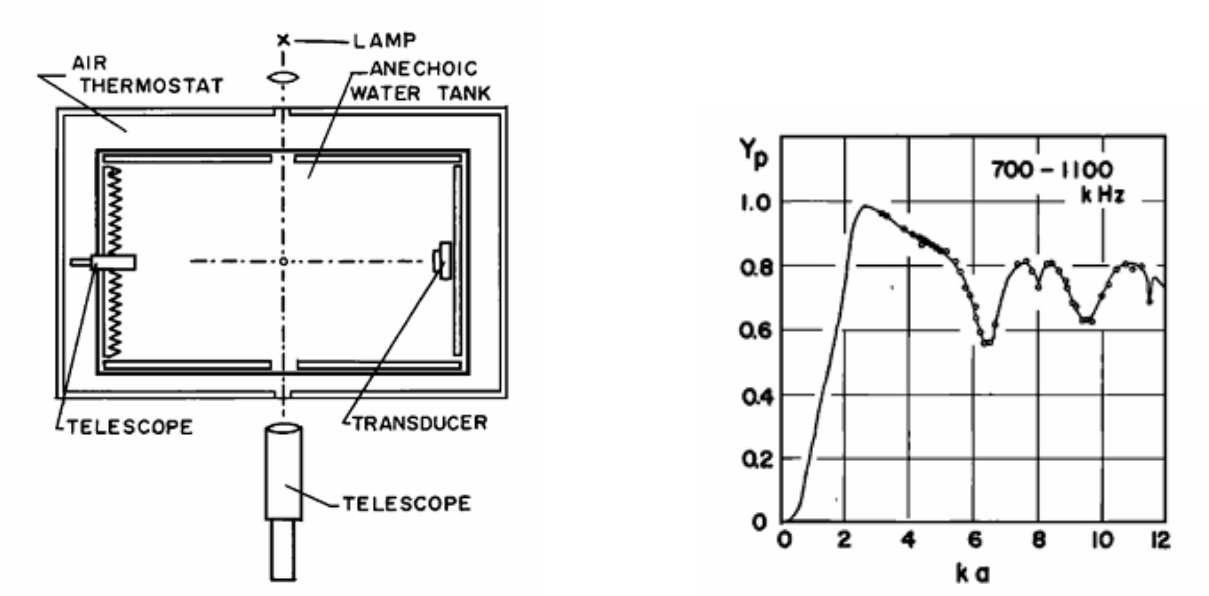

(a) Experimental Apparatus **(b)** Experimental Radiation Force Function

Figure 1.9. Hasegawa's Experimental Apparatus and Results

Anson and Chivers [37] applied Hasegawa's theory to spherical surfaces to verify it through experiments on more than 50 different types of materials immersed in water, reporting a strong correlation between the observed results and the theory. Additionally, their aim was also to find empirical relationships between the materials used and the resulting pressure curves.

Cylindrical Body

Regarding cylindrical surfaces, one of the most recent and significant studies was conducted by Wu et al. [15]. In their case, they relied on King's theory, which was later extended and developed by Embleton and Nyborg. They found a force acting on the walls of a rigid cylinder using plane wave theory and reported an error, which they considered acceptable, of around 15-20 % compared to experimental results.

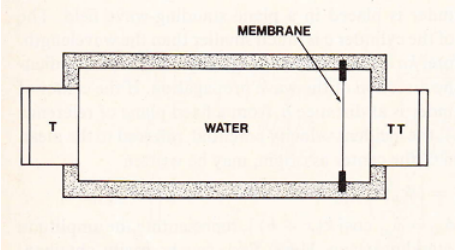

(a) Experimental Apparatus

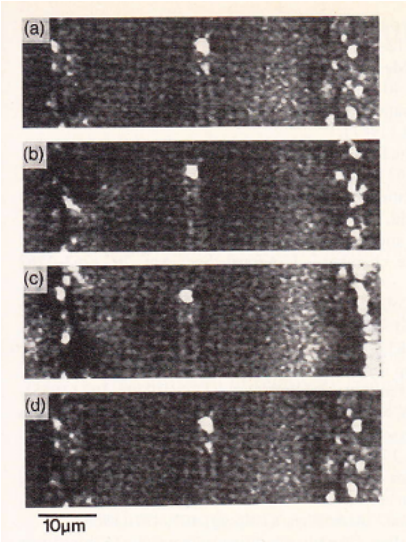

(b) Latex Particles used as tracers in a standing wave field

Figure 1.10. Wu's Apparatus and Experimental Levitated Particles

As can be seen from the various conclusions of the different authors, it seems that each of them appears to have validated or even improved upon the existing theory. Both the experimental and theoretical aspects are subject to the levels of accuracy used during the derivation of formulas, the methods by which experiments are conducted, and how boundary conditions are treated. This makes the phenomenon of radiation pressure fascinating, somewhat incomplete even in the simplest cases, and therefore stimulating in the potential to contribute further to what is thought to be universally established by the scientific community.

Chapter 2

Radiation Pressure: Technology Application

2.1 Main Applications

As mentioned earlier, the main objective of this thesis project is to control the motion of an object using radiation pressure as the driving force, derived from an acoustic field applied to it. This net force effect can be utilized for multiple purposes, including:

- Actuation: For the direct control of the movement of bodies;
- Levitation: For the lifting and/or lightening to facilitate the physical movement of certain objects, with potential applications in precision transport of small masses or even industrial transport on conveyors equipped with amplifiers;
- Medical Applications: Ultrasound applications for the control or destruction of kidney stones or any unwanted objects within the body, as well as for ultrasound imaging;

There are also potential applications in analytical chemistry, biophysics, materials science, pharmacy, and microassembly [38, 39]. In our particular case, the focus is on the first two applications, as they pertain to the direct interaction between a body and an acoustic field. These mechanisms are of a very similar nature but have subtle yet important differences for practical application.
For simple levitation, the body is typically placed in an equilibrium state where the applied acoustic field balances the object's weight by using different principles. In the case of actuation, the body is in motion, and thus, it is necessary to consider the object's position in the control operation and the phase shift in frequency.
Generally, devices used for generating the acoustic signal are piezoelectric transducers capable of producing fields at extremely high frequencies, above the audible range.

2.1.1 Static Acoustic Levitation Techniques

This type of acoustic levitation technique has the capability to lift objects with very limited mass and small dimensions into static equilibrium. The applications are diverse, ranging from laboratory-based material handling to potential uses in microgravity environments.

Standing Wave Acoustic Levitation

This technique utilizes standing wave fields to suspend particles in air, typically solid objects and liquid droplets that are smaller than the acoustic wavelength [40]. The basic setup consists of a transducer and a reflector, which create a pressure node where the levitated object is stabilized.

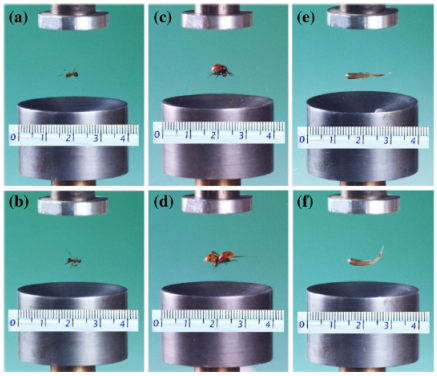

Figure 2.1. Standing Wave Acoustic Levitation of small living animals by Xie et al. [41]

Since the first ever standing wave levitation reported by August Kundt in 1866 [42] there have been further developed for applications in microgravity and materials science. There are two main types of levitation setups: single-axis levitators, which involve one or two opposing transducers, and resonant chamber levitators, which use a closed chamber to enhance the effects of standing waves.

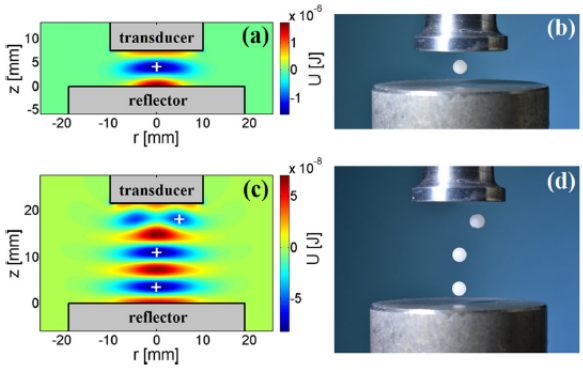

Figure 2.2. Single Axis Acoustic Levitation of Light Object by Andrade et al. [43]

Near-Field and Inverted Near-Field Acoustic Levitation

Employs the near-field force to levitate larger, planar objects just above a vibrating surface, creating a thin air film between the object and the transducer. This method can support heavier objects, leveraging the intense force generated close to the transducer surface. Commonly used for planar objects but adaptable for non-planar shapes using plates vibrating in a flexural mode. Similar to near-field levitation but the object is levitated below the transducer surface. This technique leverages an attractive acoustic force when the object's size is small relative to the acoustic wavelength, creating a gap filled by a thin air layer.

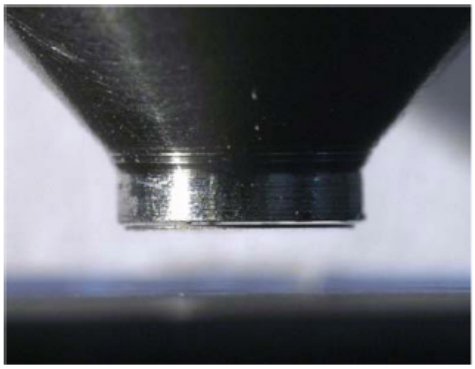

Figure 2.3. Inverted Near-Field Acoustic Levitation of a disk by Takasaki et al. [44]

Far-Field Acoustic Levitation

Involves levitating objects larger than the acoustic wavelength, using a setup that typically includes multiple transducers to generate a stable standing wave field at a distance. It can be used to levitate heavier and larger objects, providing both vertical and horizontal stabilization.

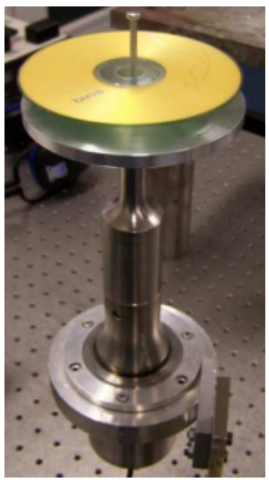

Figure 2.4. Far Field Acoustic Levitation of Large Object by Zhao et al. [45]

Single-Beam Acoustic Levitation

An advanced technique where particles are levitated using a single-sided emitter without the need for opposing acoustic elements. This method allows for more flexible configurations and is capable of trapping small particles in mid-air using highly directed acoustic beams.

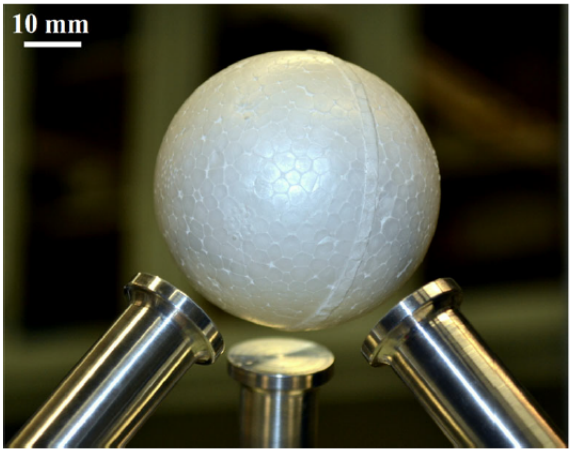

Figure 2.5. Single Beam Levitation of Light Sphere by Andrade [46]

2.1.2 Dynamic Acoustic Transportation Techniques

This method concerns the progression of acoustic levitation from static positioning to dynamic manipulation, enabling precise control over the movement of objects suspended in mid-air. The techniques discussed expand the functionality and application areas of acoustic levitation, from simple demonstrations to complex practical uses in various fields.

Manipulation by Standing Wave Acoustic Levitation

This section details methods to move levitated objects along a single axis, which is an advancement over static levitation that typically keeps objects at fixed points. The manipulation is achieved by altering the properties of the acoustic waves used in the levitation process:

- Phase Modulation: By modulating the phase of the emitted acoustic waves, researchers can create dynamic shifts in the position of pressure nodes within the standing wave field. This allows the movement of objects along the line of wave propagation, enabling controlled transportation from one point to another without physical contact;

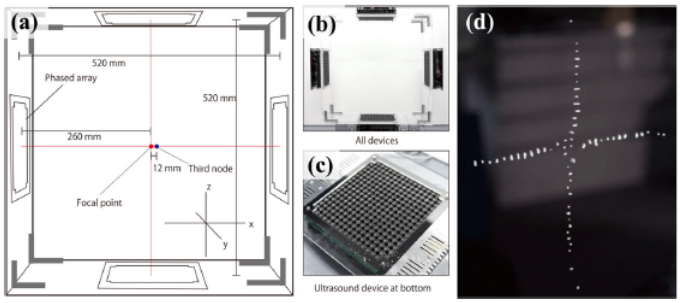

Figure 2.6. Phase Modulation Method proposed by Ochiai et al. [47]

- Amplitude Modulation: Altering the amplitude of acoustic waves can also influence the position and stability of levitated objects. This method is particularly useful for precisely controlling the height at which an object is suspended, which can be crucial for processes that require exact positioning, such as in assembling small or sensitive components.

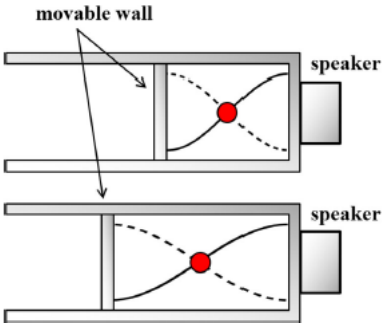

Figure 2.7. Moving Wall Manipulation Method proposed by Fletcher et al. [48]

The applications of single-axis manipulation are vast, ranging from controlled ingredient mixing in pharmaceutical development to the assembly of intricate microstructures in material sciences. The ability to move objects precisely along one axis without contact avoids contamination and damage, providing a significant advantage in sterile environments and with fragile materials. These manipulation techniques demonstrate how acoustic levitation can be adapted from a static display of technology to a functional tool in precision engineering and scientific research, highlighting its potential in industrial automation and beyond. This approach not only enhances the control over levitated objects but also paves the way for more complex manipulation strategies discussed in subsequent sections of the chapter.

Object Transport by Near-Field Acoustic Levitation Method

Near-Field Acoustic Levitation (NFAL) uses intense acoustic fields generated close to a vibrating surface to levitate and transport objects with a thin air layer acting as a buffer. This method can handle heavier objects compared to traditional acoustic levitation, which typically manages only lightweight particles. Practical applications could be:

- Industrial Automation: NFAL is particularly suited for applications requiring the clean and precise transport of flat, rigid objects such as glass sheets, silicon wafers, or metal plates in industrial settings. The non-contact nature of this method prevents contamination and damage, making it ideal for sensitive manufacturing processes.
- Microelectronic Assembly: In the assembly of microelectronic components, where precision and contamination control are paramount, NFAL provides a viable solution for manipulating and placing delicate parts without physical contact.

Technical Challenges and Solutions are:

- Stability and Control: Maintaining stable levitation while dynamically moving objects is challenging, especially under varying load conditions and speeds. Advanced control algorithms and feedback systems are employed to monitor and adjust the acoustic fields in real time.
- Scalability and Efficiency: Scaling NFAL for larger or more complex objects requires efficient management of power and precise control over a larger array of transducers. Research is ongoing to enhance the scalability and energy efficiency of these systems.

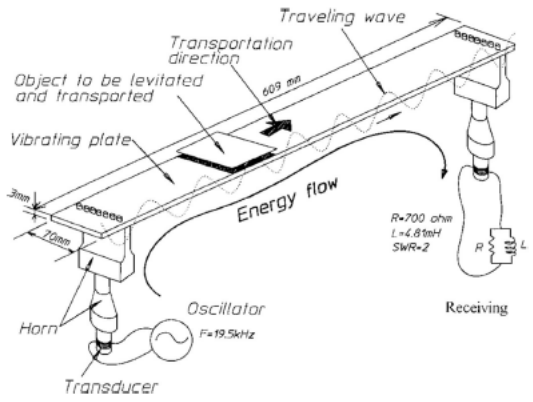

Figure 2.8. Object transport Manipulation Method proposed by Hashimoto et al. [49]

Manipulation using the Single-Beam Acoustic Levitation Method

This section explores the sophisticated approach of manipulating objects using the single-beam acoustic levitation method. Single-beam acoustic levitation offers a versatile and innovative approach for handling materials and objects in a non-contact manner [50–54].
Unlike traditional acoustic levitation that relies on standing waves created by opposing transducers, the single-beam method uses a focused beam of ultrasound to trap and manipulate particles. This is achieved through the precise control of sound wave intensity and phase, which creates a localized trap or pressure node in the path of the beam.
The manipulation is enabled by forming acoustic traps that can be moved along the path of

the beam. By adjusting the focus and direction of the beam, these traps can be dynamically re-positioned, allowing for the controlled transport of levitated objects.

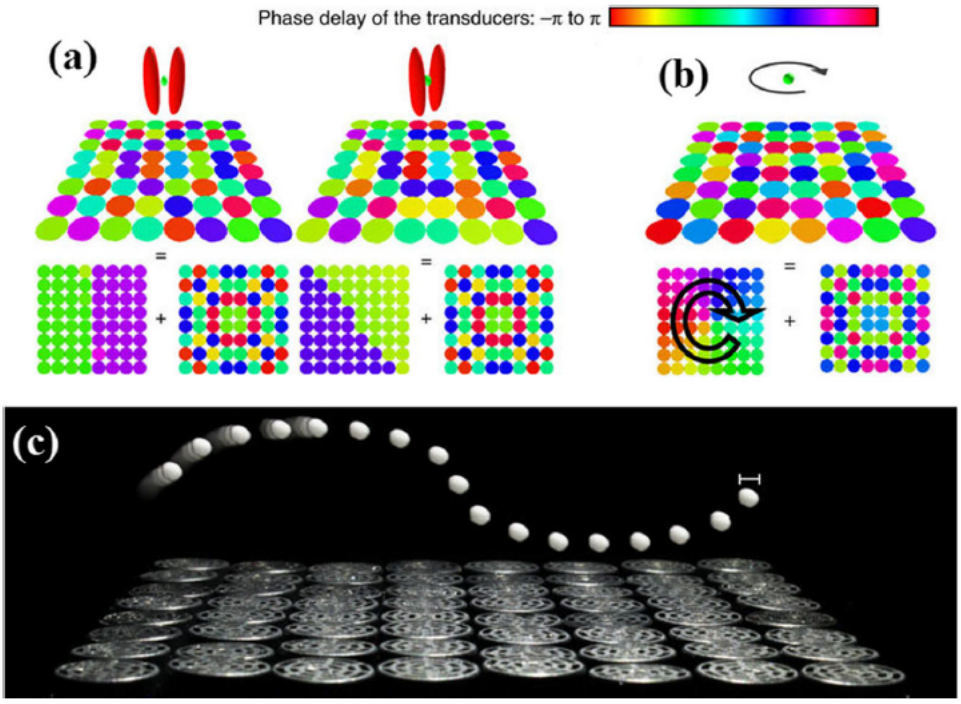

Figure 2.9. Single Beam Manipulation Method proposed by Marzo et al. [54]

Chapter 3

The mathematical formulation of the non-linear acoustics

Acoustics is a branch of physics concerned with the generation and propagation of sound waves in elastic media at a characteristic speed, c_0. Specifically, sound arises from local pressure variations induced by the propagation of acoustic waves. As a result, acoustic waves are classified as elastic waves, similar to those responsible for the vibration of structures like strings and membranes. The movement of particles determines an alternating sequence of compression and rarefaction that are, at the same time, the effect and cause of the propagation of the acoustic wave in the medium. In particular, acoustic waves are generally defined as:

- longitudinal waves: that means they oscillates in the same direction as the wave front;
- they are generally three-dimensional and their shape depends on the source;
- the medium must be elastic to guarantee rarefaction and compression to make the waves move.

Waves traveling along the interior of tubes with uniform cross-section, or those that have propagated over a long distance from their source, will closely approximate plane waves. The specific properties of acoustic wave motion in a fluid depend on several factors, including the ratios between the amplitude and frequency of the acoustic motion and the molecular mean-free-path and collision frequency. Additionally, these properties are influenced by whether the fluid is in thermodynamic equilibrium and by the shape and thermal characteristics of the boundaries enclosing the fluid.

3.1 Non-Linear Acoustics: Euler's Equation

Non-Linear acoustics deals with the description of the acoustic field under the hypothesis that small fluctuations with respect to the reference value are not negligible as in the linear acoustic

field. The derivation of the non-linear acoustic wave equation passes through the relationships between the variables that are of direct relevance to the study of sound. These equations are:

- continuity or the conservation of mass;
- force equation or the conservation of momentum;
- thermodynamic equation of state.

They generally provide a set of equations in terms of pressure P, density ρ, particle Velocity u and Temperature T that totally described the acoustic field. However, the wave equation is usually written in terms of fluctuating components:

- $P(x,t) = P_0 + p(x,t)$;
- $U(x,t) = U_0 + u(x,t)$;
- $\rho(x,t) = \rho_0 + \rho'(x,t)$;
- $T(x,t) = T_0 + T'(x,t)$;

The wave equation can thus be set up in terms of any one of these four variables. In acoustics, it is the pressure fluctuations, $p(x,t)$, that are of primary concern – i.e. noise radiation is a fluctuating pressure.
In practice, sound waves are generally three-dimensional. It is, however, convenient to commence with the derivation of the above equations in one dimension and to extend, without loss of generality, the results to three dimensions.

Continuity Equation

The mass conservation equation(continuity) provides a relationship between the density, $\rho(x,t)$, and the particle velocity, $u(x,t)$. Consider the mass flow of particles in the x-direction through an elemental, control volume, dV, for mass to be conserved, the time rate of change of the elemental mass has to equal the net mass flow into the elemental volume:
By considering the Taylor expansion of the variation of the elemental mass in the cube, one gets the classical mass conservation equation for one-dimensional flows:

$$\frac{\partial \rho}{\partial t} + \frac{\partial (\rho u_x)}{\partial x} = 0 \tag{3.1}$$

The 3.1 can be expanded up to three dimensions as:

$$\frac{\partial \rho}{\partial t} + \nabla \cdot (\rho u) = 0 \tag{3.2}$$

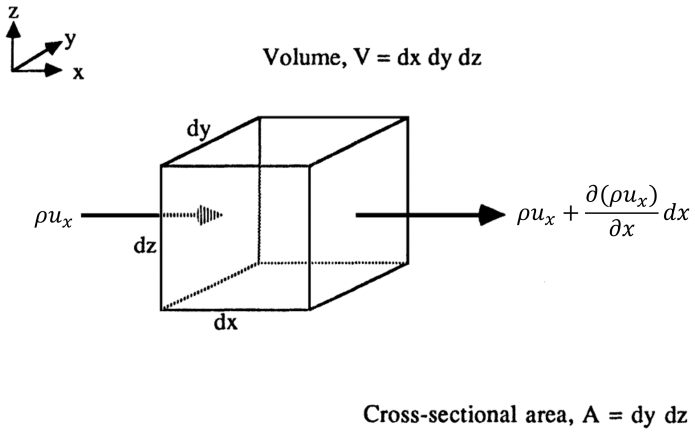

Figure 3.1. Mass Conservation

Conservation of Momentum

The momentum conservation equation provides a relationship between the pressure, $P(x,t)$, the density, $\rho(x,t)$, and the particle velocity, $u(x,t)$. Generally, it is derived either by observing the stated law of conservation of momentum with respect to an elemental, control volume in space, or by a direct application of Newton's second law.

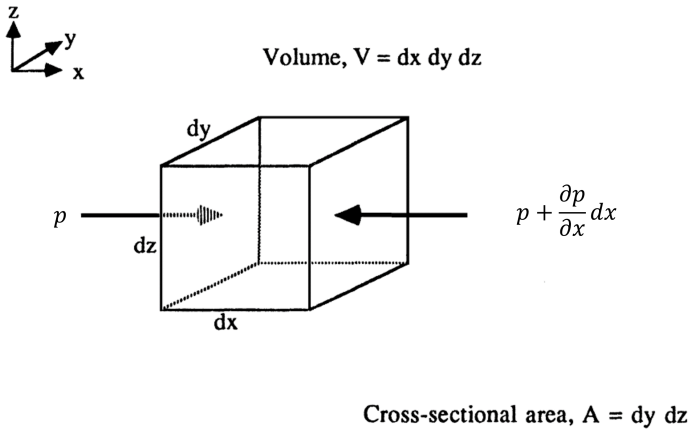

Figure 3.2. Momentum Conservation

Skipping repetitive and well-known mathematical passages present in literature, the momentum equation for one-dimensional flow looks like:

$$\rho \frac{\partial u_x}{\partial t} + \rho u_x \frac{\partial u_x}{\partial x} + \frac{\partial P}{\partial x} = 0 \tag{3.3}$$

While for three-dimensional flows it takes the vectorial form:

$$\rho \left(\frac{\partial u}{\partial t} + (u \cdot \nabla) u \right) + \nabla P = 0 \tag{3.4}$$

State Equation

The equation of state usually relates the pressure, density and absolute temperature of a fluid. For a perfect fluid it is:

$$P = \rho R T_k \tag{3.5}$$

Where P is the absolute pressure, ρ is the density of the gas, R is the gas constant, and T_k is the absolute temperature. It is worth mentioning the propagation of sound waves in air does not generally produce any significant changes of thermal energy between particles, and the entropy of the gas is constant. In addition, the thermal conductivity of the gas is very small. For these reasons the propagation of sound waves can therefore be assumed to be adiabatic. This assumption is valid for linear (small amplitude) sound waves within the audio-frequency range. Hence, the adiabatic equation of state for a perfect gas is used:

$$\frac{P}{P_0} = \left(\frac{\rho}{\rho_0}\right)^{\gamma} \tag{3.6}$$

where $\gamma = c_p/c_v$ is the ratio of specific heats, $\gamma = 1.4$ in air.

Euler Equation

In this section the time-dependent Euler system of equations are considered. These are a system of non-linear hyperbolic conservation laws that govern the dynamics of a compressible material, such as gases or liquids at high pressures, for which the effects of body forces, viscous stresses and heat flux are neglected.

There is some freedom in choosing a set of variables to describe the flow under consideration. A possible choice is the so called primitive variables or physical variables, namely, $\rho(x, y, z, t)$ = density or mass density, $p(x, y, z, t)$ = pressure, $u_x(x, y, z, t)$ = x-component of velocity, $u_y(x, y, z, t)$ = y-component of velocity, $u_z(x, y, z, t)$ = z-component of velocity.

An alternative approach is offered by the so-called conserved variables. These include mass density ρ, the x-momentum component ρu, the y-momentum component ρv, the z-momentum component ρw, and the total energy per unit mass E. Physically, these conserved quantities arise naturally from the application of fundamental laws, including the conservation of mass, Newton's Second Law, and the law of conservation of energy.

From a computational perspective, expressing the governing equations in terms of conserved variables presents several advantages. This leads to a broad class of numerical methods known as conservative methods, which will be examined later in this work. One will now state the equations in terms of the conserved variables under the assumption that the involved quantities are sufficiently smooth to permit differentiation.

It is a system of equation in which the equations 3.1, 3.3 together with the energy equation

$$\frac{\partial E}{\partial t} + \frac{\partial}{\partial x}\left[u(E + P(\rho))\right] = 0$$

with:

$$E = \rho\left(\frac{V^2}{2} + e\right)$$

where $V^2 = u_x^2 + u_y^2 + u_z^2$ and e (the specific internal energy) are used to described the non linear behavior of the acoustic field or whatever physical quantity would like to be analysed.
The system of equations is usually organized in order to have the so called, conservative form. It is a particular form in which the three equations are described in terms of a vector of variables U and a flux operator $F(U)$ to get:

$$U_t + \nabla F(U) = 0 \tag{3.7}$$

Specifically for the Euler equations in one dimensional flow, one gets:

$$U_t = \begin{pmatrix} \rho \\ \rho u \\ E \end{pmatrix}_t, \; F_x(U) = \begin{pmatrix} \rho u \\ \rho u^2 + p \\ u(E+p) \end{pmatrix}_x \tag{3.8}$$

A system of equation in the form of 3.7 has a huge advantages with respect to a classic system of PDE *(Partial Differential Equations)* written in primitive variables, namely (u, ρ, p). That's because in these decades, plenty of numerical methods were implemented by using system of equations written in the form of 3.7 and that makes 3.8 relatively easy to be solved [55].

3.2 Thompson Equation for Velocity Potential

The equation for the velocity potential in a general inviscid motion will now be derived. Under the condition of irrotational flow, where vorticity $\Omega = \nabla \times u = 0$, the particle velocity can be expressed as a function of the gradient of a potential, φ. In fact, in the study of acoustics, it is particularly advantageous to introduce a velocity potential, φ. This approach holds significant practical value and is frequently encountered in both gas dynamics and acoustics.
The in-viscid momentum conservation equation is:

$$\frac{\partial u}{\partial t} + (u \cdot \nabla)u + \frac{1}{\rho}\nabla p = 0 \tag{3.9}$$

The scalar product of the last term with u may be written

$$\frac{1}{\rho}u \cdot \nabla p = \frac{1}{\rho}\frac{Dp}{Dt} - \frac{1}{\rho}\frac{\partial p}{\partial t}$$

For isentropic flow, $dp = c^2 d\rho$; taking advantage of this fact and using the continuity equation 3.2, this becomes

$$\frac{1}{\rho}u \cdot \nabla p = -c^2 \nabla \cdot u - \frac{1}{\rho}\frac{\partial P}{\partial t}$$

The scalar product of 3.9 with u is now

$$\frac{1}{2}\frac{\partial u^2}{\partial t} + \frac{1}{2}u \cdot \nabla u^2 - c^2 \nabla \cdot u = \frac{1}{\rho}\frac{\partial p}{\partial t} \tag{3.10}$$

[in obtaining this result, the identity $(u \cdot \nabla)u = \nabla(u^2/2) - u \times \Omega$ has been used]. This is almost an equation in the velocity potential only, i.e., containing only terms involving u; To express the right-hand side in terms of the velocity potential, the time derivative of equation 3.9 is taken. This operation yields, after substituting the velocity potential $u = -\nabla\varphi$:

$$\frac{\partial^2 u}{\partial t^2} + \frac{1}{2}\nabla(\nabla\varphi)^2 + \frac{\partial}{\partial t}\left(\frac{1}{\rho}\nabla p\right) = 0 \tag{3.11}$$

Now if $f(p)$ is a function only of p, it is an identity that

$$\frac{\partial}{\partial t}\left(f(p)\nabla\varphi\right) = \nabla\left(f(p)\frac{\partial\varphi}{\partial t}\right)$$

Applying this identity to the last term, 3.11 becomes

$$\nabla\left(-\frac{\partial^2\varphi}{\partial t^2} + \frac{1}{2}(\nabla\varphi)^2 + \frac{\partial}{\partial t}\frac{p}{\rho}\right) = 0$$

The quantity in the brackets is an arbitrary function of time; this function can be incorporated into φ, so that:

$$\left(-\frac{\partial^2\varphi}{\partial t^2} + \frac{1}{2}(\nabla\varphi)^2 + \frac{\partial}{\partial t}\frac{p}{\rho}\right) = 0 \tag{3.12}$$

This can in turn be integrated with respect to time to give

$$\frac{\partial\varphi}{\partial t} - \frac{1}{2}(\nabla\varphi)^2 - \int\frac{dp}{\rho} = \text{const}$$

which is a variant of the (compressible-inviscid) Bernoulli equation. Substituting 3.12 into 3.10 and expressing u in terms of the velocity potential finally gives

$$\frac{\partial^2\varphi}{\partial t^2} - \frac{\partial}{\partial t}(\nabla\varphi)^2 + \frac{1}{2}\nabla\varphi\cdot\nabla(\nabla\varphi)^2 - c^2\nabla^2\varphi = 0$$

where the sound speed c is known in terms of the velocity potential.

$$c^2 = c_0^2\left[1 + \frac{k-1}{c_0^2}\left(\varphi_t - \frac{1}{2}|\nabla\varphi|^2\right)\right]$$

3.2.1 Kuznetsov Second Order Approximation

Despite the completeness of the Thompson equation for inviscid media, the decision to derive an approximated version up to the second order was driven by the advantage of enabling the development of semi-analytical solutions under such approximations. [56–58]. For instance, the Kuznetsov's equation 3.15, is one of the most used and credited in the field of non-linear acoustics. It was derived by assuming a second order expansion of the pressure in terms of $w = \dfrac{\rho - \rho_0}{\rho}$, instead of using the exact isentropic expression for pressure-density.

$$P = p_0\left(\rho/\rho_0\right))^\gamma \simeq p_0 + Aw + \frac{1}{2}Bw^2 \tag{3.13}$$

Where $w = \frac{\rho - \rho_0}{\rho}$ is the condensation ratio, $A = \rho c_0^2$ and $B = \rho_0^2 \left(\frac{dc^2}{d\rho}\right)_{\rho_0}$.
It is worth to notice that this approximation is one of the most used in the field of radiation pressure when the Bernoulli's theorem is introduced to get the final expression as shown in Chapter 4. The equation, written in terms of velocity potential in the one-dimensional case and in the case of absence of viscosity and thermal conductivity, is equal to:

$$\frac{\partial^2 \varphi}{\partial t^2} - \frac{\partial^2 \varphi}{\partial x^2}\left(c_0^2 + (k-1)\frac{\partial \varphi}{\partial t}\right) = 2\frac{\partial \varphi}{\partial x}\frac{\partial^2 \varphi}{\partial x t} \tag{3.14}$$

That in a more compact form is:

$$\varphi_{tt} - \varphi_{xx}\left(c_0^2 + (k-1)\varphi_t\right) = 2\varphi_x \varphi_{xt} \tag{3.15}$$

3.3 Linearised Wave Equation

For linear cases, the derivative, or gradient in three dimensions, is taken only for the particle velocity assuming that the change in density is very small compared to the other quantities. Moreover a state equation between pressure and density is supposed to be linear. This leads to a new set of linearized mass continuity equation, state equation and to the linearized conservation of momentum equation:

$$\begin{cases} \frac{\partial \rho}{\partial t} + \rho_0 c_0^2 \frac{\partial (u_x)}{\partial x} = 0 \\ \\ \frac{\partial P}{\partial x} + \rho_0 \frac{\partial (u_x)}{\partial t} = 0 \\ \\ p = (\rho - \rho_0) c_0^2 \end{cases} \tag{3.16}$$

That comes from by substituting in equation 3.3, $P(x,t) = P_0 + p(x,t)$ and $\rho(x,t) = \rho_0 + \rho'(x,t)$ and neglecting the second and higher-order terms.
Equations in 3.16 are valid for small amplitude compares to the reference pressure ($< 140dB$). At this point, there are all the ingredients to write the so called "Linearised wave equation" for acoustics. Indeed, by combining the equations in 3.16 together, and assuming that the order neglecting the constant terms in the derivation for pressure and density, one obtains:

$$\frac{\partial^2 p}{\partial t^2} = c_0^2 \frac{\partial^2 p}{\partial x^2} \tag{3.17}$$

Where the relation for $c_0^2 = \sqrt{\frac{kP_0}{\rho}}$ comes directly from the state equation assuming that:

$$c = \sqrt{\left(\frac{\partial p}{\partial \rho}\right)_{\rho = \rho_0}} \tag{3.18}$$

Consider a plane, one-dimensional, sound wave propagating in the x-direction, it is convenient to represent the solution of the wave equation in terms of complex, harmonic functions. The

general solution involves waves travelling in both the positive and negative x-directions and knowing that the general solution for equation 3.17 is $p(x,t) = F(x-ct) + G(x+ct)$, where $F(x-ct)$ is travelling in the positive direction while $G(x+ct)$ in the negative one, it is possible to rewrite the pressure field as a combination of two harmonic solutions:

$$p(x,t) = A_1 e^{\omega t - kx} + A_2 e^{\omega t + kx} \tag{3.19}$$

where $k = \omega/c$ is the wave number.

Wave Equation in Potential Form

An other way to write the wave equation is in term of a scalar potential, indeed, provided that the fluid is irrotational, that means $\nabla \times u = 0$, the velocity field could be written as a gradient of a scalar function φ, so $u = -\nabla\varphi$. After some mathematical passages, one can get the equivalence between the wave equation in terms of pressure and wave equation in terms of potential. As a consequence of substituting $\nabla \times u = 0$ into the second equation of 3.16 one obtains:

$$\nabla\left(\rho\frac{\partial\varphi}{\partial t} - p\right) = 0 \tag{3.20}$$

That leads to the famous linearised relation between pressure and potential fields:

$$p = \rho_0\frac{\partial\varphi}{\partial t} = \rho_0\varphi_t \tag{3.21}$$

At this point, considering equation 3.21 and equation 3.17 one obtains the linearised potential wave equation:

$$\frac{\partial^2\varphi}{\partial t^2} = c_0^2\frac{\partial^2\varphi}{\partial x^2} \tag{3.22}$$

Chapter 4

A Hamiltonian formulation of non-linear acoustics

The literature presents various, and sometimes controversial, interpretations of radiation pressure. These debates revolve around the scalar versus tensorial nature of acoustic stress, the choice of time-averaging framework (Lagrangian or Eulerian), the order of terms contributing to the governing equations, and the potential historical inaccuracies on the subject highlighted by several authors. Hence, this analysis aims at clarifying some of these crucial points. The object of the investigation is in essence the evaluation of the quantity:

$$F_{rad} = \int_{S_B(t)} p \cdot n \, dS$$

And its time average:

$$\langle F_{rad} \rangle = \langle \int_{S_B(t)} p \cdot n \, dS \rangle$$

The starting points can be summarized as follows:

- The model uses a general constitutive relationship between pressure and density of the barotropic form $p = p(\rho)$ and this can be specified with a certain freedoom. In other theories (see for example the equations of Westervelt, Kuznetsov, Khokhlov-Zabolotskaya-Kuznetsov (KZK), Blackstock-Crighton and Hasegawa), a second order expansion of the pressure in terms of $\rho - \rho_0$ is assumed and in some models more general, non-barotropic relationship are investigated. In this research an exact analysis is developed, without specifying any particular constitutive relationship $p = p(\rho)$ except, as a remarkable case, the application to the nonlinear adiabatic, reversible transformation;

- The model does not account for any effect related to the thermal conductivity of the gas, assumed to be vanishing;

- The model assumes the fluid is inviscid with no dissipation mechanism.

4.1 Hamiltonian Integral Formulation

Before examining this new expression for radiation pressure, it is essential to outline the Hamiltonian formulation. When dealing with a fluid system and an immersed solid body, the application of Hamilton's principle requires careful consideration. In its original formulation, Hamilton's principle applies to a set of material particles, meaning that both the kinetic and potential energy, for the application of a variational principle, must be referenced to these particles. For such systems, Hamilton's principle is equivalent to Newton's laws.

When investigating the system composed of a material body and a fluid, it is essential to extend Hamilton's principle in a rigorous manner. This requires a clear and unambiguous identification of the material system to which the kinetic and potential energy refer. To meet this need, the body and the surrounding portion of fluid are considered as a material system. It is essential that the selected portion of fluid at any time t contains the same set of fluid particles chosen at the initial time t_0. This condition allows for the application of Hamilton's principle in its original formulation, which pertains to a set of uniquely identified material particles. The requirement for material invariability of the system translates into a mathematical constraint within the variational Hamiltonian formulation.

This question is crucial because two classical approaches exist for the differential description of fluid motion: the Lagrangian and Eulerian formulations. The Lagrangian approach follows individual material particles through their motion, while the Eulerian approach does not. This distinction can lead to subtle errors when applying Hamilton's principle to a fluid described by an Eulerian framework. However, it is posited that the choice between these two approaches, when applying Hamilton's principle, ultimately depends on technical convenience. It is fundamental to begin with the Lagrangian approach when defining the material system under investigation, ensuring that an invariable set of fluid particles and the immersed body are followed, allowing for accurate application of kinetic and potential energy in the Hamiltonian method. Once Hamilton's principle is formulated for this Lagrangian set of material objects, transitioning from a Lagrangian to an Eulerian approach becomes feasible and advantageous.

Therefore, Hamilton's principle will be applied to a material system of time-invariant mass M, contained within the volume $V(t)$ bounded by an immovable surface S, as depicted in figure 1. This volume encompasses both the body of mass m and volume $V_B(t)$, enclosed by surface $S_B(t)$, as well as a portion of fluid (gas) with volume $V_F(t)$ and time-invariant mass m_F, located between surfaces S and S_B. No dissipative effects are involved in the fluid motion, and an external force F is applied to the body at point x_F, along with a torque.
The body motion can include, in general, a displacement of its gravity center $u_G(t)$ and a rotation about an axis of unit vector r, for simplicity assumed to be invariable in time. Therefore, the rotation about r is described by the angle $\theta(t)$, and the body's angular velocity is $\omega = \theta\dot{r}$. The torque applied to the body has intensity T. However, the extension to more general rotations, although mathematically tricky, is conceptually simple.

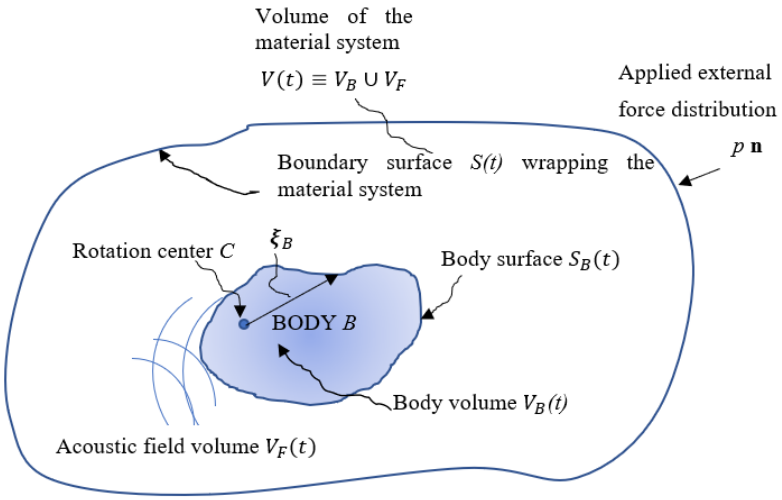

Figure 4.1. Hamilton Material Volume

The kinetic energy of this identified material system is:

$$K = \frac{1}{2}m|v_G|^2 + \frac{1}{2}J\theta^2 + \int_{V_F(t)} \frac{\rho|v|^2}{2}dV \tag{4.1}$$

ρ is the gas density, J is the moment of inertia of the body with respect to r. The potential energy of a given portion of fluid per unit volume of the fluid $u(\rho)$, related to its elastic energy storage capability, is determined as follow:

$$U = -\int_{\Omega_0}^{\Omega} p(\Omega')d\Omega'$$

Where Ω_0 and Ω are the reference material volume and the actual material volume of the gas portion, respectively. Ω must be expressed in terms of the density ρ. Since, for a generic mass μ_F of the material fluid trapped into the volume Ω, it holds $\rho\Omega = \rho_0\Omega_0 = \mu_F$, then $\rho d\Omega + \Omega d\rho = 0$ and $\frac{d\Omega}{\Omega} = -\frac{d\rho}{\rho}$, and it can be integrated leading to:

$$U = \int_{\rho_0}^{\rho} p(\rho')\Omega'\frac{d\rho'}{\rho'} = \mu_F \int_{\rho_0}^{\rho} \frac{p(\rho')}{\rho'^2}d\rho'$$

Therefore, the density (per unit volume) of the material fluid potential energy is:

$$u(\rho) = \frac{U}{\Omega} = \frac{\mu_F}{\Omega}\int_{\rho_0}^{\rho} \frac{p(\rho')}{\rho'^2}d\rho'$$

i.e.:

$$u(\rho) = \rho\int_{\rho_0}^{\rho} \frac{p(\rho')}{\rho'^2}d\rho'$$

Note $u(\rho)$ is the energy per unit volume stored by the fluid because of its compressibility and evaluated following the same material particles: its special form depends on the assumed gas constitutive relationship $p(\rho) = P(\rho) - P_0$. For example, the adiabatic reversible (isotropic) case produces:

$$u(\rho) = \rho\int_{\rho_0}^{\rho} \frac{p(\rho')}{\rho'^2}d\rho' = \frac{P_0}{(k-1)}\left(\frac{P}{P_0} - \frac{\rho}{\rho_0}\right) - P_0\left(\frac{\rho - \rho_0}{\rho_0}\right) \tag{4.2}$$

A potential additional source of potential energy could arise from the elastic effects of the body, which are not considered in the present approach but can be easily incorporated. It is important to note that the matter of our system and its mass M, contained within the volume $V(t)$, remain invariant over time. As stipulated at the outset, this refers to the same material system at any time t. The mass balance is then expressed by constant quantities as $m + m_F = M$, i.e.:

$$m + \int_{V_F(t)} \rho dV = M \rightarrow \frac{d}{dt} \int_{V_F(t)} \rho dV = 0$$

This represents the announced constraint in the Hamiltonian formulation. Therefore, the Hamilton's action A for the considered material system holds in the form:

$$A = \int_{t_1}^{t_2} \left[(K - U) + \lambda^*(t) \frac{d}{dt} \int_{V_F(t)} \rho dV \right] dt \tag{4.3}$$

This is the Lagranigan formulation of the Hamilton's principle, where $\lambda^*(t)$ is a Lagrangian multiplier to introduce the necessary constraint of conservation of mass.
Let us rewrite it, using the Reynold's theorem, as:

$$A = \int_{t_1}^{t_2} \left[(K - U) + \lambda^*(t) \int_{V_F(t)} \rho_t + \nabla \cdot (\rho v) \; dV \right] dt \tag{4.4}$$

The integrand $\rho_t + \nabla \cdot (\rho v)$ is identically vanishing at any point in the fluid, since it expresses the local balance of mass within the volume, i.e. the equation and $\rho_t + \nabla \cdot (\rho v) = 0$ holds at any point in the acoustic field. Therefore, the previous expression of the action is equivalent to:

$$A = \int_{t_1}^{t_2} \left[(K - U) + \int_{V_F(t)} \lambda^*(x,t)(\rho_t + \nabla \cdot (\rho v)) \; dV \right] dt \tag{4.5}$$

With arbitrary value for the function $\lambda(\tilde{x}, t)$. Introducing the fluid's Lagrangian density:

$$\mathcal{L}(\rho, v) = \frac{1}{2} \rho |v|^2 - u(\rho) \tag{4.6}$$

The action becomes:

$$A = \int_{t_1}^{t_2} \left[\frac{m|v_g|^2}{2} + \frac{J\dot{\theta}^2}{2} + \int_{V_F(t)} \mathcal{L}(\rho, v) + \lambda^*(x,t)(\rho_t + \nabla \cdot (\rho v)) \; dV \right] dt \tag{4.7}$$

Let for simplicity:

$$\tilde{\mathcal{L}}(\rho, v, \lambda) = \mathcal{L}(\rho, v) + \lambda^*(x,t)(\rho_t + \nabla \cdot (\rho v)) \tag{4.8}$$

Where $\tilde{\mathcal{L}}(\rho, v, \lambda)$ is the modified Lagrangian of the gas to bring into account the effect of the kinematic constraint by the continuity equation. The last considered term is the virtual work δW of the external forces acting on our material system, those applied by the distribution of pressure on the surface S, and by the external force and torque applied directly to the body:

$$\delta W = \int_{S(t)} pn \cdot \delta u_S dS + F \delta x_F + T \delta \theta \tag{4.9}$$

Finally, the Hamilton's principle stands in the form:

$$\delta A = \delta \int_{t_1}^{t_2} \left[\frac{m|v_g|^2}{2} + \frac{J\dot{\theta}^2}{2} + \int_{V_F(t)} \tilde{\mathcal{L}}(\rho, v, \lambda) dV + W \right] dt = 0 \tag{4.10}$$

Note that the volume $V_F(t)$ is changing when performing the variation, since the fluid particles move and the body moves with respect to the fluid. Therefore, the delimiting surfaces $S(t)$ and $S_B(t)$ move and they depend, respectively, on the displacement variables $u_G(t)$,$\theta(t)$ and $u_S(x,t)$, where the latter is the fluid displacement on the surface $S(t)$, and $\dot{u}_G = v_G$:

$$\delta A = \delta \int_{t_1}^{t_2} \left[\frac{m|v_g|^2}{2} + \frac{J\dot{\theta}^2}{2} + \int_{V_F(u_G,\theta(t),u_S)} \tilde{\mathcal{L}}(\rho, v, \lambda) dV + W \right] dt$$

This means the operator δ produces the variations of the entire set of variables ρ,u_S,v,λ,θ, $\dot{\theta}$,u_g,v_g. This leads to:

$$\delta A = \delta \int_{t_1}^{t_2} \left[\delta_{(u_G)} \int_{V_F(u_G,\theta(t),u_S)} \tilde{\mathcal{L}}(\rho, v, \lambda) dV + \delta_{(\theta)} \int_{V_F(u_G,\theta(t),u_S)} \tilde{\mathcal{L}}(\rho, v, \lambda) dV + \delta_{(v_G)} \frac{m|v_g|^2}{2} + \right.$$

$$\left. + \delta_{(u_S)} \int_{V_F(u_G,\theta(t),u_S)} \tilde{\mathcal{L}}(\rho, v, \lambda) dV + \int_{V_F(u_G,\theta(t),u_S)} \delta_{(\rho,v,\lambda)} \tilde{\mathcal{L}}(\rho, v, \lambda) dV + \delta_{(\dot{\theta})} \frac{J\dot{\theta}^2}{2} + \delta W \right] dt$$

Where the symbol $\delta((a, b, \dots z))$ means the variation acts on the variables $a, b, \dots z$. Therefore, the Hamilton's principle includes the six variations δA_1, δA_2, δA_3, δA_4, δA_5, δA_6:

$$\delta A_1 = \int_{t_1}^{t_2} \left[\delta_{(u_G)} \int_{V_F(u_G,\theta(t),u_S)} \tilde{\mathcal{L}}(\rho, v, \lambda) dV \right] dt, \quad \delta A_2 = \int_{t_1}^{t_2} \left[\delta_{(\theta)} \int_{V_F(u_G,\theta(t),u_S)} \tilde{\mathcal{L}}(\rho, v, \lambda) dV \right] dt$$

$$\delta A_3 = \int_{t_1}^{t_2} \left[\delta_{(u_S)} \int_{V_F(u_G,\theta(t),u_S)} \tilde{\mathcal{L}}(\rho, v, \lambda) dV \right] dt, \quad \delta A_4 = \int_{t_1}^{t_2} \left[\delta_{(\rho,v,\lambda)} \tilde{\mathcal{L}}(\rho, v, \lambda) dV \right] dt$$

$$\delta A_5 = \int_{t_1}^{t_2} \left[\delta_{(v_G)} \frac{m|v_g|^2}{2} \right] dt, \qquad \delta A_6 = \int_{t_1}^{t_2} \left[\delta_{(\dot{\theta})} \frac{J\dot{\theta}^2}{2} \right] dt$$

Let's analyze them singularly. Concerning δA_1, one shluld consider the variation over the displacement of center of gravity. Indeed:

$$\delta_{(u_G)} \int_{V_F(u_G,\theta(t),u_S)} \tilde{\mathcal{L}}(\rho, v, \lambda) dV = \int_{V_F(u_G+\delta u_G,\theta(t),u_S)} \tilde{\mathcal{L}}(\rho, v, \lambda) dV - \int_{V_F(u_G,\theta(t),u_S)} \tilde{\mathcal{L}}(\rho, v, \lambda) dV =$$

$$\int_{V_F+\delta V_F} \tilde{\mathcal{L}}(\rho, v, \lambda) dV - \int_{V_F} \tilde{\mathcal{L}}(\rho, v, \lambda) dV = \int_{\delta V_F(u_G,\theta(t),u_S} \tilde{\mathcal{L}}(\rho, v, \lambda) dV$$

This means one must calculate the integral by the variation of the volume for each element over the surface S_B, since only this surface is affected by u_G. In fact:

$$dV = \delta u_g \cdot n dS, \quad \int_{\delta V_F(u_G,\theta(t),u_S)} \tilde{\mathcal{L}}(\rho, v, \lambda) dV = \int_{S_B} \tilde{\mathcal{L}}(\rho, v, \lambda) \delta u_G \cdot n dS$$

Where n is the outward surface normal component of S_B, and δu_G is the virtual displacement at any point on S_B due to body gravity center displacement component only (the surface displacement due to the rotation component θ is analyzed by δA_2):

$$\int_{\delta V_F(u_G,u_S)} \tilde{\mathcal{L}}(\rho, v, \lambda) dV = \int_{S_B} \tilde{\mathcal{L}}(\rho, v, \lambda) \delta u_g \cdot n dS = \delta u_G \cdot \int_{S_B} \tilde{\mathcal{L}}(\rho, v, \lambda) n dS$$

The variation δA_1, with the previous calculations, follows as:

$$\delta A_1 = \int_{t_1}^{t_2} \left[\delta u_G \cdot \int_{S_B} \tilde{\mathcal{L}}(\rho, v, \lambda) n dS \right] dt$$

The second one δA_2, following an identical approach, is:

$$\delta A_2 = \int_{t_1}^{t_2} \left[\delta \theta \cdot \int_{S_B} \tilde{\mathcal{L}}(\rho, v, \lambda)(r \times \xi) n dS \right] dt$$

The third one δA_3 similarly is:

$$\delta A_3 = \int_{t_1}^{t_2} \left[\delta u_s \cdot \int_{S} \tilde{\mathcal{L}}(\rho, v, \lambda) n dS \right] dt$$

The fifth one, δA_5, is:

$$\delta A_5 = \int_{t_1}^{t_2} -\frac{d}{dt}(m v_G) \cdot \delta u_G \, dt + [m v_G \cdot \delta u_G]_{t_1}^{t_2}$$

The sixth one, δA_6, is:

$$\delta A_6 = \int_{t_1}^{t_2} -\frac{d}{dt}(J\dot{\theta}) \cdot \delta\theta \, dt + \left[J\dot{\theta} \cdot \delta\theta \right]_{t_1}^{t_2}$$

δA_4 is the more laborious and it must be manipulated as follows:

$$\delta A_4 = \int_{t_1}^{t_2} \left[\delta_{(\rho,v,\lambda)} \tilde{\mathcal{L}}(\rho, v, \lambda) dV \right] dt$$

$$= \int_{t_1}^{t_2} \left\{ \int_{V_F} \left(\rho v \cdot \delta v + \frac{|v|^2}{2} \delta\rho - \frac{du}{d\rho} \delta\rho + \left[\rho_t + \rho \nabla \cdot v + \nabla\rho \cdot v \right] \delta\lambda \right) dV \right\} dt +$$

$$\int_{t_1}^{t_2} \left\{ \int_{V_F} \left(\lambda \left[\delta\rho_t + \delta\rho \nabla \cdot v + \rho \nabla \cdot \delta v + \nabla\delta\rho \cdot v + \nabla\rho \cdot \delta v \right] \right) dV \right\} dt$$

where, collecting the different independent variations δv,$\delta\rho$,$\delta\lambda$, one gets:

$$\delta A_4 = \int_{t_1}^{t_2} \left\{ \int_{V_F} \left(\left[\rho v + \lambda \nabla\rho \right] \cdot \delta v + \lambda\rho \nabla \cdot \delta v + \left[\frac{|v|^2}{2} - \frac{du}{d\rho} - \lambda_t + \lambda \nabla \cdot v \right] \delta\rho \right) dV \right\} dt +$$

$$\int_{t_1}^{t_2} \left\{ \int_{V_F} \left(\lambda \nabla\delta\rho \cdot v + \left[\rho_t + \rho \nabla \cdot v + \nabla\rho \cdot v \right] \delta\lambda \right) dV \right\} dt + \left[\lambda\delta\rho \right]_{t_1}^{t_2}$$

Considering that:

$$\int_{V_F} \nabla \cdot (\lambda\rho\delta v) \, dV = \int_{V_F} \lambda\rho \nabla \cdot \delta v \, dV + \int_{V_F} \nabla (\lambda\rho) \cdot \delta v dV$$

i.e.:

$$\int_{V_F} \lambda\rho \nabla \cdot \delta v \, dV = \int_{V_F} \nabla \cdot (\lambda\rho\delta v) \, dV - \int_{V_F} \nabla (\lambda\rho) \cdot \delta v dV$$

Using the Gauss theorem for the first integral on the right-hand-side:

$$\int_{V_F} \lambda\rho \nabla \cdot \delta v \, dV = \int_{\partial V_F} \lambda v \cdot \nabla\delta\rho \, dS - \int_{V_F} \nabla (\lambda\rho) \cdot \delta v \, dV$$

where n is the outward normal vector along ∂V. Analogously:

$$\int_{V_F} \nabla \cdot (\lambda v \delta\rho)\, dV = \int_{V_F} \lambda v \cdot \nabla \delta\rho\, dV + \int_{V_F} \delta\rho \nabla \cdot (\lambda v)\, dV$$

i.e.:

$$\int_{V_F} \lambda v \cdot \nabla \delta\rho\, dV = \int_{V_F} \nabla \cdot (\lambda v \delta\rho)\, dV - \int_{V_F} \delta\rho \nabla \cdot (\lambda v)\, dV$$

And using again the Gauss theorem for the first integral on the right-hand-side:

$$\int_{V_F} \lambda v \cdot \nabla \delta\rho\, dV = \int_{\partial V_F} \lambda v \cdot n \delta\rho dS - \int_{V_F} \delta\rho \nabla \cdot (\lambda v)\, dV$$

Substituting back into the variation δA_4:

$$\delta A_4 = \int_{t_1}^{t_2} \left\{ \int_{V_F} \left([\rho v + \lambda \nabla\rho - \nabla(\lambda\rho)] \cdot \delta v + \left[\frac{|v|^2}{2} - \frac{du}{d\rho} - \lambda_t + \lambda \nabla \cdot v - \nabla \cdot (\lambda v) \right] \delta\rho \right) dV \right\} dt +$$

$$\int_{t_1}^{t_2} \left\{ \int_{V_F} \left[\rho_t + \rho \nabla \cdot v + \nabla\rho \cdot v \right] \delta\lambda dV + \int_{\partial V_F} (\lambda\rho n \cdot \delta v + \lambda v \cdot n \delta\rho)\, dS \right\} dt + [\lambda \delta\rho]_{t_1}^{t_2}$$

Where:

$$\int_{\partial V_F} (\lambda\rho n \cdot \delta v + \lambda v \cdot n \delta\rho)\, dS = \int_{S_B \cup S} (\lambda\rho n \cdot \delta v + \lambda v \cdot n \delta\rho)\, dS$$

A simplification comes from considering the surface S at a large distance with respect to the body, in which case one can use the Sommerfeld condition on it, i.e. the acoustic field perturbation over this surface is vanishing. This could be the case of the body generating, by its motion, waves into the acoustic field, the amplitude of which vanish at long distance. Also, a point source close to the body with respect to the distance between the body and S, is a case to which the Sommerfeld condition applies. These cases permit to write:

$$\int_{S \to S_\infty} \ldots dS \to 0$$

Leading to:

$$\delta A_4 = \int_{t_1}^{t_2} \left\{ \int_{V_F} \left([\rho v - \rho \nabla\lambda] \cdot \delta v + \left[\frac{|v|^2}{2} - \frac{du}{d\rho} - \lambda_t - \nabla\lambda \cdot v \right] \delta\rho \right) dV \right\} dt +$$

$$\int_{t_1}^{t_2} \left\{ \int_{V_F} \left[\rho_t + \rho \nabla \cdot v + \nabla\rho \cdot v \right] \delta\lambda dV + \int_{S_B} (\lambda\rho n \cdot \delta v + \lambda v \cdot n \delta\rho)\, dS \right\} dt + [\lambda \delta\rho]_{t_1}^{t_2}$$

The three terms into the volume integral leads to a system of particular equations:

$$\begin{cases} v = \nabla\lambda \\ \frac{1}{2}|\nabla\lambda|^2 - \frac{du}{d\rho} - \lambda_t - \nabla\lambda \cdot \nabla\lambda = 0 \\ \rho_t + \rho \nabla^2 \lambda + \nabla\rho \cdot \nabla\lambda = 0 \end{cases} \tag{4.11}$$

Where the first equation permits to eliminate the fluid speed. It is the first relevant result of the research, indeed it claims that the fluid particle velocity can be expressed as a potential of a scalar quantity. This is a remarkable result, as the irrotationality of the flow is no longer an

a priori assumption but rather a consequence of the chosen form of the Lagrangian, in which dissipation effects are excluded.
However, solving for the first variable, $\lambda(x,t)$, is not uniquely defined. It can be stipulated that $\lambda(x,t) = -\varphi(x,t) - \varphi_0(t)$, where the presence of $\varphi_0(t)$ does not affect the velocity field. Consequently, the equations reduce to:

$$\begin{cases} -\frac{1}{2}|\nabla\varphi|^2 - \frac{du}{d\rho} + \varphi_t + \dot{\varphi_0} = 0 \\ \rho_t - \rho\nabla^2\varphi - \nabla\rho\cdot\nabla\varphi = 0 \end{cases} \tag{4.12}$$

4.2 Analysis of the Obtained Equations

The following physical remarks about the obtained equations via the Hamilton's principle are important and they are needed to be explained in the next lines.

4.2.1 Equivalence with the Bernoulli's Equation

The analysis of the obtained equation:

$$-\frac{du}{d\rho} = -\varphi_t - \dot{\varphi_0} + \frac{1}{2}|\nabla\varphi|^2 \tag{4.13}$$

Brings important conclusions about the gas pressure that produces, in different possible forms, the Bernoulli's equation. Deriving the expression of the introduced fluid potential energy with respect to the density provides:

$$u(\rho) = \rho\int_{\rho_0}^{\rho}\frac{p(\rho')}{\rho'^2}d\rho' \rightarrow \frac{du}{d\rho} = \int_{\rho_0}^{\rho}\frac{p(\rho')}{\rho'^2}d\rho' + \rho\frac{p}{\rho^2} = \frac{u}{\rho} + \frac{p}{\rho}$$

By inserting the result into the previous equation 4.13, the following expression is obtained:

$$\frac{u}{\rho} + \frac{p}{\rho} = \varphi_t - \frac{1}{2}|\nabla\varphi|^2 + \dot{\varphi_0}$$

i.e.:

$$\frac{p}{\rho} = \varphi_t - \frac{1}{2}|\nabla\varphi|^2 + \dot{\varphi_0} - \frac{u}{\rho}$$

That produces:

$$\frac{p}{\rho} + \frac{\mathcal{E}}{\rho} - \varphi_t = \dot{\varphi_0}$$

Since at a long distance from the body, the perturbations of φ vanish, so $\mathcal{E} = \frac{1}{2}\rho|\nabla\varphi|^2 + u(\rho)$ vanishes and it follows $\dot{\varphi_0} = 0$, therefore:

$$\frac{p}{\rho} + \frac{\mathcal{E}}{\rho} - \varphi_t = 0 \rightarrow p = \rho\varphi_t - \mathcal{E}$$

Where $\mathcal{E}$ is the total energy density and this is a possible form of the Bernoulli's equation. Since:

$$\frac{u}{\rho} = \int_{\rho_0}^{\rho}\frac{p(\rho')}{\rho'^2}d\rho'$$

One can write:

$$\frac{p}{\rho}+\int_{\rho_0}^{\rho}\frac{p(\rho')}{\rho'^2}d\rho'+\frac{1}{2}\left|\nabla\varphi\right|^2-\varphi_t=0$$

Considering that:

$$d\left(\frac{p}{\rho}\right)=\frac{dp}{\rho}-\frac{p}{\rho^2}d\rho\rightarrow\frac{p}{\rho}+\int_{\rho_0}^{\rho}\frac{p(\rho')}{\rho'^2}d\rho'=\int_{P_0}^{P}\frac{dp'}{\rho(p')}$$

By which one obtains:

$$\int_{P_0}^{P}\frac{dp'}{\rho(p')}-\varphi_t+\frac{1}{2}\left|\nabla\varphi\right|^2=0 \tag{4.14}$$

This is nothing else than a familiar form of the Bernoulli's theorem for the unsteady, inviscid and compressible flow (see [59, 60]). Note the obtained expression is completely independent of the pressure-density constitutive relationship $P(\rho)$.
However, the adiabatic reversible case (isentropic transformation) deserves a specific analysis. In this case, since:

$$\frac{u}{\rho}=\frac{P_0}{\rho(k-1)}\left(\frac{P}{P_0}-\frac{\rho}{\rho_0}\right)-\frac{P_0}{\rho}\left(\frac{\rho-\rho_0}{\rho_0}\right)=\frac{1}{k-1}\left(\frac{P}{\rho}-\frac{P_0}{\rho_0}\right)-P_0\left(\frac{1}{\rho_0}+\frac{1}{\rho}\right) \tag{4.15}$$

So then:

$$\frac{p}{\rho}+\frac{1}{2}\left|\nabla\varphi\right|^2+\frac{1}{k-1}\left(\frac{P}{\rho}-\frac{P_0}{\rho_0}\right)-P_0\left(\frac{1}{\rho_0}+\frac{1}{\rho}\right)-\varphi_t=0$$

$$\left(\frac{P}{\rho}-\frac{P_0}{\rho_0}\right)+\frac{1}{2}\left|\nabla\varphi\right|^2+\frac{1}{k-1}\left(\frac{P}{\rho}-\frac{P_0}{\rho_0}\right)-\varphi_t=0$$

Or:

$$\frac{k}{k-1}\left(\frac{P}{\rho}-\frac{P_0}{\rho_0}\right)+\frac{1}{2}\left|\nabla\varphi\right|^2-\varphi_t=0$$

This is in fact, a known form of the Bernoulli's theorem for an unsteady, adiabatic, compressible flow.

4.2.2 Total Pressure Expression

Starting from the last Bernoulli's equation, considering that:

$$P(\rho)=\frac{P_0}{\rho_0^k}\rho^k \tag{4.16}$$

it follows that:

$$\frac{P}{\rho}=\frac{P_0}{\rho_0^k}\rho^{k-1} \tag{4.17}$$

thus:

$$\frac{k}{k-1}\frac{P_0}{\rho_0^k}\rho^{k-1}+\frac{1}{2}\left|\nabla\varphi\right|^2-\varphi_t=\frac{k}{k-1}\left(\frac{P_0}{\rho_0}\right)=\frac{c_0^2}{k-1}$$

or:

$$\frac{c_0^2}{k-1}\frac{\rho^{k-1}}{\rho_0^{k-1}}+\frac{1}{2}\left|\nabla\varphi\right|^2-\varphi_t=\frac{c_0^2}{k-1}$$

Collecting the density of the fluid, one obtain the exact expression for ρ:

$$\rho = \rho_0 \left[1 + \frac{k-1}{c_0^2}\left(\varphi_t - \frac{1}{2}\left|\nabla\varphi\right|^2\right)\right]^{\frac{1}{k-1}} \tag{4.18}$$

And then one can recover the exact pressure using the classic isotropic relationship between pressure and density $P(\rho) = \frac{P_0}{\rho_0^k}\rho^k$:

$$P = P_0 \left[1 + \frac{k-1}{c_0^2}\left(\varphi_t - \frac{1}{2}\left|\nabla\varphi\right|^2\right)\right]^{\frac{k}{k-1}} \tag{4.19}$$

That is the total pressure expression, itself in essence another particular form of the Bernoulli's equation.

4.2.3 Equivalence with the momentum Equation

Applying the gradient operator to the last obtained Bernoulli's equation

$$\int_{P_0}^{P} \frac{dp'}{\rho(p')} - \varphi_t + \frac{1}{2}\left|\nabla\varphi\right|^2 = 0$$

one directly obtains as usual:

$$\frac{1}{\rho}\nabla p + \nabla(\nabla\phi)\cdot\nabla\phi - \nabla\phi_t = 0$$

That with $v = -\nabla\phi$ simply produces:

$$\frac{\partial v}{\partial t} + \nabla v \cdot v = -\frac{1}{\rho}\nabla p$$

4.2.4 Equivalence with the Thompson's Equation

From the equations obtained through the variational approach, a single nonlinear equation can be determined in terms of the velocity potential. Calculating the time derivative and the gradient of $-\frac{\partial u}{\partial \rho} = \lambda_t + \frac{1}{2}\nabla\lambda^2$, one obtains:

$$-\frac{\partial^2 u}{\partial \rho^2}\rho_t = \lambda_{tt} + \nabla\lambda\cdot\nabla\lambda_t$$

$$-\frac{\partial^2 u}{\partial \rho^2}\nabla\rho = \nabla\lambda_t + \frac{1}{2}\nabla(|\nabla\lambda|^2)$$

Multiplying the continuity equation by $\frac{\partial^2 u}{\partial \rho^2}$:

$$\frac{\partial^2 u}{\partial \rho^2}\rho_t + \frac{\partial^2 u}{\partial \rho^2}\nabla\rho\cdot\nabla\lambda + \frac{\partial^2 u}{\partial \rho^2}\rho\nabla^2\lambda = 0$$

It holds:

$$\lambda_{tt} + 2\nabla\lambda\cdot\nabla\lambda_t + \frac{1}{2}\nabla(|\nabla\lambda|^2)\cdot\nabla\lambda - \frac{\partial^2 u}{\partial \rho^2}\rho\nabla^2\lambda = 0$$

Since:

$$\frac{u(\rho)}{\rho} = \int_{\rho_0}^{\rho} \frac{p(\rho')}{\rho'^2} d\rho'$$

follows:

$$\rho \frac{\partial^2 u}{\partial \rho^2} = \frac{\partial p}{\partial \rho}$$

$$\lambda_{tt} + 2\nabla\lambda \cdot \nabla\lambda_t + \frac{1}{2}\nabla(|\nabla\lambda|^2) \cdot \nabla\lambda - \frac{\partial p}{\partial \rho}\nabla^2\lambda = 0$$

Since $v = \nabla\lambda = -\nabla\varphi$ i.e. $\lambda = -\varphi$ and $\frac{\partial p}{\partial \rho} = c^2(\rho)$

$$\varphi_{tt} - c^2(\rho)\nabla^2\varphi - 2\nabla\varphi \cdot \nabla\varphi_t + \frac{1}{2}\nabla\left|\nabla\varphi\right|^2 \cdot \nabla\varphi = 0$$

In the case of the adiabatic transformation $c^2(\rho) = \frac{kp_0}{\rho_0}$ and it reduces to the Thompson's equation.

4.2.5 The Radiation Pressure in Terms of the Lagrangian $\mathcal{L}$

The derivation of the expression for radiation pressure is critical, as the literature presents various methods to determine its form, each based on different assumptions and leading to distinct results. However, in many papers of nonlinear acoustics, the role of the Lagrangian density in the expression of the radiation pressure is reported. It must be noted, however, that none of the pressure expressions obtained above explicitly involve the Lagrangian density.

$$\mathcal{L} = \frac{1}{2}\rho v^2 - u$$

It should be added that this is a natural consequence of the fact that any pressure information originates from Bernoulli's theorem, where the Hamiltonian density $\mathcal{E} = \frac{1}{2}\rho v^2 + u$ of the fluid is involved. This expression represents the total energy, comprising both kinetic and potential energy, rather than the Lagrangian density $\mathcal{L}$, which is defined as the difference between these two forms of energy.

To reconcile the two perspectives, it is demonstrated that when an approximate expression of Bernoulli's theorem is introduced at the second order, the pressure expression incorporates the Lagrangian density. In fact, let's start with the Bernoulli's theorem in the form 4.14, and since at the second order one has that the integral expansion is equal to:

$$\int_{P_0}^{P} \frac{dp'}{\rho(p')} \sim \frac{1}{\rho_0}(P - P_0) - \frac{1}{2\rho_0^2}\frac{d\rho}{dP_0}(P - P_0)^2$$

The approximate Bernoulli's equation follows:

$$-(P - P_0) + \frac{1}{2\rho_0}\frac{d\rho}{dP_0}(P - P_0)^2 + \rho_0\varphi_t - \frac{1}{2}\rho_0|\nabla\varphi|^2 \sim 0$$

$$(P - P_0)^2 - 2\rho_0\frac{dP}{d\rho_0}(P - P_0) + 2\rho_0\frac{dP}{d\rho_0}\left(\rho_0\varphi_t - \frac{1}{2}\rho_0|\nabla\varphi|^2\right) \sim 0$$

Solving the quadratic equation for $P - P_0$:

$$P - P_0 \sim \rho_0 \frac{dP}{d\rho_0} - \sqrt{\left(\rho_0 \frac{dP}{d\rho_0}\right)^2 - 2\rho_0 \frac{dP}{d\rho_0}\varepsilon}, \quad \varepsilon = \rho_0 \varphi_t - \frac{1}{2}\rho_0 |\nabla\varphi|^2$$

For small perturbation ϵ of the flow potential, the Taylor expansion at the second order produces:

$$P - P_0 \sim \epsilon + \frac{1}{2}\rho_0 \frac{d\rho}{dP_0}\epsilon^2$$

Neglecting the terms of the potential of order higher than the second, a simplified expression is produced:

$$P - P_0 \sim \left(\rho_0 \varphi_t - \frac{1}{2}\rho_0 \nabla\varphi^2\right) + \rho_0^2 \frac{d\rho}{dP_0}\varphi_t^2$$

i.e.:

$$P - P_0 \sim \rho_0 \varphi_t - \left(\frac{1}{2}\rho_0 \nabla\varphi^2 - \rho_0^2 \frac{c_0^2}{\phi_t^2}\right)$$

Since:

$$\mathcal{L}_0 \sim \frac{1}{2}\rho_0 \nabla\phi^2 - \rho_0^2 \frac{c_0^2}{\phi_t^2}$$

This formulation is consistent with those found in the literature. Indeed, provided that $p = \rho_0 \phi_t$ is valid up to the second-order quantity, it is possible to rewrite the classic acoustic Lagrangian as the summation of the kinetic and potential energy of the acoustic field.

$$\mathcal{L}_0 \sim \frac{1}{2}\rho_0 \nabla\phi^2 - \frac{p^2}{2\rho_0 c_0^2} = K - U$$

Where p is the acoustic pressure.

$$p = P - P_0 \sim \rho_0 \phi_t - \mathcal{L}_0 \tag{4.20}$$

This is valid in general and independent of the particular constitutive relationship between pressure and density and shows the dependency of the pressure on $\mathcal{L}_0$ and not on $\mathcal{E}$. This shows simply that equation 4.20 in the field of radiation pressure is nothing else than an approximate version of the Bernoulli's theorem.
The Hamilton's principle, however, permits making $\mathcal{L}$ appear in a strict form of the radiation force as shown in the next section.

4.2.6 Radiation Pressure exact expression

Finally, the Hamilton principle produces the equation $v = \nabla\lambda$ i.e. the condition that the flow is a potential one i.e. irrotational. It is not an a priori hypothesis as for the differential approach but a consequence of the assumed form for the Lagrangian. In fact, this last has been assumed as $\frac{1}{2}\rho v^2 - \frac{p(\rho)}{k-1}$ i.e. no dissipation effect, since the Lagrangian is made by only the kinetic and the potential energy (this last associated with conservative forces) without including in it any external work made by non-conservative (viscous) forces.
On the basis of the previous formulas, the total force acting on the body is determined:

$$F_{\text{rad}} = \int_{S_B} (\rho\varphi_t - \mathcal{E}) \cdot n \, dS \tag{4.21}$$

4.3 Analysis of the Boundary Terms

By employing the Hamiltonian approach, several boundary terms have been determined, originating from $\delta A_1, \delta A_2, \delta A_5$, and δA_6, along with the surface terms contained in δA_4. These terms play a significant role in the equations of motion for the body. To ensure that $\delta A = 0$, it is necessary to require that the aforementioned boundary terms vanish.
Therefore, the following equation must hold:

$$\begin{aligned}\int_{t_1}^{t_2}\left[\delta u_G \cdot \int_{S_B} \tilde{\mathcal{L}}(\rho, v, \lambda) n \, dS\right] dt + \int_{t_1}^{t_2} -\frac{d(m v_g)}{dt} \cdot \delta u_g \, dt + [m v_g \cdot \delta u_g]_{t_1}^{t_2} \\ + \int_{t_1}^{t_2}\left[\delta\theta \cdot \int_{S_B} \tilde{\mathcal{L}}(\rho, v, \lambda)(r \times \xi) n \, dS\right] dt + \int_{t_1}^{t_2} -\frac{d(J\dot{\theta})}{dt} \cdot \delta\theta \, dt + \left[J\dot{\theta} \cdot \delta\theta\right]_{t_1}^{t_2} \\ + \int_{t_1}^{t_2}\left[\int_{S_B} (\lambda\rho\delta v + \lambda v \delta\rho) \cdot n \, dS\right] + F \cdot \delta x_F + T\delta\theta dt = 0\end{aligned} \tag{4.22}$$

i.e. considering only the terms responsible for the body force (i.e. not including those terms containing $\delta\theta$) and substituting $\lambda = -\varphi$ one gets:

$$\begin{aligned}\int_{t_1}^{t_2}\left[\delta u_G \cdot \int_{S_B} \tilde{\mathcal{L}}(\rho, v, \varphi) n \, dS\right] dt + \int_{t_1}^{t_2} -\frac{d(m v_g)}{dt} \cdot \delta u_g \, dt + [m v_g \cdot \delta u_g]_{t_1}^{t_2} \\ - \int_{t_1}^{t_2}\left[\int_{S_B} (\varphi\rho\delta v + \varphi v \delta\rho) \cdot n \, dS\right] + F \cdot \delta x_F dt = 0\end{aligned} \tag{4.23}$$

4.3.1 Expression of the Radiation Force via Hamilton's Principle

The surface boundary term is:

$$-\int_{t_1}^{t_2}\left[\int_{S_B} (\varphi\rho\delta v + \varphi v \delta\rho) \cdot n \, dS\right] = 0 \tag{4.24}$$

The part of the integral associated with $\varphi v \delta\rho \cdot n$ must vanish by itself since there are no other terms at the boundary that contain $\delta\rho$. The term associated with $\varphi\rho\delta v \cdot n$ can indeed be grouped with the terms containing δu_G after suitable considerations.
Let us examine two different cases:

- The body is fixed;
- The body moves under the field pressure force and other external forces.

Body at Rest

In this case, the boundary equation simplifies as:

$$\int_{t_1}^{t_2}\left[\int_{S_B} (\varphi\rho\delta v + \varphi v \delta\rho) \cdot n \, dS\right] = 0 \tag{4.25}$$

Since $\delta\times_F = 0$ and $\delta\times_G = 0$. Therefore, it must be guaranteed that:

$$\varphi\rho\delta v \cdot n = 0, \quad \varphi v \delta\rho \cdot n = 0 \tag{4.26}$$

This implies two alternative possibilities for the first equation in 4.26:

$$\varphi = 0 \quad \text{or} \quad \delta v \cdot n = 0$$

Besides the chance of $\rho = 0$ which is not meaningful under the physical point of view. The alternatives for the second one in 4.26 indeed are:

$$\varphi = 0 \quad \text{or} \quad v \cdot n = 0 \quad \text{or} \quad \delta\rho = 0$$

Let us analyze these alternative boundary conditions. Imposing that the body boundary surface is an equipotential surface $\varphi = 0$ that would permit both the integral terms to vanish simultaneously means that the gradient of the potential along the tangent directions on the body surface vanishes, i.e. $\frac{\partial\varphi}{\partial\tau} = 0$. This, in turn, means that the tangent velocity of the fluid vanishes at the body, i.e. the fluid does not slip along the body surface. This condition is physically not consistent with the hypothesis of an inviscid body since only tangent viscous stress can prevent the fluid from slipping on the body surface. Therefore, for a body at rest, this alternative does not hold.
The condition $v \cdot n = 0$ and its consequence $\delta v \cdot n = 0$ is indeed a plausible boundary condition since it represents the body surface as impermeable to the fluid and is a classical boundary condition for a body at rest in the fluid. This condition makes both integral terms vanish simultaneously.
A final remark concerns the possible boundary condition $\delta\rho = 0$, which implies that the value of the density is prescribed at the surface of the body. For example, $p = p_0$ at the body surface is the case of a bubble of gas in a liquid fluid and p_0 is the internal pressure of the bubble. In this case, prescribing $p = p_0$ is equivalent to prescribing $\rho = \rho_0$ at the liquid interface, and one of the boundary terms vanishes. However, this case is outside the limit of our investigation and deals with a two-phase fluid for which the kinetic and potential energy of the bubble have completely different expressions with respect to the rigid body.
Therefore, the only mathematical conclusion that makes sense to the physical problem with the body at rest is $v \cdot n = 0$.

Moving Body

Following the previous hints about the boundary conditions at the body surface, let us include even in the case of a moving body the impermeability condition at the boundary. This would mean at the body surface the fluid velocity v can be decomposed into the relative velocity w_τ of the fluid particles with respect to the body purely tangent to its surface S_B since the impermeability condition compels the particles to slide along the body surface and the velocity $v_B = \dot{u_G} + \dot{\theta} r \times \xi = \dot{u_G} + \omega \times \xi$ of the body surface i.e. $v = w_\tau + v_B = v_{B_n} n + (v_{B_\tau} + w_\tau)\tau$ such that:

$$-\int_{t_1}^{t_2} \left[\int_{S_B} (\varphi\rho\delta(w_\tau + v_B) + \varphi(w_\tau + v_B)\delta\rho) \cdot n \, dS \right] dt$$

Since by definition $w_\tau \cdot n = 0$ and $\delta w_\tau \cdot n = 0$, one obtains:

$$-\int_{t_1}^{t_2}\left[\int_{S_B}(\varphi\rho\delta v_B + \varphi v_B\delta\rho)\cdot n\,dS\right]dt$$

$$-\int_{t_1}^{t_2}\left[\int_{S_B}(\varphi\rho n)\cdot\frac{d}{dt}\delta u_G + (\varphi\rho r\times\xi\cdot n)\cdot\frac{d}{dt}\delta\theta + \varphi v_B\cdot n\delta\rho\,dS\right]dt$$

Integration by parts produces (boundary time conditions are not explicitly written):

$$\int_{t_1}^{t_2}\left[\int_{S_B}\frac{d}{dt}(\varphi\rho n\cdot\delta u_G) + \frac{d}{dt}(\varphi\rho r\times\xi\cdot n)\cdot\delta\theta - \varphi v_B\cdot n\delta\rho\,dS\right]dt$$

Let us consider the first and the third term into the integral, again the only ones involved into the body force calculation (the second term is related instead to the moment of the force):

$$\int_{t_1}^{t_2}\left[\int_{S_B}\frac{d}{dt}(\varphi\rho n\cdot\delta u_G) - \varphi v_B\cdot n\delta\rho\,dS\right]dt$$

Therefore, the condition for the boundary terms to vanish is the first term is joined to the other ones containing δu_G, the second must vanish by itself since there are no other terms containing $\delta\rho$ i.e.:

$$\varphi v_B\cdot n = 0$$

Except for the special case $v_B\cdot n = 0$ that is the purely spinning sphere, in general, the term $\varphi v_B\cdot n$ to vanish must require that $\varphi = 0$ on the surface of the body. This would mean that it is spatially invariant over the body surface i.e. its tangent derivative vanishes, that is

$$\nabla\varphi\cdot\tau = -v_{B_\tau} - w_\tau = 0 \quad\rightarrow\quad w_\tau = -v_{B_\tau}$$

This implies the particles do slide along the body surface consistently with the in-viscid fluid hypothesis. As a consequence, the absolute particles speed at the body surface is purely normal in fact:

$$v = (w_\tau + v_{B_\tau})\tau + v_{B_n}n = v_{B_n}n$$

Therefore:

$$\frac{\partial\varphi}{\partial n} = -v_{B_n}$$

That is the usual impermeability condition for a moving body in a fluid, and the integral simplifies as:

$$\int_{t_1}^{t_2}\left[\int_{S_B}\frac{d}{dt}(\varphi\rho n)\cdot\delta u_G\,dS\right]dt$$

To properly express $\frac{d}{dt}(\varphi\rho n)$, it is essential to consider that the normal vector n at a given point P on the body surface varies over time due to the rotation of the body. Therefore:

$$\frac{d}{dt}(\varphi\rho n) = \frac{\partial}{\partial t}(\varphi\rho)\cdot n + \varphi\rho(\omega\times n) + \nabla(\varphi\rho n)\cdot v$$

obtained using the Poisson's formula $\frac{dn}{dt} = \omega\times n$. Moreover:

$$\nabla(\varphi\rho n)\cdot v = \rho\frac{\partial\varphi}{\partial x_j}n_iv_j + \varphi\frac{\partial\rho}{\partial x_j}n_iv_j + \rho\varphi\frac{\partial n_i}{\partial x_j}v_j = \rho(\nabla\varphi\cdot v)n + \varphi(\nabla\rho\cdot v)n + \varphi\rho(\nabla n\cdot v)$$

i.e.:

$$\int_{t_1}^{t_2} \left[\int_{S_B} (\lambda \rho \delta v + \lambda v \delta \rho) \cdot n \, dS \right] dt =$$

$$\int_{t_1}^{t_2} \left[\delta u_G \cdot \int_{S_B} (\rho \varphi_t + \varphi \rho_t - \rho v \cdot v + \varphi \nabla \rho \cdot v) \, n + \varphi \rho \, (\nabla n \cdot v) + \varphi \rho (\omega \times n) \, dS \right] dt$$

However, the boundary condition examined before requires $\varphi = 0$ along the body surface. Therefore, the integral simplifies as:

$$\int_{t_1}^{t_2} \left[\int_{S_B} (\lambda \rho \delta v + \lambda v \delta \rho) \cdot n \, dS \right] dt = \int_{t_1}^{t_2} \left[\delta u_G \cdot \int_{S_B} (\rho \varphi_t - \rho v \cdot v) \, n \, dS \right] dt$$

Collecting all the boundary terms that exhibit δu_G:

$$\int_{t_1}^{t_2} \delta u_G \cdot \left[\int_{S_B} (\mathcal{L} + \rho \varphi_t - \rho v \cdot v) \, n \, dS - \frac{d}{dt}(m v_G) + F \right] dt = 0$$

That permits us to conclude the analysis with:

$$F_{\text{rad}} = \int_{S_B} (\mathcal{L} + \rho \varphi_t - \rho v \cdot v) \, n \, dS$$

Or equivalently since $\mathcal{L} - \rho v \cdot v = -\mathcal{E}$:

$$F_{\text{rad}} = \int_{S_B(t)} (\rho \varphi_t - \mathcal{E}) \, n \, dS$$

That is perfectly consistent with the same form examined in the previous section. The second-order approximation of the integrand, as shown in the previous subsection 4.2.5, produces:

$$F_{\text{rad}} = \int_{S_B} (\rho_0 \varphi_t - \mathcal{L}_0) \, n \, dS$$

That reminds some results obtained in the literature.

4.4 Radiation Pressure Derived by the Momentum Conservation

Let us examine separately a reasoning that is considered in many papers in the literature and is at the basis of several statements about radiation pressure. It is interesting to clarify some of the debates about the momentum flux arguments, frequently appearing when dealing with the calculation of the radiation pressure.

Let us apply the momentum Q conservation to the fluid volume $V(t)$:

$$\dot{Q} = \frac{d}{dt} \int_{V(t)} \rho v dV$$

Now, a different definition of the volume with respect to the one considered in the Hamiltonian approach is presented: V is the volume trapped by S_B, the body surface, as in the Hamiltonian

approach, but the wrapping surface S is indeed now considered unmovable. The integral over S to express the force acting on the body has been used, in fact $F = \dot{Q}$:

$$-\int_{S_B} p \cdot n \, dS - \int_S p \cdot n \, dS = \frac{d}{dt} \int_{V(t)} \rho v \, dV$$

$$-F_{\text{rad}} - \int_{S_B} p \cdot n \, dS = \int_{V(t)} \frac{\partial}{\partial t}(\rho v) dV + \int_S (\rho v) v \cdot n D v + \int_{S_B} \rho v (v - v_B) \cdot n dS$$

And since $v_B \cdot n = v \cdot n$, the momentum flux through the body surface clearly vanishes:

$$F_{\text{rad}} = -\int_{V(t)} \frac{\partial}{\partial t}(\rho v) \, dV - \int_S p \cdot n + \rho v \otimes v \cdot n \, dS$$

Let us consider now the special case of a periodic time evolution of all the physical quantities. This is the important case of a harmonic source present as excitation in the field. Because of nonlinearities, several harmonic components emerge generating a periodic response of the acoustic field of period T. In order to evaluate the time average of the quantities involved in the previous equation, the integral form over which the average is calculated is:

$$\langle F_{\text{rad}} \rangle = -\langle \int_{V(t)} \frac{\partial}{\partial t}(\rho v) \, dV \rangle - \langle \int_S p \cdot n + \rho v \otimes v \cdot n \, dS \rangle$$

$$\langle G \rangle = \frac{1}{T} \int_t^{t+T} G(\tau) \, d\tau$$

$\langle G \rangle$ is still a function of time, the average producing the smoothing of the fast fluctuation within the period T. Consider that $\int_{V(t)} \frac{\partial}{\partial t}(\rho \mathbf{v}) \, dV$ is calculated over a time varying volume $V(t)$. Its variations are because of the motion of the body that modifies S_B. The motion of the body decomposes into a fluctuating motion superimposed to a slow drift effect. One may assume that along the period T the effect of the drift is negligible. Moreover, if the volume V is large enough, the volume fluctuations due to the body motion are negligible too, leading to conclude the volume $V(\tau) \sim V(t)$ for $\tau \in [t, t+T]$.

$$\langle F_{\text{rad}} \rangle = -\int_{V(t)} \langle \frac{\partial}{\partial t}(\rho v) \rangle \, dV - \int_S \langle p \cdot n + \rho v \otimes v \cdot n \rangle \, dS$$

Where because of the periodicity of the acoustic field:

$$\langle \frac{\partial}{\partial t}(\rho v) \rangle = \rho v_{t+T} - \rho v_t = 0$$

That permits to state the final formula:

$$\langle F_{\text{rad}} \rangle = -\int_S \langle p \cdot n + \rho v \otimes v \cdot n \rangle \, dS \tag{4.27}$$

That with slightly different details (and sometimes obscure points) in its derivations is one of the most credited formulas for the radiation pressure calculation (for example in [10,25,61–63]).

4.5 Critical Analysis between the Two Expressions for Radiation Pressure

Hamiltonian principle has been used to derive the force acting on a moving body immersed into an inviscid compressible fluid without approximations. The aim of the present section is a critical comparison between the exact expression obtained here:

$$F_{\text{rad}} = \int_{S_B(t)} (\rho\varphi_t - E)\, n\, dS$$

and the ones frequently proposed in the literature:

$$F_{\text{rad}} = -\int_S (p \cdot n + \rho v \otimes v \cdot n)\, dS \tag{4.28}$$

The equation 4.28, although it calculates the total force on the body, does not express the integral over the body surface S_B but over another separated and independent surface S (somehow arbitrary and vague). This choice is singular and strange since, as shown before, it is possible to calculate the pressure integral over the body surface, and it follows directly using the pressure expression coming from Bernoulli's theorem and its approximated form. Moreover, it is simply shown in the next points that this choice leads to avoidable complications and some misleading interpretations of the acoustic stress tensor.

It is just the case to emphasize that 4.28 is not useful in the limit $S \to S_B$ because in this case:

$$\int_{S \to S_B} \langle p \cdot n + \rho v \otimes v \cdot n \rangle\, dS = \int_{S_B} \langle p \cdot n \rangle\, dS$$

and the momentum flux across the body surface vanishes, and equation 4.28 becomes useless and trivial and gives back the obvious equation:

$$\langle F_{\text{rad}} \rangle = -\int_S \langle p \cdot n \rangle\, dS$$

Note that only by invoking the Bernoulli equation for the pressure, the previous equation becomes useful:

$$p = \rho\varphi_t - E$$

$$F_{\text{rad}} = -\int_S (\rho\varphi_t - E) \cdot n + \rho(v \otimes v) \cdot n\, dS$$

Where now, comparing it with the form of the radiation force previously determined, it appears that:

- The extra term $\rho v \otimes v$ is an unmotivated complication just coming from the geek choice of considering another surface S instead of S_B the body surface to make the integral.
- The result of the last equation is valid only using time average, while the equation:

$$F_{\text{rad}} = \int_{S_B(t)} (\rho\varphi_t - E)\, n\, dS$$

is valid in general and, of course, also after time averaging.

- The equation is, in fact, an approximation since the exact equation provides:

$$\langle F_{\text{rad}} \rangle = -\langle \int_{V(t)} \frac{\partial}{\partial t}(\rho v)\, dV \rangle - \langle \int_S p \cdot n + \rho v \otimes v \cdot n\, dS \rangle$$

and one needs approximations to neglect the term $\langle \int_{V(t)} \frac{\partial}{\partial t}(\rho v)\, dV \ \rangle$.
- The existence of an acoustic stress tensor is inferred by the equation:

$$\langle F_{\text{rad}} \rangle = -\int_S \langle p \cdot n + \rho v \otimes v \cdot n \rangle\, dS$$

that claims for the following acoustic stress tensor expression:

$$\langle \sigma_{\text{rad}} \rangle = -\langle p \cdot I + \rho v \otimes v \rangle$$

Although the quantity $\langle \sigma_{\text{rad}} \rangle$ is defined along the surface S, the tensor part $\rho v \otimes v$ does not generate purely normal stress to the surface but leads also to tangent stress component. However, it is perfectly clear from the previous analysis this has nothing to do with physical tangent stresses arising on the surface S or S_B. Along this surface, by the physical hypotheses made about the inviscid fluid, only normal stress pressure exists. In fact, this expression of the radiation force comes from the balance:

$$-\int_{S_B} p \cdot n\, dS - \int_S p \cdot n\, dS = \frac{d}{dt} \int_{V(t)} \rho v\, dV$$

That is, the forces over the two considered surfaces are $\int_{S_B} p \cdot n\, dS$ and $\int_S p \cdot n\, dS$ respectively, meaning the surface forces are only due to the normal pressure without any tangent stress. It is the volume term $\frac{d}{dt} \int_{V(t)} \rho v\, dV$ that is the rate of the fluid volume momentum that by using a mathematical manipulation produces for its calculation the momentum flux. Therefore, the momentum flux term integrated over the surface S is only a mathematical way to calculate a volume effect, nothing to do with the surface local force transmitted to the fluid through S_B or S.
In this sense, the choice to express the radiation force through

$$\langle F_{\text{rad}} \rangle = -\int_S \langle p \cdot n + \rho v \otimes v \cdot n \rangle\, dS$$

This approach is neither useful nor accurate, particularly when attempting to introduce the acoustic stress tensor σ_{rad} as a local quantity. Its purpose is solely to function under surface integration to mathematically represent a volume effect.

Chapter 5

Finite Difference Solutions and Results

To begin with, the main challenge is trying to solve highly complicated partial differential equations like:

$$\varphi_{tt} - c^2(\rho)\nabla^2\varphi - 2\nabla\varphi \cdot \nabla\varphi_t + \frac{1}{2}\nabla\left|\nabla\varphi\right|^2 \cdot \nabla\varphi = 0 \tag{5.1}$$

In this case, aside from the choice between one model and another, the equation of interest is highly complex and typically does not have an analytical solution, often requiring approximate methods. As a result, there arises a need to use numerical tools to simulate the solution.
In this specific domain, i.e., computational fluid dynamics (CFD), there are numerous numerical methods available for solving such highly non-linear partial differential equations (PDEs). In particular, in CFD analysis, the classification of a PDE is crucial for selecting the most efficient numerical scheme, which depends on the associated quadratic form. Starting form the definition of a linear PDE in the general form, one gets:

$$A(x,t)\varphi_{xx} + 2B(x,t)\varphi_{xt} + C(x,t)\varphi_{tt} + D(x,t)\varphi_x + E(x,t)\varphi_y + F(x,t)\varphi + G(x,t) = 0$$

Specifically, a PDE could be elliptic, parabolic or hyperbolic depending on the value of the discriminant ($\Delta = B^2 - 4AC$). Indeed:

- if $\Delta < 0$, the PDE is elliptic;
- if $\Delta = 0$, the PDE is parabolic;
- if $\Delta > 0$, the PDE is hyperbolic.

In this case, the PDE is not linear, so it is impossible to get the value for $A(x,t)$, $B(x,t)$ or $C(x,t)$. Hence, the necessity of using a different approach based on characteristic's line to find the nature of the equation arises. In order to accomplish this task, it is necessary to reduce a second order equation 5.1 into a so called 'Conservative System' of a first order ones.

5.1 Conservative Laws

The central postulate, leading to the formulation of conservation laws, is one of balance in a physical system. The postulate states that the production of an entity, e.g., mass, energy, or charge, in a closed volume is exactly balanced by the flux of the entity across the boundary of the volume. In other words, an entity in a volume can only increase if more of it flows into the volume than what leaves.

Whereas the derivation of physical models based on conservation principles arises naturally, solving the resulting models, using either computational or mathematical means, remains a substantial challenge and an active area of research with numerous open questions. On the mathematical side, many fundamental questions of existence and uniqueness of the solutions remain open once the minimum of the spatial dimension and the size of the system exceeds one. In other words, scalar problems in multiple dimensions and nonlinear systems in one dimension are reasonably well understood, but many fundamental properties of systems in more than one spatial dimension remain poorly understood. Unfortunately, this latter case is exactly the most relevant for applications across science and engineering. Without a rigorous mathematical understanding of the fundamental conservation laws, there are limits to the achievable rigor when one seeks to develop numerical solution techniques. Nevertheless, the last four decades have witnessed tremendous progress in the development and analysis of computational techniques for the solution of complex systems of conservation laws and the success of these models is unquestioned. A central goal of this text is to offer the reader an overview of many of these developments, supported by some analysis of the algorithms and accompanied with insights into the implementation of these algorithms.

Conservation is a fundamental principle applied to model the physical world, stretching across quantum mechanics, continuum mechanics, and gravitational physics, with prominent examples including the Euler equations of gas dynamics, Navier's equations of elasticity, Maxwell's equations of electromagnetics, and Einstein's equations of gravitation [64]. It is therefore no surprise that the mathematical analysis of conservation laws is a deep research area with contributions stretching back to Leibniz. The evelopment of efficient and accurate computational methods to solve such problems have occupied scientific pioneers such a von Neumann, Lax, and Lions. Unfortunately, despite the apparent simplicity of the problem, a closer examination reveals significant challenges when attempting to understand the basic conservation law and the nature of its solutions.

Actually, conservation laws are time-dependent laws of partial differential equations (usually non-linear) with a relatively simple mathematical structure. In one dimensional case, the general equation takes the form:

$$\frac{\partial u(x,t)}{\partial t} + \frac{\partial}{\partial x} f(u(x,t)) = 0 \tag{5.2}$$

where u is a scalar unknown and $f(u(x,t))$ is the flux of the state variable. Equation 5.2 can

be easily extended to three dimensions, without loss of generality, obtaining:

$$\frac{\partial U(x,t)}{\partial t} + \nabla F(U(x,t)) = 0 \tag{5.3}$$

In this case, U and $F(U(x,t))$ are vectors. At this point, the Jacobian of flow function, J, is introduced:

$$J = \frac{\partial F(U)}{\partial U} = \frac{\partial f_i}{\partial u_j} = A(U)$$

It is evident that conservative systems can be written in almost linear form using the formula for calculating the derivative of a compound function:

$$\frac{\partial F(U)}{\partial x} = \frac{\partial F(U)}{\partial U}\frac{\partial U}{\partial x} = A(U)U_x$$

Leading to a quasi-linear system of equations written as:

$$U_t + A(U)U_x = 0 \tag{5.4}$$

Therefore, these seemingly complex differential systems can be easily traced back to a greatly simplified form, the solution of which is far easier and more immediate with respect to a second order non-linear PDE, which usually needs complicated time integration algorithm, as Runge-Kutta 4^{th} order method, to get stability and sufficient accuracy on the results [56].
Typically the flux functions are non-linear functions of u, leading to non-linear systems of partial differential equations ($PDEs$). In general it is not possible to derive exact solutions to these equations, and hence the need to devise and study numerical methods for their approximate solution. Of course the same is true more generally for any non-linear PDE and, to some extent, the general theory of numerical methods for non-linear $PDEs$ applies in particular to systems of conservation laws.
Regardless, there are several reasons for studying this particular class of system instead of solving directly 5.1:

- Many practical problems in science and engineering involve conserved quantities and lead to $PDEs$ of this class;
- Difficulties associated with solving these systems (as in case of shock formation or any other spontaneous source or formation of discontinuity in the solution) that are not seen elsewhere and must be dealt with carefully in developing numerical methods;
- Loss of reversibility along the characteristic lines due to the intersection of them at the discontinuity;
- Inadequacy of the differential form of the conservation law due to loss of smoothness and loss of classic solutions;
- Preservation of conservation properties.

- Development of several numerical schemes and solution using conservation laws were developed in the last decades with good results [65].

So one of the goal of this project is to find a direct and rigorus approach to find the associated conservation form to 5.1. There are relatively few works on that [66] and it is still a rather challenging task to perform this kind of reduction form a highly-non-linear-second-order partial differential equation, into a relatively simple quasi-linear first order conservative scheme.

5.1.1 First Order Reduction

At this point, the main goal is to write a system of first order PDE written in the well-known conservative form:

$$\frac{\partial U}{\partial t} + \frac{\partial F(U)}{\partial x} = 0$$

With this intention, this change of variable has been made by using the relationships derived from the Hamiltonian's analysis:

$$\begin{cases} \varphi_x = -u \\ \varphi_t = \frac{1}{2}u^2 + \frac{k}{k-1}\left(\frac{P_0^{\frac{1}{k}}}{\rho_0}P^{\frac{k-1}{k}} - \frac{P_0}{\rho_0}\right) \end{cases} \tag{5.5}$$

Then, let's substitute these equations into equation 5.1,together with the Schwartz Theorem condition $\varphi_{xt} = \varphi_{tx}$ (valid for smooth solutions), to obtain the first order reduction. In this treatment, it was decided to keep the speed of sound constant and only the one dimensional case is considered. In so doing, the new reference equation is:

$$\varphi_{tt} - \varphi_{xx}(c_0^2 - \varphi_x^2) - 2\varphi_x\varphi_{xt} = 0 \tag{5.6}$$

and the substitution of 5.5 produces:

$$\begin{cases} \left(\frac{1}{2}u^2 + \frac{k}{k-1}\left(\frac{P_0^{\frac{1}{k}}}{\rho_0}P^{\frac{k-1}{k}} - \frac{P_0}{\rho_0}\right)\right)_t = -u_x(c_0^2 - u^2) + 2uu_t \\ u_t = -\left(\frac{1}{2}u^2 + \frac{k}{k-1}\left(\frac{P_0^{\frac{1}{k}}}{\rho_0}P^{\frac{k-1}{k}} - \frac{P_0}{\rho_0}\right)\right)_x \end{cases} \tag{5.7}$$

Where the subscripts xt mean respectively the space and time derivative.
To write down the system in a conservative form all the time derivatives must be on the left-hand side of the equation while the space derivatives must be on the right-hand side. Knowing that:

$$\frac{\partial u^2}{\partial t} = 2uu_t$$

And

$$u_x(c_0^2 - u^2) = \left(\frac{u^3}{3} - c_0^2 u\right)_x$$

One can write the system as:

$$\begin{cases} \left(-\frac{1}{2}u^2 + \frac{k}{k-1}\left(\frac{P_0^{\frac{1}{k}}}{\rho_0}P^{\frac{k-1}{k}} - \frac{P_0}{\rho_0}\right)\right)_t - \left(\frac{u^3}{3} - c_0^2 u\right)_x = 0 \\ u_t + \left(\frac{1}{2}u^2 + \frac{k}{k-1}\left(\frac{P_0^{\frac{1}{k}}}{\rho_0}P^{\frac{k-1}{k}} - \frac{P_0}{\rho_0}\right)\right)_x = 0 \end{cases} \tag{5.8}$$

The last step is to have only two variables the system must depend on, so let's make a change of variable in the first equation. I call "fake pressure" the quantity:

$$\tilde{p} = -\frac{1}{2}u^2 + \frac{k}{k-1}\left(\frac{P_0^{\frac{1}{k}}}{\rho_0}P^{\frac{k-1}{k}} - \frac{P_0}{\rho_0}\right) = -\frac{1}{2}u^2 + \frac{c_0^2}{k-1}\left(\left(\frac{P}{P_0}\right)^{\frac{k-1}{k}} - 1\right) = \varphi_t - u^2 \tag{5.9}$$

By substituting the expression for $\tilde{p}$ and performing some straightforward mathematical manipulations, the final system in terms of the two variables u and $\tilde{p}$ is obtained. This results in a system that is significantly simpler to implement and solve numerically:

$$\begin{cases} \tilde{p}_t + \left(c_0^2 u - \frac{u^3}{3}\right)_x = 0 \\ u_t + \left(\tilde{p} + u^2\right)_x = 0 \end{cases} \tag{5.10}$$

If the conservative form is used the U and $F(U)$ vectors are:

$$U = \begin{pmatrix} \tilde{p} \\ u \end{pmatrix}, F(U) = \begin{pmatrix} c_0^2 u - \frac{u^3}{3} \\ \tilde{p} + u^2 \end{pmatrix}$$

The system 5.10 is a novelty in literature since a new formula for the time derivative of the potential has been used to reduce the system. Indeed, in [66–68] there is such as reduction for similar equations, e.g. Lighthill equation, Blackstock–Crighton equation and the inviscid Kutsetsov equation, but using a different relation for φ_t such as:

$$\varphi_t = \frac{(1-\rho)}{\varepsilon}$$

that is completely different than in our case and it does not consider second order quantities.

5.1.2 Evaluation of Eigenvalues of the System

One of the key notions underlying the behavior of the solutions of 5.10 is the concept of *hyperbolicity*. For scalar equations, the notion of hyperbolicity referred to the property of finite speed of propagation. Such a notion will hold true for a system.

Hyperbolic system The linear system 5.4 is hyperbolic if the matrix $A(U)$ is diagonalizable and has m real eigenvalues (with m the dimension of the matrix $A(U)$) for all U, t. The system is termed strictly hyperbolic if the eigenvalues are distinct.

$$\lambda_1 \leq \lambda_2 \leq \cdots \leq \lambda_i$$

This definition can be extended to the nonlinear case 5.2 if the flux f is at least C^1 in U. A system is hyperbolic if for any state U in the range of f, the Jacobian matrix $\nabla_U f$ is diagonalizable in $\mathbb{R}$.
In this case, it is possible to reduce the nonlinear system into a quasi-linear system as 5.4, indeed:

$$\nabla F(U) = \begin{pmatrix} c_0^2 u - \frac{u^3}{3} \\ \tilde{p} + u^2 \end{pmatrix}_x = \begin{pmatrix} 0 & c_0^2 - u^2 \\ 1 & 2u \end{pmatrix} \begin{pmatrix} \tilde{p} \\ u \end{pmatrix}_x = A(U)U_x \tag{5.11}$$

In this case, it can be shown that the hyperbolicity is guaranteed as long as the particle velocity is less than the characteristic speed of sound of the medium, often denoted by c_0.
Indeed, performing some linear algebra calculations, one gets:

$$\lambda_i = det\left[A(U) - \lambda \mathit{I}\right] = \begin{vmatrix} -\lambda & c_0^2 - u^2 \\ 1 & 2u - \lambda \end{vmatrix} = \lambda^2 - 2u\lambda + u^2 - c_0^2 = 0$$

That has the solution equal to:

$$\lambda_{1,2} = u \pm \sqrt{u^2 - u^2 + c_0^2} = u \pm c_0$$

This represents the characteristic wave directions associated with each characteristic velocity, λ_i. This result indeed demonstrates the hyperbolic nature of this system of equations, which is consistent with what one would expect from a wave equation system, even in the presence of nonlinearities.

5.2 Finite Difference Method: A Brief Overview

With a general understanding of the key properties that numerical methods for conservation laws must possess, it is now turn to a more detailed discussion of a specific class of methods, known as finite difference methods. These methods are arguably the first family of approaches proposed to solve differential equations, dating back to von Neumann (1903–1957) and even predating the introduction of the digital computer. In fact, the basic principles behind finite difference approximations were known to Euler (1707–1783), and the first analysis of finite difference methods for initial value problems was presented in the seminal paper by Courant, Friedrichs, and Lewy (1928), where the CFL condition was introduced [69].
The foundation of a finite difference scheme lies in the use of finite difference approximations of derivatives in both space and time. The development and analysis of such schemes is a classic topic in numerical analysis, and it shall not be attempted to cover it exhaustively here.
Hyperbolic partial differential equations ($PDEs$) are typically solved using either the Finite Difference Method (FD) or the Finite Volume Method (FV). The FD method is the most straightforward approach for discretizing partial differential equations. In essence, each point in space where the continuous representation of the equations is considered is replaced with

a set of discrete equations, known as finite-difference equations. The FD method is usually defined on a regular, fixed grid, which allows for highly efficient solution methods.
Although newer techniques such as the Finite Difference Time Domain ($FDTD$) method have been developed in recent decades [70], FD methods are not commonly used for irregular evaluation domains but are more frequently applied to rectangular or block-shaped models. Despite some applications involving moving boundaries and complex geometries, the FV method is generally preferred by experts in computational fluid dynamics (CFD) [71].
As the complexity of the equation, boundary conditions, and problem geometry increases, the FV method becomes more suitable for simulation, particularly due to its natural ability to discretize complex domains using irregular cells. This makes it more accurate for domains with complicated shapes, especially in the presence of curved geometries. However, it is more time-consuming and complex to implement compared to the classic FD method.
In simple cases such as one-dimensional problems or square and rectangular domains—the two methods yield similar results. Thus, the FD method is chosen as the first approach to the numerical solution of our problem due to its simplicity. The Finite Difference method approximates partial differential equations ($PDEs$) by using finite difference formulas at evenly spaced grid points. This approach allows the transformation of a PDE into a system of algebraic equations, which is relatively easier to solve compared to the original form. In order to solve any type of differential equation, it is essential to discretize the solution at each point within the domain. In this case, the domain is a plane grid $[x, t]$, where x represents the physical domain and t represents the time domain. In the FD method, the solution is calculated exactly at the grid points (or nodes) (x_i, t_j) within the domain, specifically:

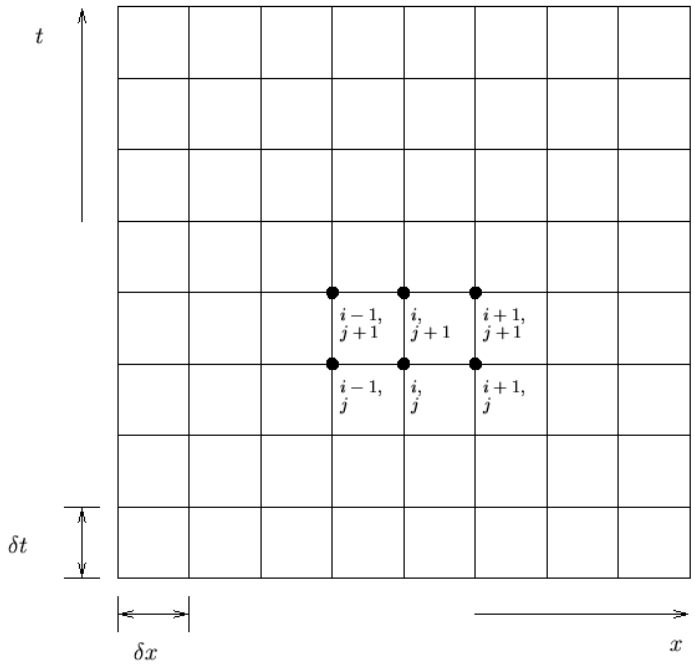

Figure 5.1. Numerical Grid

$$x_i = ih,\ t_j = jk$$

where $\delta x = h$ is the space interval and $\delta t = k$ is the time step. In adaptive mesh cases, both h and k could vary to achieve better results for more complex geometry.
The strategy of the finite difference method, is to calculate the point values assumed by the solution of the differential problem in each node of the computational domain. Specifically, the value of the generic approximate solution u in the node x_i at time t_j is represented by the notation:

$$U_i^j = u(x_i, t_j)$$

Time and space derivatives in the partial differential equation are approximated using the finite difference formulas. There are several ways to approximate the derivative depending on the direction and on the order of the derivative, here there are two of the most used schemes for time and space derivatives:

$$FT(Forward - Time) = \frac{\partial u(x_i, t_j)}{\partial t} \simeq \frac{u(x_i, t_{j+1}) - u(x_i, t_j)}{k} = \frac{U_i^{j+1} - U_i^j}{k} + O(\delta t)$$

$$CS(Centred - Space) = \frac{\partial u(x_i, t_j)}{\partial x} \simeq \frac{u(x_{i+1}, t_j) - u(x_{i-1}, t_j)}{2h} = \frac{U_{i+1}^j - U_{i-1}^j}{2h} + O(\delta h^2)$$

Where the $O(\delta h^2)$ and $O(\delta t)$ represent the order of the truncation error, so the accuracy of the numerical scheme towards the exact solution.

Courant Number

A very important parameter in FD simulations, is the so called *Courant Number*. It is the ratio between the time and space grid size times the characteristic speed of the PDE equation. It represents numerically the speed of the 'numerical solution' with respect to the 'actual solution'. Indeed, numerical methods inevitably introduce some undesired effects, specifically diffusion and dispersion [55,72], and the Courant Number is an important parameter in this sense. The closer the Courant Number is to 1, the best the approximated solution is, but it can easily lead to instability. Such that choice hihgly depends on the non-linearity in the equation/system to be solved.
The *Courant-Friedrichs-Levy* (CFL) condition is one of the most used one to determine the maximum value of the Courant number for linear cases, unfortunately there is no a general theory for non-linear equations [55, 64, 65, 73, 74]. The CFL condition that is used for most numerical schemes is:

$$0 < c = \frac{c_0 k}{h} < 1 \tag{5.12}$$

However, condition in 5.12 could vary depending on the FD scheme used to solve the equation.

5.2.1 First and Second Order-Numerical Schemes

Depending on whether the truncation error of the finite difference approximation is proportional to the first or second power of the grid spacing k or h, one may get significant issues and differences in the solutions even though the problem would appear relatively easy.
Indeed, when solving partial differential equations numerically, the choice between the so called first-order or second-order finite difference schemes tremendously impacts the accuracy, stability, and computational cost of the solution. Here there are the main differences between these two types of schemes.

First-Order Numerical Scheme

A first-order numerical scheme is one where the truncation error of the finite difference approximation is proportional to the first power of the grid spacing δx or δt. The truncation error decreases linearly with decreasing grid spacing.
Classic examples of a first-order forward and backward difference approximations for the first derivative are:

$$\text{Forward difference:} \quad \frac{\partial u}{\partial x} \approx \frac{u(x+\Delta x) - u(x)}{\delta x}$$
$$\text{Backward difference:} \quad \frac{\partial u}{\partial x} \approx \frac{u(x) - u(x-\Delta x)}{\delta x}$$

and the accuracy of a first-order scheme is $O(\delta x)$. First-order schemes are generally simpler and more stable under certain conditions but may require finer grids to achieve a desired level of accuracy compared to higher-order schemes. As an advantage, the computational cost is relatively low because the stencil (the number of grid points involved in the computation) is usually smaller than a second order one.
The main problem of a first-order numerical scheme is what is defined as dissipation (or artificial viscosity). Indeed, even if these kind of schemes usually provides stable and convergent solutions, the amplitude is usually smaller with respect to the exact one as it propagates through the computational domain. It tends to smooth out the solution by reducing the amplitude of high-frequency components. However, this can be beneficial for stabilizing the solution, particularly in the presence of strong discontinuities (e.g., shock waves), but it can also lead to a loss of important details in the solution. The accuracy in magnitude is always related to:

- Refinement of the mesh: the finer the mesh is, the more accurate the result will be;
- Courant Number: the closer it is to 1, the closer to exact the result is.

Courant Number equals to 1 is possible only in linear problems, in any other situation it will be always less than 1 and it should be tailored depending on the non-linearity of the problem and on the refinement of the mesh. For this reason, dissipation that occurs in a first-order mesh is always a combination of the two factor both.

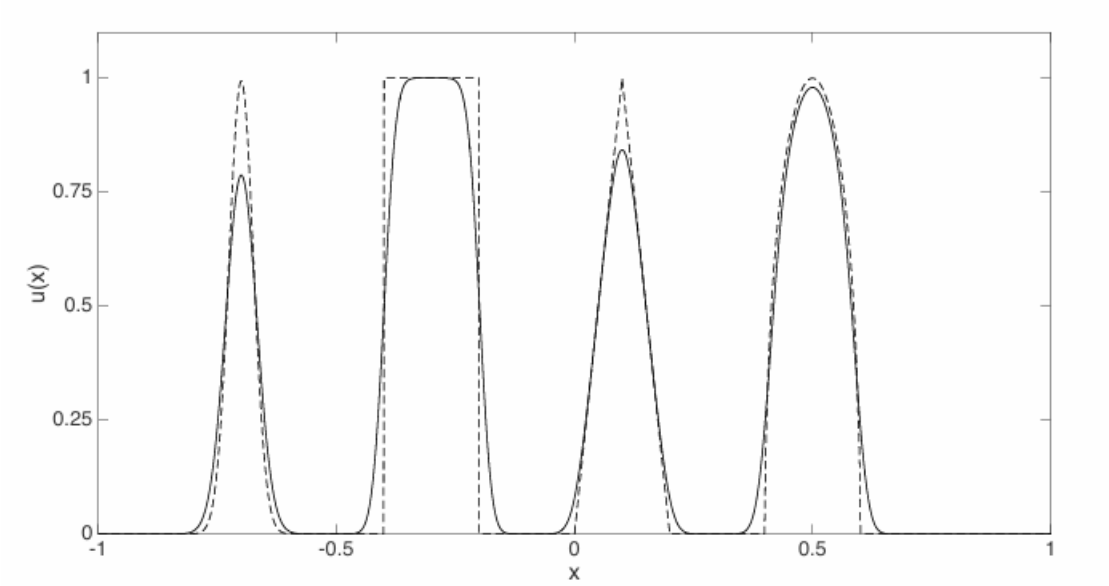

Figure 5.2. Diffusion effect on a generic initial profile [64]

Second-Order Numerical Scheme

A second-order numerical scheme is one where the truncation error of the finite difference approximation is proportional to the square of the grid spacing δx^2 or δt^2. The truncation error decreases quadratically with decreasing grid spacing.
A typical second-order central difference approximation for the first derivative is:

$$\frac{\partial u}{\partial x} \approx \frac{u(x+\delta x) - u(x-\delta x)}{2\delta x}$$

Where its accuracy is proportional to $O(\delta x^2)$. Second-order schemes generally provide higher accuracy for a given grid spacing compared to first-order schemes. However, they can be less stable under certain conditions, requiring careful consideration of the numerical stability criteria (smaller Courant Number with respect to a first-order scheme). In these kind of schemes, dispersion phenomena is the main issue on solving PDEs.
Dispersion refers to the artificial spreading of different frequency components of the wave at different speeds. This results in a phase error, where the numerical wave speed deviates from the physical wave speed. Consequently, oscillations and phase inaccuracies arise in the solution, causing waves to propagate either faster or slower than their true speed. While higher-order schemes reduce dissipation, they tend to increase dispersion, making the waveforms oscillate and potentially leading to non-physical results. This can be extremely restrictive on finding some stable quantities in a certain point for very long period of time (e.g. Radiation Pressure on a fixed wall), leading to unpredictable results.

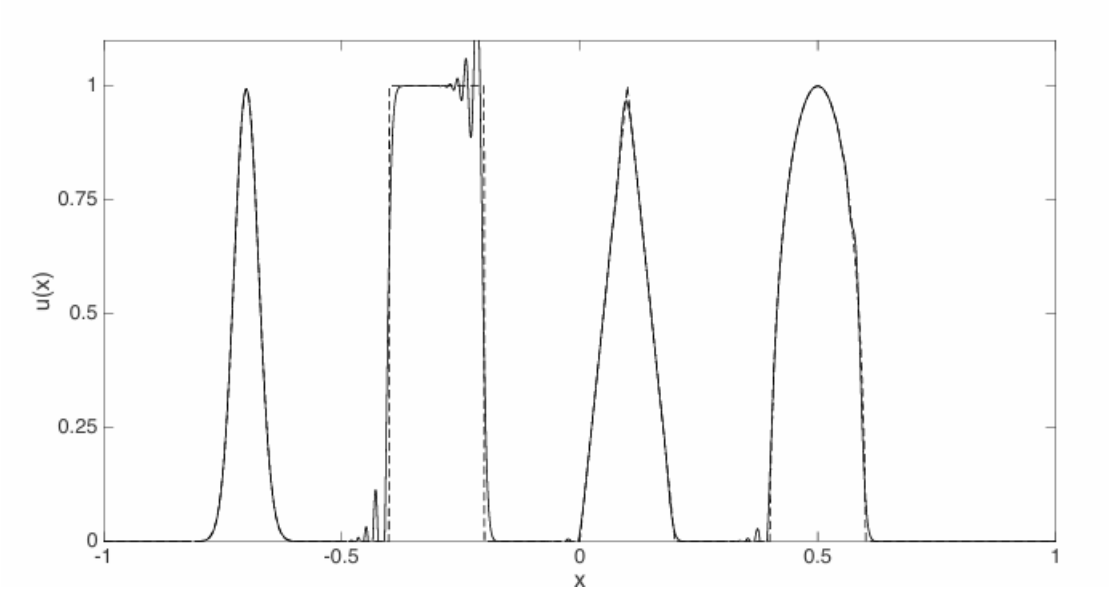

Figure 5.3. Dispersion effect on a generic initial profile [64]

Generally, the computational cost is higher than that of first-order schemes because of the more complexity of the stencil that involves more grid points. Understanding these differences is crucial when selecting a numerical scheme for solving partial differential equations, as it directly impacts the trade-off between accuracy, stability, and computational efficiency.

	First-Order	**Second-Order**
Truncation Error	$O(\delta x)$	$O(\delta x^2)$
Accuracy	Linear Accuracy	Quadratic Accuracy
Stability	More Stable	Less Stable, requiring careful consideration of stability conditions
Computational Cost	Lower	Higher due to larger stencil
Grid Spacing Requirement	Requires finer grid to achieve high accuracy	Achieves higher accuracy with coarser grid compared to first-order

Table 5.1. Table: Summary of First and Second Order Numerical Scheme

5.2.2 Numerical Schemes for Conservative Laws

When one attempts to solve nonlinear conservation laws numerically, it will run into additional difficulties not seen in standard linear equations. Moreover, the non-linearity makes everything

harder to analyze. In spite of this, a great deal of progress has been made in recent years.
For smooth solutions to nonlinear problems, the numerical method can often be linearized and results from the theory of linear finite difference methods applied to obtain convergence results for nonlinear problems [72]. For nonlinear problems there are important difficulties that can arise:

- The method might be non-linearly unstable, i.e., unstable on the nonlinear problem even though linearized versions appear to be stable. Often oscillations will trigger nonlinear instabilities.
- The method might converge to a function that is not a weak solution of our original equation (or that is the wrong weak solution, i.e., does not satisfy the entropy condition).

The possibility of converging to an incorrect weak solution is not entirely surprising; if multiple weak solutions exist, there is no guarantee that convergence will lead to the correct one. Moreover, the occurrence of convergence to a function that is not a weak solution at all is more perplexing. This issue stems from the ability to derive various conservation laws that are equivalent for smooth solutions but yield different weak solutions. Fortunately, a straightforward and natural requirement can be imposed on numerical methods to ensure that convergence does not lead to non-solutions. This requirement involves enforcing consistency with the underlying physical laws represented by the conservation equations, thus ensuring that the numerical scheme aligns with the expected behavior of the solutions.
By adhering to this principle, it becomes possible to establish a framework that mitigates the risk of converging to invalid solutions, thereby enhancing the reliability and accuracy of numerical simulations in fluid dynamics and related fields. This is the requirement that the method be in conservation form like 3.7, which means it has the form:

$$U_i^{j+1} = U_i^j - \frac{k}{h}\left[F^j_{i+\frac{1}{2}} - F_{i-\frac{1}{2}}\right] \tag{5.13}$$

Where $F^j_{i+\frac{1}{2}}$ and $F_{i-\frac{1}{2}}$ are the numerical flux evaluated at the intermediate cells in the grid. Depending on $F(U_{i+\frac{1}{2}})$ it is possible to have a first order, a second order or a higher order numerical scheme as MUSCL, ENO, WENO, Sweby and others [71]. The necessary condition is that the numerical flux must be expressed in a conservative form and that makes the conservation form extremely flexible to use.
Based on the previous considerations regarding the advantages and disadvantages of different types of numerical schemes, a decision has been made to opt for first-order methods. The choice was dictated by:

- The simplicity of the computational domain in one dimension allows us to use very fine meshes, thereby limiting the phenomenon of dissipation;
- The stability and robustness of the numerical solution is essential to find a second-order quantity that can be easily distorted by artificial oscillatory phenomena (dispersion);

- The computational cost is not very significant at this level as long as the solution domain is very simple.

Lax-Friedrichs Scheme

One of the most popular first-order numerical scheme is the so called Lax-Friedrichs (LF) scheme. This numerical scheme is a well-known method for solving hyperbolic partial differential equations, particularly conservation laws. It is named after Peter Lax and Kurt O. Friedrichs, who introduced the scheme [75, 76]. It is an explicit method that combines a central difference in space with a forward difference in time and adds an artificial dissipation term for stability. The Lax-Friedrichs update formula for a one-dimensional conservation law is given by:

$$U_i^{j+1} = U_i^j - \frac{k}{h}\left[{F_{LF}}^j_{i+\frac{1}{2}} - F_{LF_{i-\frac{1}{2}}}\right]$$

Where F_{LF} means the flux of the conservative system evaluated using the LF method:

$$\begin{cases} F_{LF}(U_{i+\frac{1}{2}}) = \frac{1}{2}\left[F(U_i^j) + F(U_{i+1}^j)\right] - \frac{h}{2k}\left[U_{i+1}^j - U_i^j\right] \\ F_{LF}(U_{i-\frac{1}{2}}) = \frac{1}{2}\left[F(U_i^j) + F(U_{i-1}^j)\right] - \frac{h}{2k}\left[U_i^j - U_{i-1}^j\right] \end{cases}$$

Using the notation:

- U_i^j is the numerical approximation of the solution at grid point i and time level j.
- k is the time step size.
- h is the spatial grid size.

The Lax-Friedrichs scheme is conditionally stable. The stability condition, often referred to as the Courant-Friedrichs-Lewy (CFL) condition, requires that:

$$\frac{\Delta t}{\Delta x} \leq \frac{1}{|a|}$$

where a is the maximum eigenvalue of the Jacobian of the flux function $f(u)$. For the linear wave equations it is equivalent to have $c = \frac{c_0 k}{h} \leq 1$.
The Lax-Friedrichs scheme is known for its high numerical dissipation and for its first-order accuracy in both time and space. The scheme is relatively simple to implement but may require a finer grid to achieve a desired level of accuracy.

Lax-Friedrichs-Rusanov Scheme

In this case, the Lax-Friedrichs-Rusanov (LFR) scheme, also called local Lax-Friedrichs scheme or simply Rusanov scheme, is used. It is a first-order numerical scheme that discretizes the function $F(U_{i+\frac{1}{2}})$ in this manner:

$$U_i^{j+1} = U_i^j - \frac{k}{h}\left[{F_{LFR}}^j_{i+\frac{1}{2}} - F_{LFR_{i-\frac{1}{2}}}\right]$$

With:

$$\begin{cases} F_{LFR}(U_{i+\frac{1}{2}}) = \frac{1}{2}\left[F(U_i^j) + F(U_{i+1}^j)\right] - \frac{|f'(U_i^j)|}{2}\left[U_{i+1}^j - U_i^j\right] \\ F_{LFR}(U_{i-\frac{1}{2}}) = \frac{1}{2}\left[F(U_i^j) + F(U_{i-1}^j)\right] - \frac{|f'(U_i^j)|}{2}\left[U_i^j - U_{i-1}^j\right] \end{cases}$$

Where F_{LFR} means the flux of the conservative system evaluated using the LFR method. Where $|f'(U_i^j)|$ is the local speed of sound $c_0 + |u_i^j|$ evaluated at each node. This method is of first-oredr accuracy in time and space ($\varepsilon \sim (\delta x, \delta t)$) too, but it guarantees much less dissipation and same stability with respect to LF method in same operative conditions. For the considerations above, the LFR was the chosen method for future analysis.

5.2.3 Numerical Boundary Conditions

Boundary conditions are crucial in numerical analysis because they specify different kinds of constraints on the values of a solution, or of its derivatives, at the boundary of the domain where the PDE is defined.

So far, methods for updating the cell average U_i^j have only been studied assuming that neighboring cell values U_{i-1}^j and U_{i+1}^j are known and perhaps values farther away as needed in order to compute the fluxes $F_{i-1/2}^j$ and $F_{i+1/2}^j$. In practice, one must always compute on some finite set of grid cells covering a bounded domain, and in the extremes cells it is impossible to obtain some numerical information. Instead, it is needed to set some physical boundary conditions, that are already known from the external environment, that should be used in updating these grid values.

One of the most credited approach is to include a few additional cells on either end, called ghost cells, whose values are set at the beginning of each time step in some manner that depends on the boundary conditions type. Let's assume the physical grid is a vector in the variable x defined as $x = \{1, 2, \ldots, N\}$.

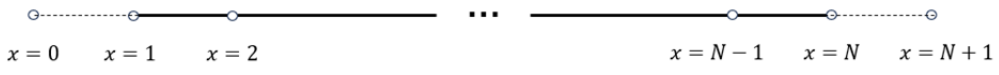

Figure 5.4. Numerical Grid

Figure 5.4 shows a grid with two ghost cells at each boundary in $x = 0$ and $x = N + 1$. These values provide the neighboring-cell values needed in updating the cells near the physical domain. The updating formula is then exactly the same in all cells, and there is no need to develop a special flux-limiter method, say, that works with boundary data instead of initial data. Instead, the boundary conditions must be used in deciding how to set the values of the ghost cells, but this can generally be done in a way that depends only on the boundary conditions and is decoupled entirely from the choice of numerical method that is then applied.

Based on the values assigned at the boundary, three types of boundary conditions can be identified.

Dirichlet

It specifies the value of the function (solution) itself on the boundary of the domain. The mathematical representation is like:

$$U(x_b, t) = g(t) \quad \text{for} \quad x_b \in \partial\Omega$$

Where $g(x)$ is usually a known function of time and $\partial\Omega$ is the boundary domain.

Neumann

It assigns the value of the derivative of the solution normal to the boundary. It is always in the form:

$$\frac{\partial U}{\partial n}(x_b, t) = h(t) \quad \text{for} \quad x_b \in \partial\Omega$$

Robin

It sets the value either of the function or of the derivative of the function normal to the boundary. It is also referred as mixed boundary conditions due to the mixing of both properties of Dirichlet and Neumann:

$$aU(x_b, t) + b\frac{\partial U}{\partial n}(x_b, t) = r(t) \quad \text{for} \quad x_b \in \partial\Omega$$

Dirichlet, Neumann and Robin boundary conditions are three fundamental types used in the context of solving differential equations, particularly partial differential equations (PDEs).

5.2.4 Acoustic Boundary Conditions

In Acoustics, boundary conditions can be extrapolated from physical quantities directly. In a seminal work of Poinsot and Lele [77] a very detailed discussion about the concept of well-posed boundary conditions for fluid flow based on the theory of characteristics is explained. It is considered a milestone for boundary conditions definition in the case of Navier-Stokes or Euler's equations for complex cases in which both kinematic and thermal boundary conditions are required.
This case is a little bit different, indeed neither thermal transformation are involved by definition of in-viscid fluid flow, nor Euler's equation are used. In particular, as it will be shown in Section 5.3, boundary conditions of interest are:

- Solid Walls
- Oscillating Walls.

Solid Walls

Consider a tube of gas with a solid wall at one end. In this case one would expect acoustic waves to reflect at this boundary. For a solid wall at $x = a$ the boundary condition for particle velocity is usually defined as:

$$u(a, t) = 0$$

In terms of pressure and particle velocity in the numerical grid domain, this condition is written for each time step in this way:

$$\begin{cases} \text{for } U_0: & p_0 = p_1 & u_0 = -u_1 \\ \text{for } U_{-1}: & p_{-1} = p_2 & u_{-1} = -u_2 \end{cases}$$

This imposes the necessary symmetry at the start of each time step. This assumes that the solid-wall boundary condition can be set by reflecting all components of U and then negating the second component.

Oscillating Walls

Now the solid wall is oscillating at $x = a$ with very small amplitude generating an acoustic sound wave in the tube of boundaries $a \leq x \leq b$. This is a common situation in acoustics because sound waves are usually generated by a very small amount of molecular vibrations of surfaces. For very small-amplitude motions, linear acoustics solution can be still used on a fixed grid domain with the boundary condition:

$$u(b, t) = A(t)$$

For a fixed frequency oscillation one may get:

$$A(t) = \epsilon \sin(\omega t)$$

As in the previous case, one can write this physical kinematic conditions in the numerical grid domain in terms of pressure and particle velocity as:

$$\begin{cases} \text{for } U_0: & p_0 = p_1 & u_0 = 2A(t_j) - u_1 \\ \text{for } U_{-1}: & p_{-1} = p_2 & u_{-1} = 2A(t_j) - u_2 \end{cases}$$

It is worth mentioning, that the condition on particle velocity comes directly from a linear interpolation of quantities among the extreme of physical grid and the two cells surrounding it.

5.3 Statement of the Problem

The study of the one-dimensional system is proposed. The system is a closed tube of total length L containing air, of known physical properties and subject to an adiabatic transformation.

At the left-end of the tube, there is a perfectly reflecting fixed wall; at the right-end there is a speaker able to spread in the tube a beam of monochromatic plane waves. The oscillatory dynamics of the speaker membrane are reproduced by the motion of a piston with known kinematics.
The first goal of the analysis is to implement a FD numerical scheme in MATLAB® and to check the validity of the solutions in different scenarios. Then, the final goal will be the representation of radiation pressure effect over a fixed surfaces as a function of the driven frequency of the piston. That would lead to have a preliminary idea of what one can imagine as a future control law to manipulate the force over a perfect reflecting object.

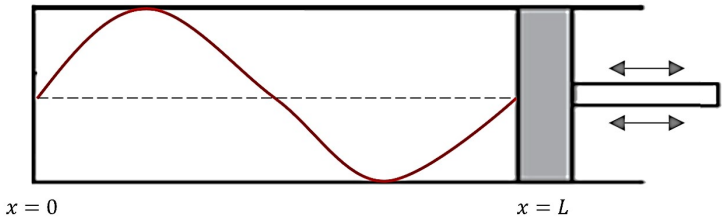

Figure 5.5. Piston pipe scheme

To begin with, the inviscid gas equation 5.6 with a constant the speed of sound $c(\rho)$ is used for the problem. This leads the equation to be much simpler and still valid in case of absence of high non-linearity. At this point, the general system of equation expressed in terms of velocity potential is the following:

$$\begin{cases} \varphi_{tt} - \varphi_{xx}(c_0^2 - \varphi_x^2) = 2\varphi_x\varphi_{xt} \\ \varphi_x(0,t) = 0 \\ \varphi_x(L,t) = -A_p(t) \\ \varphi_t(x,0) = 0, \quad \varphi(x,0) = 0, \end{cases} \tag{5.14}$$

Where $A_p(t)$ is the kinematic boundary condition imposed by the piston, and the negative sign is justified by the convention of $u = -\nabla\varphi$. As previously mentioned in Sec.5.1, an equation like that is useless to perform any kind of numerical or an analytical analysis, hence the system is reduced to 5.10. At this point, only initial and acoustic boundary conditions must be set to completely and uniquely defined the problem and its solution.

Initial Conditions

The initial conditions must be set on real quantities, i.e. particle velocity and pressure, which represents the acoustic field without any initial perturbation. In this case:

$$\begin{cases} P(x,0) = P_0 \\ u(x,0) = 0 \end{cases} \tag{5.15}$$

These two conditions reflect to the numerical variable the numerical scheme actually evaluates step by step. Indeed, numerical initial conditions are:

$$\begin{cases} \tilde{p}(x,0) = 0 \\ u(x,0) = 0 \end{cases} \tag{5.16}$$

The zero initial value for $\tilde{p}$ it is a consequence of its definition, indeed by substituting the real initial values for particle velocity and pressure one obtains:

$$\tilde{p} = -\frac{1}{2}u(x,0)^2 + \frac{c_0^2}{k-1}\left(\left(\frac{P(x,0)}{P_0}\right)^{\frac{k-1}{k}} - 1\right) = 0$$

Boundary Conditions

Concerning boundary conditions, particle velocity is described by Dirichlet's type either on the rigid wall, or on correspondence of the piston because the value is always fixed during the entire simulation:

$$\begin{cases} u(0,t) = 0, & (Rigid\ Wall) \\ u(L,0) = A_p(t), & (Moving\ Piston) \end{cases} \tag{5.17}$$

Where $A_p(t)$ represents the velocity of the piston at the right-hand side of the cylinder.
Regarding the boundary conditions on $\tilde{p}$, it is necessary to identify the condition on the actual pressure's derivative, then substitute them into new variable's derivative. Real case needs reflecting boundary conditions on the left and the conservation of momentum on the right, leading to this set of boundary conditions:

$$\begin{cases} P_x(0,t) = 0 & (Rigid\ Wall) \\ P_x(L,0) = -\rho\dot{u}(L,t) & (Moving\ Piston) \end{cases} \tag{5.18}$$

Where $\dot{u}(L,t)$ is always provided analytically because of prescribed motion of the piston.
At this point, by progressively applying the Rusanov numerical scheme to the conservative system 5.10 one might finally solve the nonlinear system of equation. The starting point is the knowledge of the assumed values of the fictitious pressure and speed at the initial instant and at every point of the space grid. The next step is to calculate the values of the state variables in each node at $t = 1$.
As is clear, to determine $\tilde{p}_1^j$ and u_1^j it is necessary to know the values assumed by the fake pressure and by the fluid velocity in the previous node ($x = 0$), which is outside the physical grid. Similarly, the same circumstance occurs in the calculation of $\tilde{p}_N^j$ and u_N^j, with the difference that the values assumed by the state variables in the next node ($x = N + 1$) are unknown.
Therefore, to proceed with the calculation it is necessary to assign the values assumed by the state variables at points outside the physical grid or ghost points. By simply applying the relationships found in the previous subsection 5.2.4, at the fixed wall ($x = 1$) the following conditions are defined for each time step j:

$$\begin{cases} u_0 = -u_2 \\ p_0 = p_2 \end{cases}$$

At this point, let's see how this condition is flow down to the numeric variable $\tilde{p}$ at the ghost node.

$$\tilde{p}_0 = -\frac{1}{2}(-u_2)^2 + \frac{c_0^2}{k-1}\left(\left(\frac{P_2}{P_0}\right)^{\frac{k-1}{k}} - 1\right) = -\frac{1}{2}u_2^2 + \frac{c_0^2}{k-1}\left(\left(\frac{P_2}{P_0}\right)^{\frac{k-1}{k}} - 1\right) = \tilde{p}_2$$

So the symmetry with respect to the node $x = 1$ is unchanged for the fake pressure quantity in case of fixed wall.

Instead, if one uses the suggested acoustic boundary conditions at the moving wall ($x = N$) the expressions of the values assumed in node $N + 1$ should be as follows:

$$\begin{cases} u_{N+1} = -u_{N-1} + 2u(L,t) \\ p_{N+1} = p_{N-1} \end{cases}$$

This condition of symmetry of pressure value with respect to the right-hand side ghost node, is usually implemented to get the simulation faster and easier to implement [78] even though there is the presence of an oscillating wall with the problem of mass flow conservation.

The derivative of pressure at the boundary must correspondingly adjust with the acceleration of the piston, as indicated by the boundary conditions referenced in 6.73. Numerous authors have endeavored to enhance the precision of their solutions by employing the momentum conservation equation [77, 79–81], which may include the implementation of a moving mesh to accommodate high amplitudes at the boundary. This aspect warrants careful consideration, as one seeks a second-order quantity where accuracy is paramount to achieve results that are as realistic as possible, even if this necessitates a more computationally intensive algorithm. Consequently, the pressure at node $N + 1$ will be assessed using this methodology.

$$\begin{cases} u_{N+1} = -u_{N-1} + 2u(L,t) \\ p_{N+1} = p_{N-1} - 2h\rho\dot{u}(L,t) \end{cases}$$

Assuming to know the values in the fictitious nodes, the numerical scheme can be implemented in a recursive way by reconstructing the trend of the quantities of interest along the tube length. In particular, the boundary value on the oscillating piston node for the variable $\tilde{p}$ is evaluated by substituting the physical quantities evaluated at the ghost node:

$$\tilde{p}_{N+1} = -\frac{1}{2}(-u_{N+1})^2 + \frac{c_0^2}{k-1}\left(\left(\frac{p_{N+1}}{p_0}\right)^{\frac{k-1}{k}} - 1\right) = -\frac{1}{2}u_2^2 + \frac{c_0^2}{k-1}\left(\left(\frac{p_{N+1}}{p_0}\right)^{\frac{k-1}{k}} - 1\right)$$

5.3.1 Test Configurations and Assumptions

The simulations were made considering normalized quantities for excitation frequency, piston stroke and simulation time. Specifically, the latters were defined as:

$$\begin{cases} \tilde{\omega} = \frac{\omega_f}{\omega_1} \\ \\ \tilde{L} = \frac{A_p(\omega_f)}{L} \\ \\ \tilde{t} = \frac{p_k}{2\pi\omega_f} \end{cases} \tag{5.19}$$

ω_f is the excitation frequency, $\omega_1 = \frac{c_0}{2L}$ is the first resonance frequency, p_k is the number of cycles of the piston and L_p is the ratio between the piston's stroke and the length of the tube L. For every simulation, a unitary length of the tube $L = 1$ was considered. The use of normalized quantities is good practice whether to replicate the same physical conditions throughout an experiment. The tests were performed assuming that:

- the maximum magnitude value of the piston's stroke is fixed and small compared to the grid dimension;
- the frequency of the signal is monochromatic, so no superposition of harmonic waves are expected in the solution except for some non linear effects;
- the amplitude of the signal is modulated such that the homogeneous part of the solution disappears. It is necessary since no viscosity effects are involved and the solution would present the homogeneous part of the solution for the entire simulations affecting the steady-state response.

One more consideration should be made about the last assumption because it is necessary to distinguish between numerical and viscous damping. The first one is related to the numerical scheme implemented to find the approximated solution of the problem, the second one is the actual damping of the system that decreases naturally the effect of the homogeneous part of the solution. In our case, since the artificial viscosity introduced by the numerical scheme behaves in a completely different way from the physical viscosity of the air, the necessity to modulate the signal in a way the homogeneous part of the solution is null arises. With such technique, only the steady-state component of the response survives.
Now, a series of three different simulations are shown to see how the radiation pressure varies. In fact, it will be seen that radiation pressure strongly depends on the normalized frequency $\tilde{\omega}$ and on the relative amplitude of the stroke respect to the tube length. Clearly, the stroke of the piston cannot be greater than the space grid length to respect the finite difference scheme

accuracy. That's because a fixed grid has been used to perform simulations, so only small displacement of the piston are allowed [73]. Considering that, the simulations have been performed considering these range of values:

- Amplitude range varies from 0.0001% to 0.0005% of L
- Frequency bandwidth from 0 to $5\,\omega_1$

In this manner, the displacement of the piston results to be infinitesimal, while the frequencies analysed are up to the fifth of resonance one. Here, a table that shows the parameters for each simulation.

Table 5.2. Table: Cases 1-3

Case #	Piston Stroke / Tube Length	$\tilde{\omega}$
1	0.0001 %	2.3
2	0.0002 %	2.3
3	0.0001 %	0-5

These values are chosen to highlight how the non linear effects affect the acoustic field and how the radiation pressure varies depending on the amplitude of the excitation.

Case 1 This is the case where the effects of non linearity are not relevant. The system behaves like it is described by the linear wave equation, and one could foresee that the radiation pressure on the rigid wall will be equal to zero.

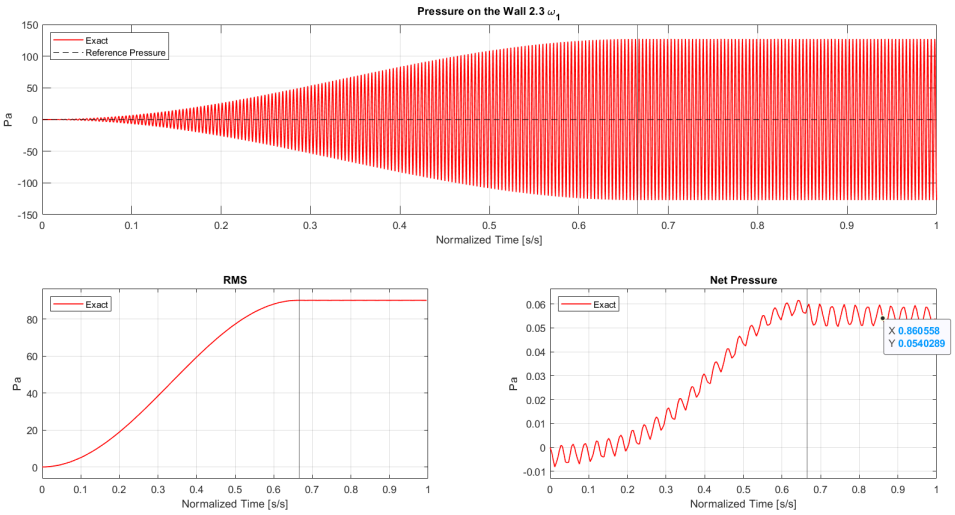

Figure 5.6. Radiation Pressure Case 1

However, even if the acoustic field behaves as linear, the radiation pressure equation presents non linear terms that makes its value different from zero, as it is shown next. Figure 5.6 is composed by three different plots: the top one, shows the trend of the radiation pressure on the fixed wall during time; in the bottom left side there is the root-mean-squared value of the signal over time; in the bottom right, instead, there is the mean value of the radiation pressure over time. The latter, in particular, is the most interesting because it demonstrates the net shift of the pressure with respect the reference one. This last is not expected in linear acoustic theory, and it shows how the consideration of higher-order terms in the wave equation is crucial to see that effect. It is worth mentioning that the first half of the net radiation pressure trend (bottom-right part of the figure 5.6) has, apparently, a strange behaviour. The main reason is the modulated input signal driven by a quadratic sine function. That makes the signal's magnitude to change over time and the time average value is affected until steady-state condition is accomplished. Then, the steady state part of that graph is from vertical black line to the end of the simulation.

Case 2 Now, the piston stroke is the double with respect to the previous case. Indeed, the response is generally increased and the mean value of the has increased quadratically. The figure 5.6 is composed as the previous one. In figure 5.6 the net value is around 0.054 Pa, while in 5.7 the pressure is 0.219 Pa. This result may be interesting in the case a control of the net radiation pressure could be expressed by some mathematical relationship in terms of amplitude modulation. It is worth mentioning that the first half of the net radiation pressure

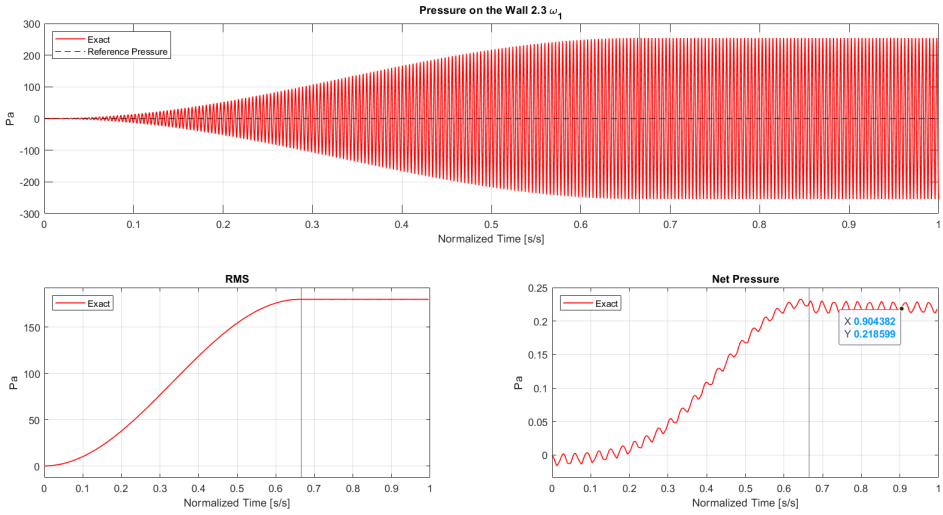

Figure 5.7. Radiation Pressure Case 2

trend (bottom-right part of the figure 5.6) has, apparently, a strange behaviour. The main reason is a modulated input signal, driven by a quadratic sine function. That makes the signal's magnitude to change over time and the time average value is affected until steady-state condition is accomplished. Basically, the fundamental part of that graph is from half to the end

of the simulation.

Case 3 Of another kind, is the subject of the figure 5.8. Indeed, it shows the average value of the radiation pressure from 0 to the 5^{th} resonance. Here, the scale for Pressure is expressed in dB.

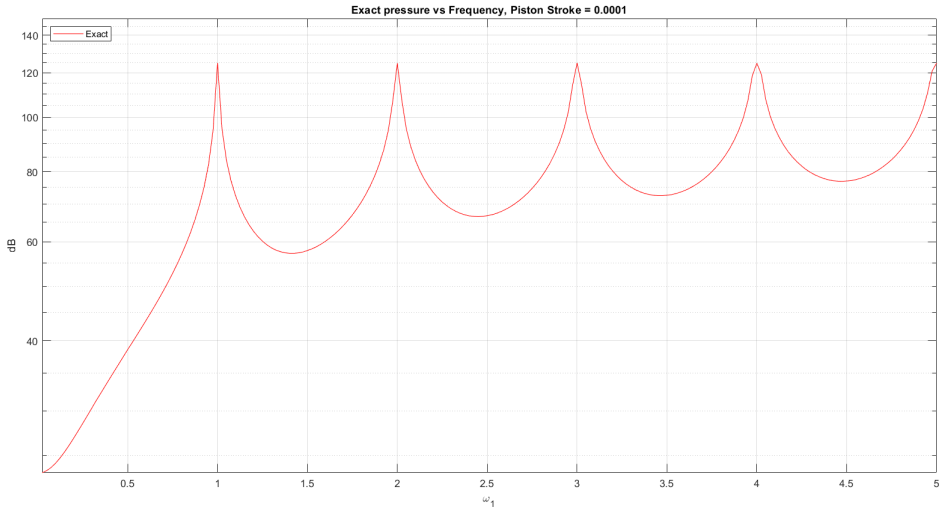

Figure 5.8. Radiation Pressure over frequency Case 3

It is clear that peaks occur in correspondence of integer multiple of the first resonance, and the minimum value are exactly in the middle near the frequencies of the open-rigid tube configuration. It seems to appear a very regular trend about the radiation pressure value between resonance frequencies, it can be very interesting on finding some analytical expression to derive it, together with the quadratic relationship with respect to the amplitude, to get an helpful control law to manipulate the pressure on a body.

5.3.2 Radiation Pressure Models comparison

The next tests are performed to compare the results for different radiation pressure models:

- Exact Formula: $p = \rho\varphi_t - \mathcal{E}$;
- Lagrangian Formula: $p = \rho_0\varphi_t - \mathcal{L}_0$;
- King's Formulation: $p = \rho_0\varphi_{1_t} - \mathcal{L}_0$ with φ_{1_t} solution of the linear wave equation.

Specifically, the study is made to see how the different formulas differs in the solutions. From the analytical studies, one should expect a very tiny difference between the first two cases by the fact that the Lagrangian formulation is a second order approximation of the exact one. The third case would appear more different because of the strong approximation between the linear and nonlinear wave equations. In the next cases 4 and 5 the excitation frequency is closer to

the second resonance frequency in order to increase non-linearity effects and to enhance the differences between the radiation pressure models. Case 6 will show the difference of the models among a wide range of frequencies as in case 3.

Table 5.3. Table: Cases 4-7

Case #	Piston Stroke / Tube Length	$\tilde{\omega}$
4	0.01 %	1.85
5	0.05 %	1.85
6	0.01 %	0-5
7	0.05 %	0-5

Case 4 This case shows how the three models collapse because of the absence of high non-linear effects on the radiation pressure. In particular, it also demonstrates the quality of the numerical simulations since, as it is predicted, the models must produce close results in presence of very small perturbation acting on the system. Figure 5.9 shows also that the model used by King to determine the radiation pressure would appear unsatisfactory and too approximated. Indeed, the amount of radiation pressure evaluated is roughly the half of the pressure using the exact and the Lagrangian formula.

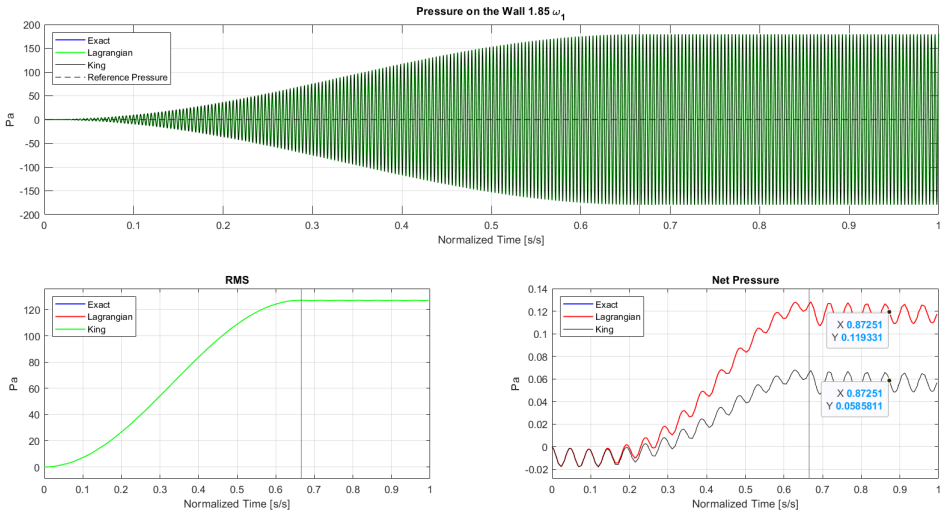

Figure 5.9. Radiation Pressure Case 4

Case 5 This figure 5.10 shows how the two nonlinear models differ because of a more effect of high non-linear on the system. In particular, even if the two pressure models slightly differs, the exact pressure model seems to be a little bit higher with respect to the Lagrangian one. Indeed, it is a natural consequence of having introduced non-linearity that differ up to third-order in

to the system by increasing the amplitude of the oscillating piston. However, the Lagrangian approximation appears to be still a very good attempt to describe radiation pressure near the linear case or far from resonance regime.

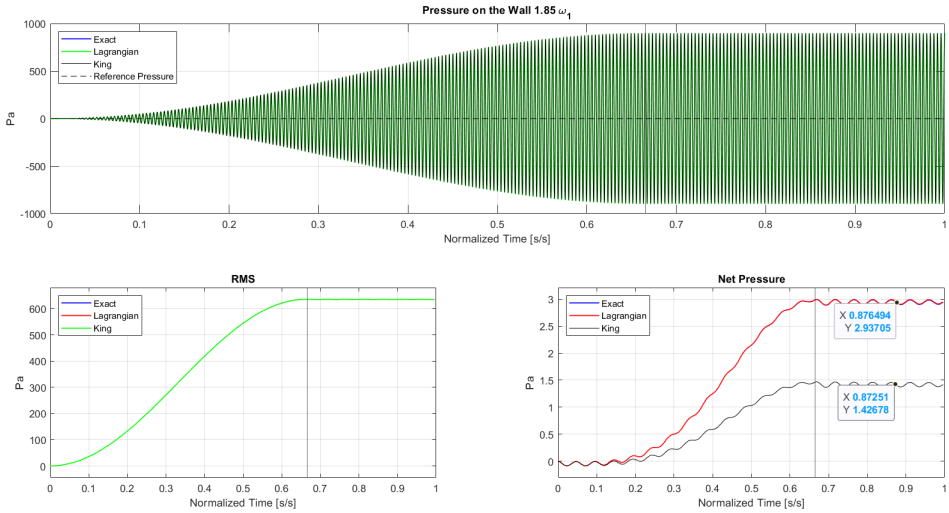

Figure 5.10. Radiation Pressure Case 5

A close look to the figure 5.11 highlights the little difference between the two models in the two cases 4 and 5.

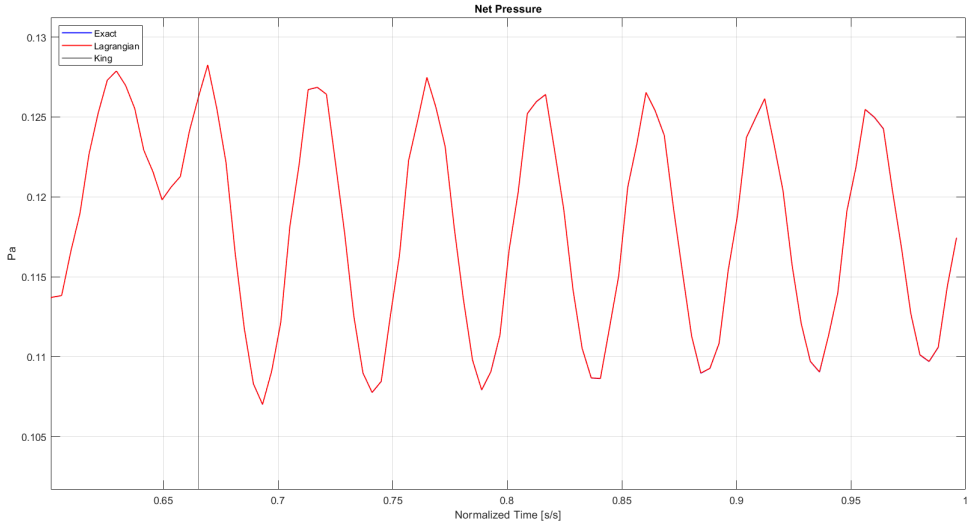

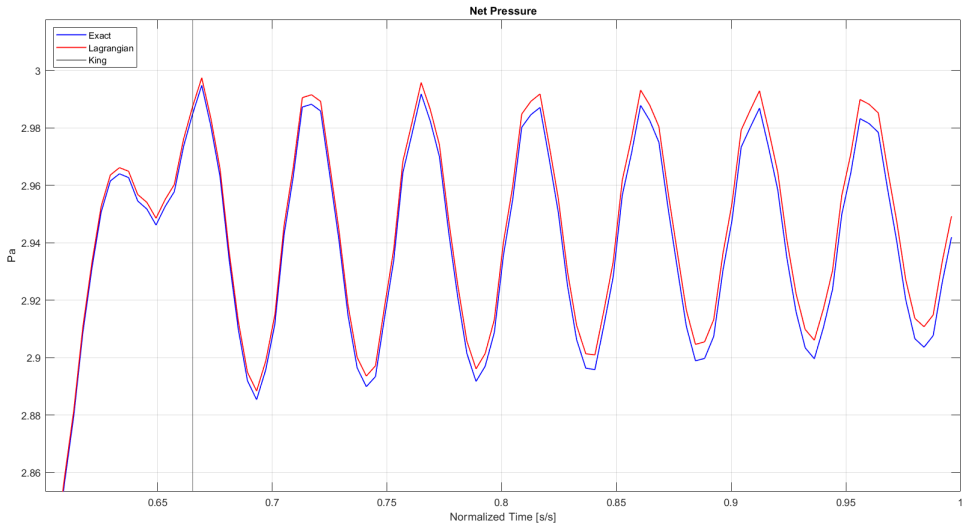

Figure 5.11. Comparison between Exact and Lagrangian Expression

Case 6 The next figure concerns the same simulation made in case 3 but with all the radiation pressure models. As one might image, the difference is very small compared to their magnitude and it is present only in correspondence of resonant conditions. This phenomenon is the main cause of the divergence of the values for the three models. The differences are more evident in figure 5.13 where the error is represented in a logaritmic scale. The green line represents the error between the exact and the Lagrangian model. As it can clearly seen, the more one is close to resonant condition, the more the error is evident between the models. However, for small oscillation of the piston the error between the two is at maximum around 2 or 3 % near resonances and it is very low anywhere else.

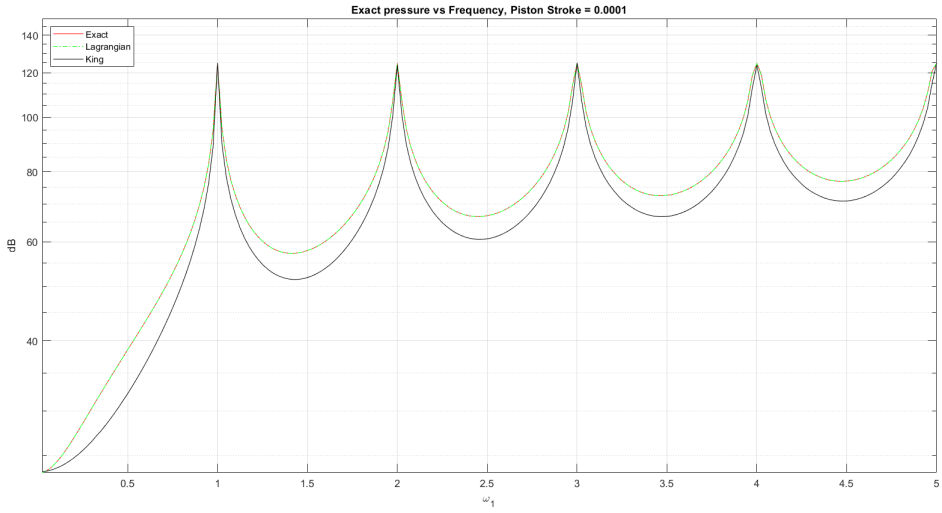

Figure 5.12. Radiation Pressure over frequency Case 6

The black line represents the error between the exact model and the King's one and it seems to oscillate a little around 50 % outside resonance frequencies. Close to resonance conditions, the physical model may failed because of no viscosity introduced into the system.

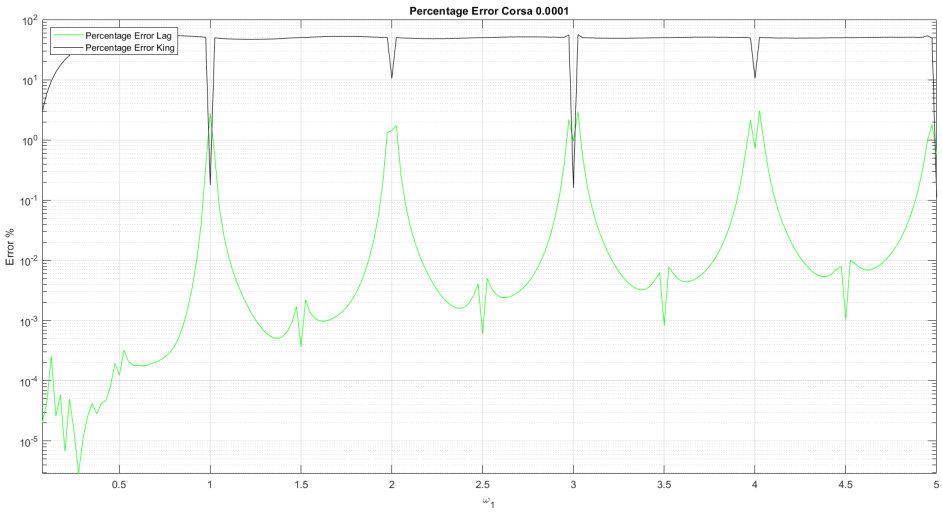

Figure 5.13. Error over frequency Case 6

Case 7 The next figure concerns the same simulation made in case 6 but with a larger piston stroke to induce more non-linearity into the system. In this way, the difference between the models increases a lot compared to the previous case shown in 5.12 and it could be well seen in correspondence of resonant conditions..

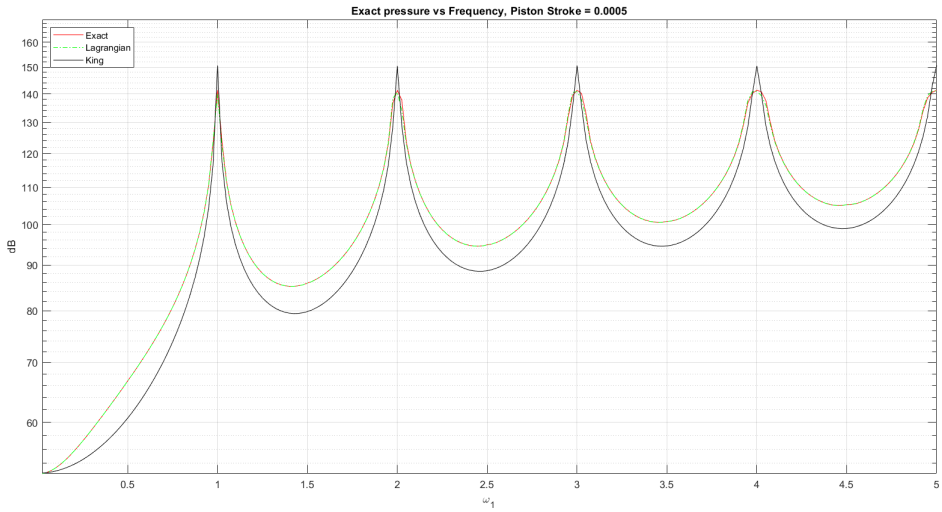

Figure 5.14. Radiation Pressure over frequency Case 7

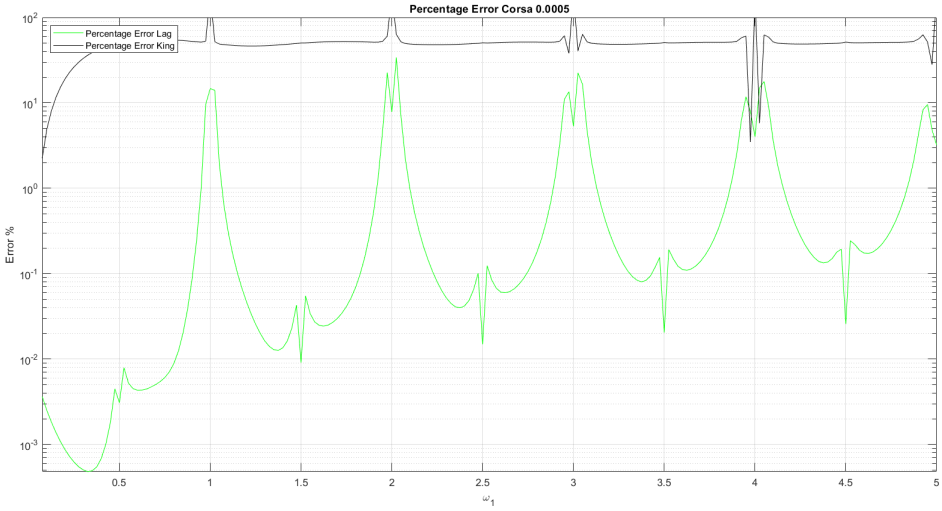

Figure 5.15. Error over frequency Case 7

Even in this case, the blue line represents the error between the exact and the Lagrangian model. As it can clearly seen in the figure above, the larger induced oscillation of the piston the greater the error is between the two models. Forthwith, the maximum error is now around 30 % near resonances but it is still very low anywhere else.
The black line represents the error between the exact model and the King's one. The error seems to oscillate a little around 50 % outside resonance frequencies and it has greater peaks at the latter ones.

Chapter 6

Perturbation Approach for the Acustic Radiation Pressure

The numerical results seen in the previous chapter 5 give us a new insight into the problem of acoustic radiation pressure. In fact, there seems to be a pattern that repeats between resonant frequencies with a pattern that is quadratic in relation to the piston's stroke amplitude. This drives us to go beyond pure numerical analysis, which can still be prone to error, investigating the possibility of finding an approximate analytical solution.
Finding an analytical relationship between the magnitude of the acoustic field and the radiation pressure would allow us to go to verify and validate the results found and could add an important contribution in this field which, for more than a century now, has been struggling to find a unique formulation of this phenomenon. The starting equation is always the same, and the mathematical model is exactly the same as the numerical equations previously implemented:

$$\begin{cases} \varphi_{tt} - \varphi_{xx}(c_0^2 - \varphi_x^2) = 2\varphi_x\varphi_{xt} \\ \varphi_x(0,t) = 0 \\ \varphi_x(L,t) = -A_p(t) \\ \varphi_t(x,0) = 0 \end{cases} \tag{6.1}$$

In this case, the presence of the double nonlinearity of the acoustic field does not allow us to find a trivial analytical solution. In addition, having a limited domain with uneven boundary conditions increases the complexity of the problem. Although there is some possibility of implementing an exact solution for mobile domains, the complexity of the resolution and the solution itself leads to an impracticability of such a method. It presents solutions as developments in infinite sets of functions, making the future development of a real-time monitoring tool virtually impossible. Looking for new semi-analytical resolution techniques of partial-drift equations implemented in recent decades, the Adomian Decomposition Method [82] and Homotopy Perturbation Method [83] seem to be among the most promising. In the case of HPM proposed by Dr. Huan He is a combination of homotopy in topology and classic perturbation techniques,

he provides us with a convenient way to obtain analytic or approximate solutions for a wide variety of problems arising in different fields. They are polynomial expansion techniques of the solution and work very well if they have information about a possible form of the solution to the regime even going to find, in some cases, the exact solution of the problem [84–88]. From a historical point of view, it takes inspiration from the classic method of perturbations, going to extend its scope even in cases where there is not a very small scale parameter within the problem. These methods are based on an iterative process that depends strictly on the guess solution given at the first step that depends strongly on the initial conditions and can often be ineffective by finding a solution that diverges over time. Moreover, there is still no general line of how to use this technique in a rigorous manner, but it seems that everyone is solving their problem heuristically using some trick. In addition to this, methods were rarely used in the case of finite domains and given the absence of strict application of the method, it was decided to use the classic perturbation method.

6.1 Perturbation Method: a brief introduction

Most of the physical problems facing engineers, physicists, and applied mathematicians today exhibit peculiarity which preclude the knowledge of the exact analytical solutions. Some of these features are non-linearity, variable coefficients, complex boundary shapes, and nonlinear boundary conditions at known or, in some cases, unknown boundaries. Even if the exact solution of a problem can be found explicitly, it may be useless for practical applications, interpretation or numerical evaluation. Examples of such problems are Bessel functions of large argument and large-order and doubly periodic functions. Thus, in order to obtain information about solutions of equations, one is forced to resort to approximations, numerical solutions, or combinations of both. Foremost among the approximation methods are perturbation (asymptotic) methods. According to this technique, the solution is represented by the first few terms of an asymptotic expansion, usually not more than two terms. The expansions may be usually carried out in terms of a small parameter which appears naturally in the equations, or which may be artificially introduced for convenience as it will be done in the next section. Such expansions are called parameter perturbations. Alternatively, the expansions may be carried out in terms of a coordinate; these are called coordinate perturbations. The latter case is very helpful in case of secular terms appearance [89].

Many physical problems involving the function $u(x, \varepsilon)$ can be represented mathematically by the differential equation $L(u, x, \varepsilon) = 0$ and the boundary condition $B(u, \varepsilon) = 0$, where x is a scalar or vector independent variable and ε is a parameter. In general, this problem cannot be solved exactly. However, if there exists an ε for which the above problem can be solved, one seeks to find the approximated solution for small ε in, say, powers of ε; that is equal to:

$$u(x, \varepsilon) = u_0(x) + \varepsilon u_1(x) + \varepsilon^2 u_2(x) + \cdots$$

Where u_n, is independent of ε and $u_0(x)$ is the solution of the zero order problem in case of zero non-linearity. One then substitutes this expansion into $L(u, x, \varepsilon) = 0$ and $B(u, \varepsilon) = 0$, expands for small ε, and collects coefficients of each power of ε.
Since these equations must hold for all values of ε, each coefficient of ε must vanish independently because sequences of ε are linearly independent. These usually are simpler equations governing u, which can be solved successively by iterating the solution.

6.2 Perturbation Method: Application on a fixed screen

As it has been known, the starting equation is:

$$\varphi_{tt} - \varphi_{xx}(c_0^2 - \varphi_x^2) = 2\varphi_x\varphi_{xt}$$

From the Section 6.1, perturbation method consists of expressing the solution as a power series in a small parameter ε. Frequently, in nonlinear vibration problems, the small parameter ε compares in the dynamic equation as referred to a small non-linearity that 'perturbs' the dynamic of the equivalent linear system. In our case, this kind of parameters does not seem to appear, leading to the incapacity of using the method. However, this can be avoided if the small perturbation appears as a forcing term, or as a boundary condition (see [90]). In this case, an equivalent non-dimensional problem is solved in order to make a perturbation of order ε clearly appear as forcing term at the boundary.

Dimensionless Wave Equation

Let's write the dimensionless quantities as follow:

$$x = L\tilde{x}, \quad t = \frac{L}{c_0}\tilde{t}, \quad \varphi(\tilde{x}, t) = c_0 L\psi(\tilde{x}, \tilde{t})$$

In so doing, even the derivatives must be affected by the transformation:

$$\frac{\partial}{\partial\tilde{x}} = \frac{1}{L}\frac{\partial}{\partial\tilde{x}}, \quad \frac{\partial}{\partial t} = \frac{c_0}{L}\frac{\partial}{\partial\tilde{t}},$$

With this in mind, the derivatives of the potential becomes:

$$\varphi_t = c_0 L\frac{c_0}{L}\psi_{\tilde{t}} = c_0^2\psi_{\tilde{t}}, \quad \varphi_x = c_0 L\frac{1}{L}\psi_{\tilde{x}} = c_0\psi_{\tilde{x}}, \quad \varphi_{tt} = c_0 L\frac{c_0^2}{L^2}\psi_{\tilde{t}\tilde{t}} = \frac{c_0^3}{L}\psi_{\tilde{t}\tilde{t}},$$

$$\varphi_{xx} = c_0 L\frac{1}{L^2}\psi_{\tilde{x}\tilde{x}} = \frac{c_0}{L}\psi_{\tilde{x}x}, \quad \varphi_{xt} = c_0 L\frac{c_0}{L^2}\psi_{\tilde{x}\tilde{t}} = \frac{c_0^2}{L}\psi_{\tilde{x}\tilde{t}},$$

Now substituting these relations, one gets the non-dimensional nonlinear wave equation:

$$\psi_{\tilde{t}\tilde{t}} - \psi_{\tilde{x}\tilde{x}} = -\psi_{\tilde{x}}^2\psi_{\tilde{x}\tilde{x}} + 2\psi_{\tilde{x}}\psi_{\tilde{x}\tilde{t}} \tag{6.2}$$

Eventually, the system becomes:

$$\begin{cases} \psi_{\tilde{t}\tilde{t}} - \psi_{\tilde{x}\tilde{x}} = -\psi_{\tilde{x}}^2\psi_{\tilde{x}\tilde{x}} + 2\psi_{\tilde{x}}\psi_{\tilde{x}\tilde{t}} \\ \psi_{\tilde{x}}(0,\tilde{t}) = 0 \\ \psi_{\tilde{x}}(1,\tilde{t}) = -\frac{A_p(t)}{c_0} = -\frac{B}{c_0}\sin\left(\frac{\omega_f L}{c_0}\tilde{t}\right) = -\varepsilon\sin(\omega_a\tilde{t}) \\ \psi(\tilde{x},0) = 0, \quad \psi_t(\tilde{x},0) = 0 \end{cases} \tag{6.3}$$

Where:

- $\varepsilon = \frac{B}{c_0}$ is the local Mach Number;
- $\omega_a = \frac{\omega_f L}{c_0}$ is a normalized frequency.

It is clear that the small parameter ε can be referred to the Mach number, indeed it is the ratio between the speed of the piston and the speed of sound in air. Moreover, in our analysis this number is much less than 1, leading to the chance to express the solution using the perturbation method expansion. With this intention, the solution can be rewritten as:

$$\psi(\tilde{x},\tilde{t}) = \varepsilon\psi_1(\tilde{x},\tilde{t}) + \varepsilon^2\psi_2(\tilde{x},\tilde{t}) + o(\varepsilon^3)$$

And substituting it in to 6.3, one one gets two systems of equation of order ε and ε^2.

$$\begin{cases} \psi_{1_{\tilde{t}\tilde{t}}} - \psi_{1_{\tilde{x}\tilde{x}}} = 0 \\ \psi_{1_{\tilde{x}}}(0,\tilde{t}) = 0 \\ \psi_{1_{\tilde{x}}}(1,\tilde{t}) = -\sin(\omega_a\tilde{t}) \\ \psi_1(\tilde{x},0) = 0, \quad \psi_{1_t}(\tilde{x},0) = 0 \end{cases} \tag{6.4}$$

and:

$$\begin{cases} \psi_{2_{\tilde{t}\tilde{t}}} - \psi_{2_{\tilde{x}\tilde{x}}} = 2\psi_{1_{\tilde{x}}}\psi_{1_{\tilde{x}\tilde{t}}} \\ \psi_{2_{\tilde{x}}}(0,\tilde{t}) = 0 \\ \psi_{2_{\tilde{x}}}(1,\tilde{t}) = 0 \\ \psi_2(\tilde{x},0) = 0, \quad \psi_{2_t}(\tilde{x},0) = 0 \end{cases} \tag{6.5}$$

6.2.1 Order ε Solution

The first order system looks like a linear wave equation problem defined in a limited domain of unit length and in-homogeneous boundary conditions. It aims at representing a simple case of a rigid pipe closed at one end with a fixed and perfectly reflecting wall while on the other end the presence of an oscillating piston is modeled. This problem is a little more complicated compared to the standard homogeneous case; indeed, the presence of non-homogeneous boundary conditions needs to be treated carefully. A standard mathematical way to solve this problem [91], suggests splitting the analytical solution into two parts:

- ψ_b that always satisfies the boundary conditions.
- ψ_s that, considering ψ_b, is able to satisfy the related modified system of equations with homogeneous Boundary Conditions.

So the solution is split in:

$$\psi_1(\tilde{x},\tilde{t}) = \psi_b(\tilde{x},\tilde{t}) + \psi_s(\tilde{x},\tilde{t}) \tag{6.6}$$

In order to always satisfy boundary conditions, ψ_b must be equal to:

$$\psi_b(\tilde{x},\tilde{t}) = \tilde{x}\psi_{\tilde{x}}(0,\tilde{t}) + \frac{\tilde{x}^2}{2}\left(\psi_{\tilde{x}}(1,\tilde{t}) - \psi_{\tilde{x}}(0,\tilde{t})\right) = -\frac{\tilde{x}^2}{2}\sin(\omega_a\tilde{t})$$

By substituting 6.6 into the 6.4, one obtains a new system of equations in terms of ψ_s. Indeed:

$$\psi_{b_{\tilde{t}\tilde{t}}} + \psi_{s_{\tilde{t}\tilde{t}}} = \psi_{b_{\tilde{x}\tilde{x}}} + \psi_{s_{\tilde{x}\tilde{x}}} \tag{6.7}$$

With:

$$\psi_{b_{\tilde{t}\tilde{t}}} = \frac{\tilde{x}^2}{2}\omega_a^2\sin(\omega_a\tilde{t}), \quad \psi_{b_{\tilde{x}\tilde{x}}} = -\sin(\omega_a\tilde{t})$$

Leading to a new system of equations in terms of ψ_s:

$$\begin{cases} \psi_{s_{\tilde{t}\tilde{t}}} = \psi_{s_{\tilde{x}\tilde{x}}} - \frac{\tilde{x}^2}{2}\omega_a^2\sin(\omega_a\tilde{t}) - \sin(\omega_a\tilde{t}) \\ \psi_{s_{\tilde{x}}}(0,\tilde{t}) = 0 \\ \psi_{s_{\tilde{x}}}(1,\tilde{t}) = 0 \\ \psi_s(\tilde{x},0) = 0, \quad \psi_{s_t}(\tilde{x},0) = \frac{\tilde{x}^2}{2}\omega_a \end{cases} \tag{6.8}$$

Now the system is no longer homogeneous in the wave equation but it is homogeneous in Boundary Conditions and this simplifies a lot the calculations to find the analytical solution. The general solution for ψ_s is $\psi_s = \psi_{s,H} + \psi_{s,P}$, where $\psi_{s,H}$ is related to the homogeneous solution, while $\psi_{s,P}$ on the particular one. Since the absence of any kind of dissipation in the model will preserve the homogeneous part of the solution, which will corrupt the final result at steady state, one can neglect the homogeneous solution of the problem and solving only the particular one.
It is essential to mention that ignoring the homogeneous part of the solution could be acceptable for the approximation of the solution at steady state. Indeed, as previously mentioned in 5.3.1 a similar thing had been made in numerical simulations trying to minimize the effect of the homogeneous part of the solution through a modulation of the input signal, leading to a numerical representation of only the particular solution at steady state even in absence of any viscous effect.

Particular Solution

In particular, since the forcing function is in the form $v(\tilde{x})\sin(\omega_a t)$, one can use the separation of variables technique to find a particular solution in the form $\psi_{s_P} = v(\tilde{x})\sin(\omega_a t)$, leading to:

$$\omega_a^2 v(\tilde{x})\sin(\omega_a t) + v''(\tilde{x})\sin(\omega_a t) = \left(1 + \frac{\tilde{x}^2\omega_a^2}{2}\right)\sin(\omega_a t) \tag{6.9}$$

Canceling out the sine term, one gets an ODE in $\tilde{x}$:

$$\omega_a^2 v(\tilde{x}) + v''(\tilde{x}) = \left(1 + \frac{\tilde{x}^2\omega_a^2}{2}\right) \tag{6.10}$$

Leading to the general solution as:

$$v(\tilde{x}) = C_1 \sin(\omega_a \tilde{x}) + C_2 \cos(\omega_a \tilde{x}) + \frac{\tilde{x}^2}{2} \tag{6.11}$$

With boundary conditions $v'(0) = v'(1) = 0$, the constants are:

$$C_1 = 0, \quad C_2 = \frac{1}{\omega_a \sin(\omega_a)} \tag{6.12}$$

Finally:

$$v(\tilde{x}) = \frac{\cos(\omega_a \tilde{x})}{\omega_a \sin(\omega_a)} + \frac{\tilde{x}^2}{2} \tag{6.13}$$

So the solution will be:

$$\psi_{s_P}(\tilde{x}, t) = \left[\frac{\cos(\omega_a \tilde{x})}{\omega_a \sin(\omega_a)} + \frac{\tilde{x}^2}{2}\right]\sin(\omega_a \tilde{t}) \tag{6.14}$$

Complete Solution

Now it is possible to write the complete solution for $\psi_1(\tilde{x}, \tilde{t}) = \psi_b(\tilde{x}, \tilde{t}) + \psi_s(\tilde{x}, \tilde{t})$ that satisfies both the general equation and boundary conditions.

$$\psi_1(\tilde{x}, \tilde{t}) = \psi_b + \psi_{s_P} = -\frac{\tilde{x}^2}{2}\sin(\omega_a \tilde{t}) + \left[\frac{\cos(\omega_a \tilde{x})}{\omega_a \sin(\omega_a)} + \frac{\tilde{x}^2}{2}\right]\sin(\omega_a \tilde{t}) \tag{6.15}$$

That leads to:

$$\psi_1(\tilde{x}, \tilde{t}) = \frac{\cos(\omega_a \tilde{x})}{\omega_a \sin(\omega_a)}\sin(\omega_a \tilde{t}) \tag{6.16}$$

This result is already known in literature. Indeed, in [23] an attempt on finding the nonlinear expression for radiation pressure in a fixed domain was done and they started the analysis based on the solution above for the linear case and an oscillating piston on a side. The interesting part is the presence of a sinusoidal function at the denominator that make the denominator equals to zero at certain frequencies. From the definition in 6.3 the critical cases are:

$$\omega_a = \frac{\omega_f L}{c_0} = k\pi$$

If one would relate the driven frequency to the first resonant one, just recall the relationship used in 5.19 to know when resonance occurs:

$$\omega_a = \tilde{\omega}\omega_1 \frac{L}{c_0} = \tilde{\omega}\frac{2\pi c_0}{2L}\frac{L}{c_0} = k\pi$$

$$\tilde{\omega} = k, \quad k \in \mathbb{N}$$

And it is truly consistent with the result found in 5 where peaks towards infinity are located into integer values of $\tilde{\omega}$.
A similar form of the solution is present in [20] for open field, obviously there is no chance to face resonance conditions so the denominator is not a sine.

Radiation Pressure Expression in the Linear Case

It is now appropriate to articulate the solution for radiation pressure by utilizing the solution of the linear wave equation alongside a nonlinear expression for pressure. The first effort to ascertain the actual value of radiation pressure was undertaken by Lord King [8]. However, it will be demonstrated that this approximation is of the same order of magnitude as the actual solution.
From the dimensionless relationships one can come back to the actual velocity potential, indeed:

$$\varphi(x,t) = c_0 L \psi(\tilde{x},\tilde{t}) = c_0 L \varepsilon \psi_1(\tilde{x},\tilde{t})$$

$$\varphi(x,t) = \frac{c_0 L}{\omega_a}\frac{B}{c_0}\frac{\cos(\omega_a \tilde{x})\sin(\omega_a \tilde{t})}{\sin(\omega_a)} = \frac{c_0 B}{\omega_f}\frac{\cos\left(\frac{\omega_f}{c_0}x\right)\sin(\omega_f t)}{\sin\left(\frac{\omega_n L}{c_0}\right)} \tag{6.17}$$

By performing the time derivative of 6.17 one finds:

$$\varphi_t(x,t) = B c_0 \frac{\cos\left(\frac{\omega_f}{c_0}x\right)\sin(\omega_f t)}{\sin\left(\frac{\omega_n L}{c_0}\right)} \tag{6.18}$$

Let's see if this solution is consistent with theory. Indeed, if one would use the linear relationship between pressure and potential, one found that the mean value over a period is null. This is exactly what happens because 6.18 is a linear sinusoidal function which mean value is always zero. Indeed, assuming a period of $T = \frac{2\pi}{\omega_f}$ one gets:

$$\langle p_{\text{rad}}(x,t)\rangle = \frac{1}{T}\int_0^T \rho_0 \varphi_t(x,t)dt = \frac{\rho_0 B c_0}{T}\int_0^T \frac{\cos\left(\frac{\omega_f}{c_0}x\right)\sin(\omega_f t)}{\sin\left(\frac{\omega_n L}{c_0}\right)}dt = \frac{\rho_0 B c_0}{T\sin\left(\frac{\omega_n L}{c_0}\right)}\int_0^T \sin(\omega_f t)dt = 0$$

In case of Lord King's formula, where the Lagrangian function is involved, one gets a value different from zero:

$$\langle p_{\text{rad}}(x,t)\rangle = \rho_0\phi_t - \mathcal{L} = \rho_0\phi_t + \frac{\rho_0^2 c_0^2 \varphi_t^2(x,t)}{2} - \frac{\rho_0 \varphi_x^2(x,t)}{2} = \rho_0\phi_t + \frac{\rho_0^2 c_0^2 \varphi_t^2(x,t)}{2}$$

One can neglect the kinetic contribution at the fixed wall because this boundary condition must hold for every time:

$$u(0,t) = -\varphi_x(0,t) = 0$$

For this specific case, one gets a non-zero mean value indeed:

$$p_{\text{rad}}(x,t) = \frac{1}{T}\int_0^T \frac{\rho_0^2 c_0^2 \varphi_t^2(x,t)}{2}dt = \frac{\rho_0}{T}\int_0^T \frac{1}{2}\rho_0^2 c_0^2 \left(\frac{B c_0 \cos\left(\frac{\omega_f x}{c_0}\right)}{\sin\left(\frac{\omega_f L}{c_0}\right)}\cos(\omega_f t)\right)^2 dt$$

Since:

$$\frac{1}{T}\int_0^T \cos^2(\omega_f t)\,dt = \frac{1}{2} \quad \text{and} \quad T = \frac{2\pi}{\omega_f}$$

One finally gets:

$$\overline{p}_{\text{rad}} = \frac{\rho_0 B^2 \cos^2\left(\frac{\omega_f x}{c_0}\right)}{4\sin^2\left(\frac{\omega_f L}{c_0}\right)}$$

At the fixed boundary located at $x = 0$ the value is:

$$\overline{p}_{\text{rad}} = \frac{\rho_0 B^2}{4\sin^2\left(\frac{\omega_f L}{c_0}\right)} = E$$

Where E is the total energy density of the acoustic wave.

6.2.2 Order ε^2 Solution

The second order system is described by the equation:

$$\begin{cases} \psi_{2_{\tilde{t}\tilde{t}}} - \psi_{2_{\tilde{x}\tilde{x}}} = 2\psi_{1_{\tilde{x}}}\psi_{2_{\tilde{x}\tilde{t}}} \\ \psi_{2_{\tilde{x}}}(0,\tilde{t}) = 0 \\ \psi_{2_{\tilde{x}}}(1,\tilde{t}) = 0 \\ \psi_2(\tilde{x},0) = 0, \quad \psi_{2_t}(\tilde{x},0) = 0 \end{cases} \tag{6.19}$$

In this case, the ε^2 order system is completely homogeneous on boundary conditions. With this intention, it is possible to build the forcing functions $\psi_{2_{\tilde{x}\tilde{t}}}$, indeed knowing the partial derivatives and multiplying them together one obtains:

$$\psi_{1_{\tilde{x}}} = -\frac{\sin(\omega_a\tilde{x})\sin(\omega_a\tilde{t})}{\sin(\omega_a)}, \quad \psi_{1_{\tilde{x}\tilde{t}}} = -\omega_a\frac{\sin(\omega_a\tilde{x})\cos(\omega_a\tilde{x})}{\sin(\omega_a)}$$

Hence, one gets:

$$2\psi_{1_{\tilde{x}}}\psi_{1_{\tilde{x}\tilde{t}}} = 2\omega_a\frac{\sin^2(\omega_a\tilde{x})\cos(\omega_a\tilde{t})\sin(\omega_a\tilde{t})}{\sin^2(\omega_a)} = \omega_a\frac{\sin^2(\omega_a\tilde{x})\sin(2\omega_a\tilde{t})}{\sin^2(\omega_a)} \tag{6.20}$$

This simplifies our system to:

$$\begin{cases} \psi_{2_{\tilde{t}\tilde{t}}} - \psi_{2_{\tilde{x}\tilde{x}}} = \omega_a\frac{\sin^2(\omega_a\tilde{x})\sin(2\omega_a\tilde{t})}{\sin^2(\omega_a)} \\ \psi_{2_{\tilde{x}}}(0,\tilde{t}) = 0 \\ \psi_{2_{\tilde{x}}}(1,\tilde{t}) = 0 \\ \psi_2(\tilde{x},0) = 0, \quad \psi_{2_t}(\tilde{x},0) = 0 \end{cases} \tag{6.21}$$

This system of partial differential equation looks like to the general form treated in [92] where a general solution is given in terms of Green's function convolution:

$$\begin{cases} \psi_{2_{\tilde{t}\tilde{t}}} - \psi_{2_{\tilde{x}\tilde{x}}} = \Phi(\tilde{x},\tilde{t}) \\ \psi_{2_{\tilde{x}}}(0,\tilde{t}) = g_1(\tilde{t}) \\ \psi_{2_{\tilde{x}}}(1,\tilde{t}) = g_2(\tilde{t}) \\ \psi_2(\tilde{x},0) = f_0(\tilde{x}), \quad \psi_{2_t}(\tilde{x},0) = f_1(\tilde{x}) \end{cases} \tag{6.22}$$

Where $\Phi(x,t)$ is an arbitrary forcing function. The general solution, is given by the formula:

$$\psi_2(x,t) = \frac{\partial}{\partial \tilde{t}} \int_0^1 f_0(\xi) G(\tilde{x},\xi,\tilde{t})\, d\xi + \int_0^1 f_1(\xi) G(\tilde{x},\xi,\tilde{t})\, d\xi + \int_0^1 \int_0^{\tilde{t}} \Phi(\xi,\tau) G(\tilde{x},\xi,\tilde{t}-\tau)\, d\xi\, d\tau$$

$$- \int_0^{\tilde{t}} g_1(\tau) G(\tilde{x},0,\tilde{t}-\tau)\, d\tau + \int_0^{\tilde{t}} g_2(\tau) G(\tilde{x},L,\tilde{t}-\tau)\, d\tau \tag{6.23}$$

Where $G(x,\xi,t)$ is the Green's function for the wave equation in case of reflecting boundary conditions [93]:

$$G(\tilde{x},\xi,\tilde{t}) = \tilde{t} + \frac{2}{\pi} \sum_{n=1}^{\infty} \frac{1}{n} \cos(n\pi\tilde{x}) \cos(n\pi\xi) \sin(n\pi\tilde{t}) \tag{6.24}$$

The function $\Phi(x,t)$ for our specific case is simply:

$$\Phi(\tilde{x},\tilde{t}) = \omega_a \frac{\sin^2(\omega_a \tilde{x}) \sin(2\omega_a \tilde{t})}{\sin^2(\omega_a)} \tag{6.25}$$

by using the same notation, functions $g_1(t)$, $g_2(t)$, $f_0(x)$, and $f_1(x)$ are identically set to zero, simplifying the integration evaluation of 6.23 and resulting in:

$$\psi_2(\tilde{x},\tilde{t}) = \int_0^1 \int_0^{\tilde{t}} \Phi(\xi,\tau) G(\tilde{x},\xi,\tilde{t}-\tau)\, d\xi\, d\tau \tag{6.26}$$

Then by substituting the actual forcing function, one obtains:

$$\psi_2(\tilde{x},\tilde{t}) = \int_0^1 \int_0^{\tilde{t}} \omega_a \frac{\sin^2(\omega_a \tilde{x}) \sin(2\omega_a \tau)}{\sin^2(\omega_a)} \left(\tilde{t}-\tau\right)\, d\xi\, d\tau +$$

$$\int_0^1 \int_0^{\tilde{t}} \omega_a \frac{\sin^2(\omega_a \xi) \sin(2\omega_a \tilde{t})}{\sin^2(\omega_a)} \left[\frac{2}{\pi} \sum_{n=1}^{\infty} \frac{1}{n} \cos(n\pi\tilde{x}) \cos(n\pi\xi) \sin(n\pi(\tilde{t}-\tau))\right] d\xi\, d\tau \tag{6.27}$$

Then, by solving the integration one obtain the solution for the second order system:

$$\psi_2(\tilde{x},\tilde{t}) = \frac{\omega_a}{\sin^2(\omega_a)} \left[\frac{(\sin(2\omega_a\tilde{t}) - 2\tilde{t}\omega_a)(\sin(2\omega_a) - 2\omega_a)}{16\omega_a^3}\right] +$$

$$\sum_{n=1}^{\infty} \frac{4(-1)^{n+1}\omega_a^2 \cos(\pi n\tilde{x})}{n\pi \tan(\omega_a)(4\omega_a^2 - n^2\pi^2)^2} \left[2\omega_a \sin(n\pi\tilde{t}) - n\pi \sin(2\omega_a\tilde{t})\right], \text{for}\, \omega_a \neq \frac{n_i\pi}{2} \tag{6.28}$$

The second part of the solution appears to yield no mean value over a period due to the presence of linear sinusoidal functions, which inherently possess a zero mean value over their respective

periods. However, the derived expression seems to become undefined in the specific case where $\omega_a = \frac{r\pi}{2}$ with $r = n_i$.

This scenario, in which the denominator approaches zero, can be circumvented because it occurs when the excitation frequency coincides with the resonance frequency of the tube, a condition that is prohibited by hypothesis. The alternative situation arises when the excitation frequency is precisely situated between two resonance frequencies, resulting in a modified form of the additional term in 6.28 as follows:

$$-\cos(r\pi\tilde{x})\frac{(\sin(r\pi\tilde{t}) - r\pi\tilde{t}\cos(r\pi\tilde{t}))}{8c_0 r\pi((-1)^r - 1)} \tag{6.29}$$

The solution presented bears a striking resemblance to scenarios in which secular terms emerge in perturbation method problems, necessitating careful treatment. It appears to exhibit a mean value that deviates from zero, which must be taken into account when evaluating radiation pressure. The term under consideration is:

$$r\tilde{t}\cos(r\pi\tilde{t})$$

Indeed, after the time derivative it becomes:

$$r\cos(r\pi\tilde{t}) - r^2\pi\tilde{t}\sin(r\pi\tilde{t})$$

The mean value is significantly influenced by the evaluation period, with the sign of the contribution also contingent upon the value of r.

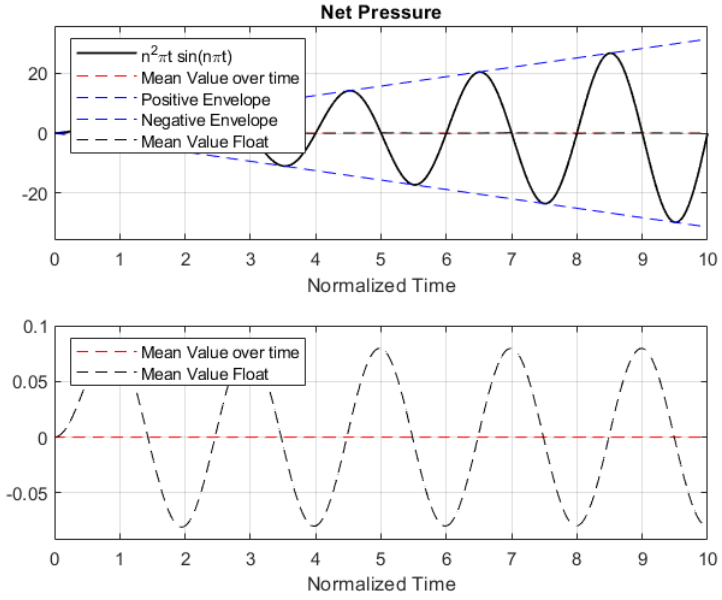

Figure 6.1. Solution over Time and mean value trend

In practice, although the mean value over a specific period may appear to deviate from zero, the overall mean contribution tends to stabilize around zero, as illustrated in figure 6.1. Consequently, this stabilization is of little relevance for the assessment of radiation pressure. Since a

zero mean value is expected in the calculation of radiation pressure, one can disregard the entire second part of the solution associated with the infinite summation. Furthermore, the validity of this type of solution is confined to short time intervals, rendering that term relatively negligible in our context.
Given this consideration, the approximate solution derived from the perturbation method is expressed as the sum of 6.28 and 6.16.

$$\psi(\tilde{x},\tilde{t}) = \varepsilon\psi_1(\tilde{x},\tilde{t}) + \varepsilon^2\psi_2(\tilde{x},\tilde{t}) + o(\varepsilon^3)$$

$$\psi(\tilde{x},\tilde{t}) \simeq \varepsilon\frac{\cos(\omega_a\tilde{x})}{\omega_a\sin(\omega_a)}\sin(\omega\tilde{t}) + \varepsilon^2\frac{\omega_a}{\sin^2(\omega_a)}\left[\frac{(\sin(2\omega_a\tilde{t}) - 2\tilde{t}\omega_a)(\sin(2\omega_a) - 2\omega_a)}{16\omega_a^3}\right] \tag{6.30}$$

Radiation Pressure: Final Expression

In order to get back to physical quantities, it is necessary to substitute back the opposite relations one used at the beginning of the chapter. In so doing, one gets:

$$\varphi(x,t) = c_0L\psi(\tilde{x},\tilde{t}) = c_0L\left\{\varepsilon\frac{\cos(\omega_a\tilde{x})}{\omega_a\sin(\omega_a)}\sin(\omega\tilde{t}) + \varepsilon^2\frac{\omega_a}{\sin^2(\omega_a)}\left[\frac{(\sin(2\omega_a\tilde{t}) - 2\tilde{t}\omega_a)(\sin(2\omega_a) - 2\omega_a)}{16\omega_a^3}\right]\right\} \tag{6.31}$$

Then, let's substitute the relation for ω_a, ε, $\tilde{x}$ and $\tilde{t}$ to obtain the physical velocity potenital:

$$\varphi(x,t) = \frac{Bc_0}{\omega_f}\frac{\cos\left(\frac{\omega_f x}{c_0}\right)\sin(\omega_f t)}{\sin\left(\frac{\omega_f L}{c_0}\right)} + \frac{B^2}{\sin^2\left(\frac{\omega_f L}{c_0}\right)}\left[\frac{(\sin(2\omega_f t) - 2t\omega_f)(c_0\sin\left(2\frac{\omega_f L}{c_0}\right) - 2\omega_f L)}{16\omega_f^2 L}\right] \tag{6.32}$$

Since pressure is expressed in terms of the derivative of potential, one must evaluate the time derivative:

$$\varphi_t = \varphi_{1_t} + \varphi_{2_t} = Bc_0\frac{\cos\left(\frac{\omega_f x}{c_0}\right)\cos(\omega_f t)}{\sin\left(\frac{\omega_f L}{c_0}\right)} + \frac{B^2}{\sin^2\left(\frac{\omega_f L}{c_0}\right)}\left[\frac{(2\omega_f\cos(2\omega_f t) - 2\omega_f)(c_0\sin\left(2\frac{\omega_f L}{c_0}\right) - 2\omega_f L)}{16\omega_f^2 L}\right] \tag{6.33}$$

Finally, to get the net radiation pressure at the fixed boundary, a time average over the period $T = \frac{2\pi}{\omega_f}$ is necessary. Now, if the time average is performed over the period T,$\langle\varphi_{1_t}\rangle = 0$, the $\cos(2\omega_f t)$ part in φ_{2_t} placed at the numerator of the second order solution is identically zero while the remaining part appears to be constant:

$$\langle\varphi_{2_t}\rangle = \frac{1}{T}\int_0^T \varphi_{2_t}dt = \frac{B^2}{\sin^2\left(\frac{\omega_f L}{c_0}\right)}\left[\frac{4\omega_f^2 L - 2\omega_f c_0\sin\left(\frac{2\omega_f L}{c_0}\right)}{16\omega_f^2 L}\right] = \frac{B^2}{4\sin^2\left(\frac{\omega_f L}{c_0}\right)}\left[1 - \frac{c_0\sin\left(\frac{2\omega_f L}{c_0}\right)}{2\omega_f L}\right] \tag{6.34}$$

Now, concerning the Lagrangian part of the radiation pressure definition one consideration should be made. Before proceeding further, it would be good practice to not have too many terms in the radiation expression to make a critical analysis of the main terms. Indeed, different order of magnitude between the terms appears in the complete expression. In one hand, the

first-order solution is proportional to Bc_0, while the second order one is proportional to B^2. That leads to neglect the second order contribution into the quadratic term in the potential energy term $U = \frac{\rho_0}{2c_0^2}\varphi_t^2$, this passage leads to a slight loss of accuracy in the final analytical result but allows for a very simple expression to study later on. So one can state that:

$$\langle \varphi_t^2 \rangle \simeq \langle \varphi_{1_t}^2 \rangle \tag{6.35}$$

On the opposite hand, $\langle \varphi_t \rangle$ seems to dramatically contribute in the linear part of the radiation pressure expression. Indeed, while the first-order solution has a zero-mean value, the second order one does not, leading to almost twice the value of the radiation pressure considering the linear acoustic field solution. For this reason, it is necessary to consider the second order solution in the pressure expression. By putting everything together, the final expression for the mean value of the radiation pressure is:

$$\overline{p}_{rad} = \frac{B^2}{4\sin^2\left(\frac{\omega_f L}{c_0}\right)}\left[1 - \frac{c_0 \sin\left(\frac{2\omega_f L}{c_0}\right)}{2\omega_f L}\right] + \frac{B^2}{4\sin^2\left(\frac{\omega_f L}{c_0}\right)} = \frac{B^2}{4\sin^2\left(\frac{\omega_f L}{c_0}\right)}\left[2 - \frac{c_0 \sin\left(\frac{2\omega_f L}{c_0}\right)}{2\omega_f L}\right] \tag{6.36}$$

The ratio between the fully non-linear acoustic field solution and the linear field solution using the same expression for the radiation pressure is:

$$\mu = \frac{\overline{p}_{rad}}{\overline{p}_{rad_{lin}}} = 2 - \frac{c_0 \sin\left(\frac{2\omega_f L}{c_0}\right)}{2\omega_f L}$$

The $\frac{\omega_f L}{c_0}$ ratio is the well-known Helmholtz number $He = kL = \frac{\omega_f L}{c_0}$. Hence, the ration becomes:

$$\mu = 2 - \frac{\sin(2He)}{2He} \tag{6.37}$$

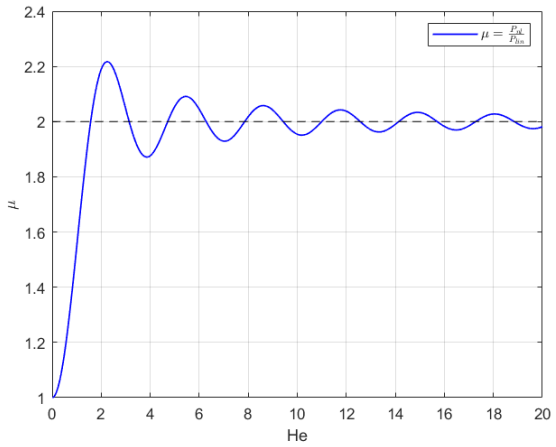

Figure 6.2. μ over Helmholtz number

In the limit of high Helmholtz number, the limits tend to:

$$\lim_{He \to \infty} \mu = 2 \tag{6.38}$$

While for low Helmholtz number, nonlinear and linear acoustic theory collapse to the same result. Indeed:

$$\lim_{He \to 0} \mu = 1 \tag{6.39}$$

The results found in 6.38 means that for a fixed geometry, namely L, non-linearity is playing an important role at high frequency while it is not in case of low frequencies 6.39 collapsing to the results of Lord King's.

6.2.3 Results Comparison: Analytical vs Numerical

In this section, the comparison graphs between the results of the tests conducted in 5.3.2 and the pressure trends predicted by formula 6.36 are presented.

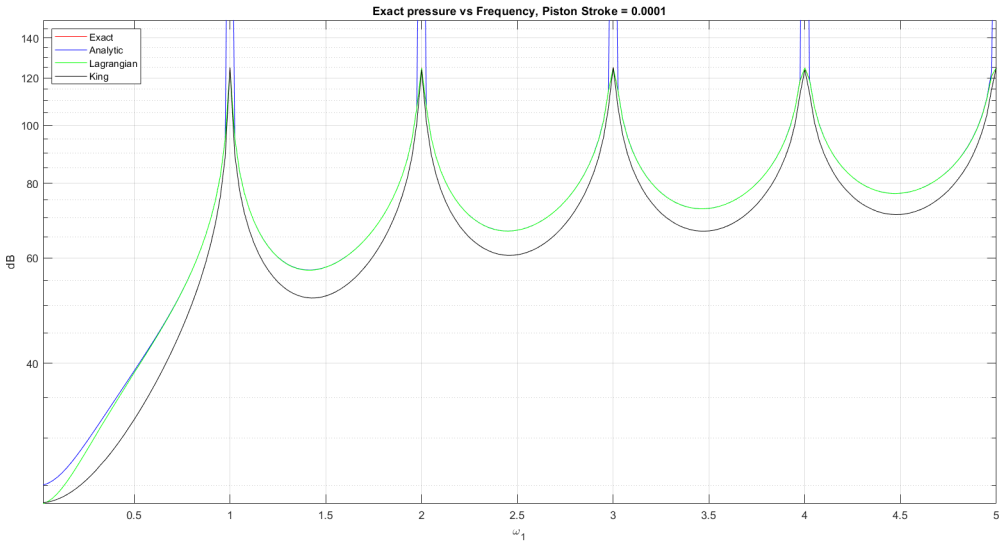

Figure 6.3. Radiation Pressure over frequency Comparison

As is clearly shown in the two figures above, the analytical formula proves to be extremely accurate and yields results very similar to the numerical ones.

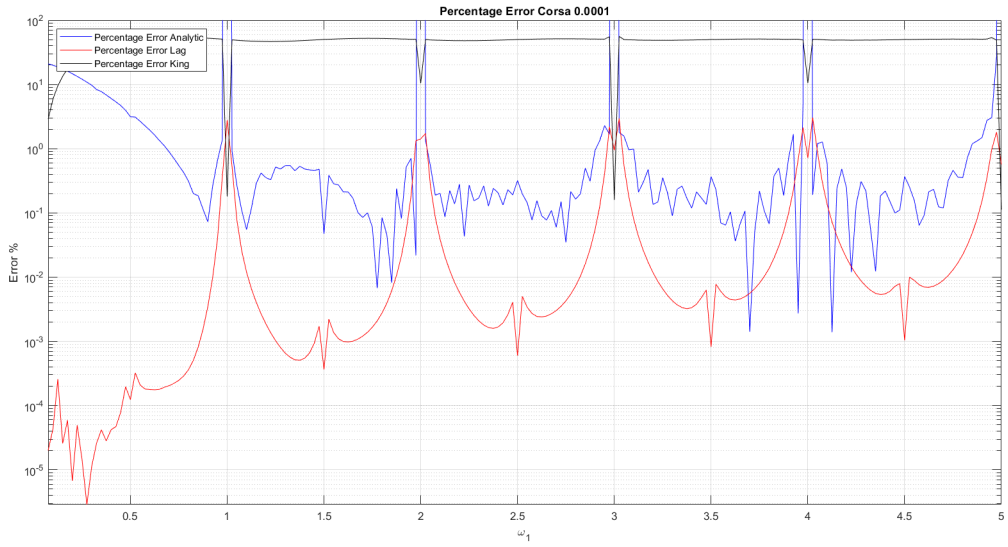

Figure 6.4. Error over frequency

Except for the resonance frequencies and those in their vicinity ($\pm 0.05\,\omega_1$), the error is always below 1%. This demonstrates the validity of the analytical result and how it can facilitate the development of a semi-analytical model on which to implement a control strategy.

6.3 The problem of the moving boundary

While in the previous Section 6.2 the problem of a fixed reflected screen was investigated, the problem of a moving boundary subjected to an acoustic wave is finally analysed. Indeed, the study of wave equations with moving boundaries is essential to understand how waves interact with free bodies and how the interaction force is possibly modified by the boundary's speed.

This problem is relevant in various fields such as acoustics, electromagnetism, and fluid dynamics and the main challenge lies in solving wave equations where the domain changes over time due to the movement of boundaries, which can either be in uniform motion or exhibit acceleration [94]. The leading goal is to predict how wave properties such as amplitude, frequency, and phase shift when they encounter moving boundary and which kind of influence they produce on its motion.

This phenomena is very complex and has deep historical roots in scientific literature either in case of acoustic or electromagnetic waves. Concerning acoustic interaction between bodies at constant speed and waves, Doppler [95] gave a fundamental contribution as well as Einstein [96] for the electromagnetic counterpart. However, the problem of finding the exact solution for arbitrarily moving boundary is still under debate for its intrinsic complexity and uncertainty on mathematical passages. Moreover, the problem is often split in two different parts, one related to the generation of waves from moving boundaries and one related to the nonlinear interactions

of a moving wall under the effect of incoming and reflected wave.
Many works as the one of Balazas [97] or Gaffour [98] treated the problem of generation of waves in semi-infinite, or finite domain, caused by a moving wall at constant speed $v << c_0$. Even though it appears to be an easy case at first, the found solutions were quite tricky. Later on, Dan Censor analyzed the effect of incoming waves on a moving wall with different speed in his works [99, 100]. He showed as, for constant boundary speed, the wave equation solution seems to be modified by a Doppler coefficient that modifies the frequency of the reflected wave as expected from Doppler effect's theory . Later on, he demonstrated how to improve its method considering also a sinusoidal component of the speed of the boundary to see how the reflected wave's frequency would be different from the case of constant speed. In addition, he also studied a solution for oblique incident waves case on sinusoidally oscillating bodies.
These contributions belongs to a class of works where the boundary movement is assigned *a priori*. Who instead went further was Cooper that analyzed the general case of electromagnetic waves impinging on an arbitrary wall with arbitrary speed [101]. He started his analysis founding the exact equations for the electromagnetic field, as valid as for the acoustic counterpart, in case of rigid body in a arbitrary position r_0 ion case of perfect reflecting wall. By calling $\Psi(x,t)$ the general solution of electromagnetic field, he found that:

$$\Psi(x,t) = Ae^{i(\omega t - kx)}e^{2ikr_0} \tag{6.40}$$

Where r_0 is the position of the wall with respect of a generic coordinate system. At the same time, in case of moving boundary with constant velocity defined as v, the solution assumes the form obtained by Lorentz and in agreement with the results of Doppler shift in frequency:

$$\Psi(x,t) = A\left[\frac{1+\frac{v}{c}}{1-\frac{v}{c}}\right]\exp\left\{i\left[\left(\frac{1+\frac{v}{c}}{1-\frac{v}{c}}\right)(\omega t - kx) + 2ik\left(\frac{r_0 - vt}{1-\frac{v}{c}}\right)\right]\right\} \tag{6.41}$$

He stated that in case of non-stationary boundary, or it does not move with a constant velocity, the exact solution cannot be computed in a simple way because it involves the solution itself to define the actual position of the boundary leading to a sort of loop of information that cannot be solved analytically. However, he considered what he called the quasi-stationary approximation that consists on substituting the actual value of the position of the boundary in the solution of 6.40, leading to a solution that satisfies Maxwell's equation to the order $\beta = \frac{v(t)}{c_0}$. Further on the paper, he introduced a second order approximation called Uniform Doppler Approximation that regards the solution of 6.41. Indeed, substituting the actual value of the speed one can obtain a solution whose error would be of the order $\gamma = \frac{a}{c_0^2}$.
These two approximations, in case of sinusoidal moving boundary, lead to the same order of accuracy and for very small quantities it provides very good results. For this reason, taking into account the symmetry of acoustic and electromagnetic fields and solutions and the fact that $\frac{v}{c_0} \ll 1$, these approximations will be used in the next passages to find the solution of the moving boundary problem.

6.3.1 Linear Impedance Representation

In this very first case, the solution of the oscillating piston and a free moving wall problem in a tube will be found in terms of particle velocity. There are three main reasons to justify this approach with respect of solving the exact same problem in terms of velocity potential as it was for the fixed boundary case:

- Simplicity of boundary conditions: in case of particle velocity the boundary conditions are of Dirichlet's type instead of Neumann's reducing the complexity of the analytical passages to find the solution;
- Kinematic conditions: the kinematic of the wall can be directly related to the acoustic impedance at the moving wall in terms of mass, stiffness and coupling between the body and the fluid;
- Equivalence of the solution: the linear solution found in terms of velocity potential can be recovered by using the linear relationship: $\varphi_t(x,t) = -\int c_0^2 u_x(x,t)dt$.

Linear Problem

Let's analyse the case in which the perfect reflector is free to move and it is represented numerically by an acoustic impedance $Z_w = r + j\omega_f M - j\frac{k_s}{m}$. r, k and M are respectively the a global friction coefficient that includes the fluid-structure loading value $\rho_0 c_0$, a possible stiffness of the system and the mass of the reflector. By using the linear relationship for plane waves $Z_w = \frac{p}{u}$ one can write the new system with this new boundary condition approximated to the first order:

$$\begin{cases} u_{tt} = c_0^2 u_{xx} \\ u(x_w,t) = -\frac{p(x_w,t)}{r+j\left(\omega_f M - \frac{k_s}{\omega_f}\right)} \\ u(L,t) = A(t) \\ u(x,0) = 0, \quad u_t(x,0) = 0 \end{cases} \tag{6.42}$$

Where x_w is the location of the moving wall. Even in this case, one can split the solution for $u(x,t) = u_1(x,t) + u_2(x,t)$ where $u_1(x,t)$ always satisfies boundary conditions. In this case, $u_1(x,t)$ looks like:

$$u_1(x,t) = A(t)\left(\frac{x-x_w}{L-x_w}\right) - \frac{p(x_w,t)}{r+j\left(\omega_f M - \frac{k_s}{\omega_f}\right)}\left(\frac{L-x}{L-x_w}\right)$$

and, using the quasi-uniform approximation as in [101] one can assume $\dot{x}_w \simeq 0$, leading to:

$$u_{1_{tt}}(x,t) = \ddot{A(t)}\left(\frac{x-x_w}{L-x_w}\right) - \frac{\ddot{p}(x_w,t)}{r+j\left(\omega_f M - \frac{k_s}{\omega_f}\right)}\left(\frac{L-x}{L-x_w}\right)$$

In this case, harmonic boundary conditions in time are assumed for both the piston and the moving wall. Since the problem is linear at this stage, it is assumed that the pressure at the

moving wall has the same frequency as the oscillating piston, with a phase shift to be evaluated later. A complex representation is used to simplify the computations in deriving the solution. Specifically: $u(L,t) = Be^{j\omega_f t}$ and $p(x_w,t) = p(x_w)e^{j(\omega_f t+\Phi)}$.
Since the primary interest lies in the steady-state solution, initial conditions are no longer considered as part of the system. With these considerations, the system becomes:

$$\begin{cases} u_{2_{tt}} = c_0^2 u_{2_{xx}} + \frac{B\omega_f^2(x-x_w)}{L-x_w}e^{j\omega_f t} + \frac{\omega_f^2 p(x_w)}{r+j\left(\omega_f M - \frac{k_s}{\omega_f}\right)}\left(\frac{x-L}{L-x_w}\right)e^{j(\omega_f t+\Phi)} \\ u_2(x_w,t) = 0 \\ u_2(L,t) = 0 \end{cases} \tag{6.43}$$

Whereas the problem is linear in u_2, the solution can be split into two parts: one related to the first forcing term $\frac{B\omega_f^2(x-x_w)}{L-x_w}e^{j\omega_f t}$ and the other to the second forcing term $\frac{\omega_f^2 p(x_w)}{r+j\left(\omega_f M - \frac{k}{\omega_f}\right)}\left(\frac{x-L}{L-x_w}\right)e^{j(\omega_f t+\Phi)}$.
The solution is fairly straightforward, and after a few simple mathematical steps, the complete solution is obtained:

$$u(x,t) = B\frac{\sin\left(\frac{\omega_f(x-x_w)}{c_0}\right)}{\sin\left(\frac{\omega_f(L-x_w)}{c_0}\right)}e^{j\omega_f t} - \frac{p(x_w)}{r+j\left(\omega_f M - \frac{k_s}{\omega_f}\right)}\frac{\sin\left(\frac{\omega_f(L-x)}{c_0}\right)}{\sin\left(\frac{\omega_f(L-x_w)}{c_0}\right)}e^{j(\omega_f t+\Phi)} \tag{6.44}$$

That satisfies both boundary conditions and the wave equation. It claims that there are two standing waves present in the tube. To simplify the notation, one writes:

$$k = \frac{\omega_f}{c_0}$$

In light of the assumption of symmetry between the particle velocity and the potential solutions, one can derive the expression for the potential. According to linear theory, one can express this relationship as follows:

$$\varphi_t(x,t) = -\int c_0^2 u_x(x,t)dt$$

Hence, the spatial derivative of 6.44 is:

$$u_x(x,t) = \frac{B\omega_f}{c_0}\frac{\cos\left(k(x-x_w)\right)}{\sin\left(k(L-x_w)\right)}e^{j\omega_f t} + \frac{p(x_w)\omega_f}{c_0\left(r+j\left(\omega_f M - \frac{k_s}{\omega_f}\right)\right)}\frac{\cos\left(k(L-x)\right)}{\sin\left(k(L-x_w)\right)}e^{j(\omega_f t+\Phi)} \tag{6.45}$$

and after time integration, the result follows:

$$\varphi_t(x,t) = jBc_0\frac{\cos\left(k(x-x_w)\right)}{\sin\left(k(L-x_w)\right)}e^{j\omega_f t} + j\frac{p(x_w)c_0}{\left(r+j\left(\omega_f M - \frac{k_s}{\omega_f}\right)\right)}\frac{\cos\left(k(L-x)\right)}{\sin\left(k(L-x_w)\right)}e^{j(\omega_f t+\Phi)} \tag{6.46}$$

At this juncture, it appears that the solution is self-referential. To mitigate this issue, one may consider the definition of linear pressure to ascertain the value at the boundary of the moving wall.

$$p(x_w,t) = \rho_0\varphi_t(x_w,t)$$

In so doing, one is able to find the magnitude and phase of the pressure at the wall. Indeed:

$$p(x_w)\left[\frac{\left(r+j\left(\omega_f M-\frac{k_s}{\omega_f}\right)\right)\sin(k(L-x_w))-j\rho_0c_0\cos(k(L-x_w))}{\left(r+j\left(\omega_f M-\frac{k_st}{\omega_f}\right)\right)\sin(k(L-x_w))}\right]e^{\Phi}=\frac{jBc_0\rho_0}{\sin(k(L-x_w))}$$

$$p(x_w)e^{\Phi}=\frac{jBc_0\rho_0\left(r+j\left(\omega_f M-\frac{k_s}{\omega_f}\right)\right)}{\left(r+j\left(\omega_f M-\frac{k_s}{\omega_f}\right)\right)\sin(k(L-x_w))-j\rho_0c_0\cos(k(L-x_w))}$$

At this stage, it is observed that the pressure at the moving wall is represented as a complex quantity. Therefore, consideration will be given to its magnitude and phase.

$$|p(x_w)|=Bc_0\rho_0\frac{\sqrt{r^2+\left(\omega_f M-\frac{k_s}{\omega_f}\right)}}{\sqrt{\left(r\sin(k(L-x_w))\right)^2+\left[\left(\omega_f M-\frac{k_s}{\omega_f}\right)\sin(k(L-x_w))-\rho_0c_0\cos(k(L-x_w))\right]^2}} \tag{6.47}$$

$$\Phi=\frac{\pi}{2}+\arctan\left(\frac{\omega_f M-\frac{k_s}{\omega_f}}{r}\right)-\arctan\left(\frac{\left(\omega_f M-\frac{k_s}{\omega_f}\right)\sin(k(L-x_w))-\rho_0c_0\cos(k(L-x_w))}{r\sin(k(L-x_w))}\right) \tag{6.48}$$

To simplify the expression one uses:

$$\gamma=\arctan\left(\frac{\omega_f M-\frac{k_s}{\omega_f}}{r}\right)-\arctan\left(\frac{\left(\omega_f M-\frac{k_s}{\omega_f}\right)\sin(k(L-x_w))-\rho_0c_0\cos(k(L-x_w))}{r\sin(k(L-x_w))}\right)$$

to get:

$$\Phi=\frac{\pi}{2}+\gamma$$

Now, it is possible to write the equation for the potential by substituting magnitude and phase into 6.46. Indeed, one obtains:

$$\varphi_t(x,t)=jBc_0\frac{\cos\left(k(x-x_w)\right)}{\sin\left(k(L-x_w)\right)}e^{j\omega_f t}+ \tag{6.49}$$

$$j\frac{Bc_0^2\rho_0\left(r-j\left(\omega_f M-\frac{k_s}{\omega_f}\right)\right)\frac{\cos(k(L-x))}{\sin(k(L-x_w))}e^{j(\omega_f t+\Phi)}}{\sqrt{\left[r^2+\left(\omega_f M-\frac{k_s}{\omega_f}\right)^2\right]\left[\left(r\sin(k(L-x_w))\right)^2+\left[\left(\omega_f M-\frac{k_s}{\omega_f}\right)\sin(k(L-x_w))-\rho_0c_0\cos(k(L-x_w))\right]^2\right]}}$$

Or it can be written collecting the plane wave impedance value ρ_0c_0:

$$\varphi_t(x,t)=jBc_0\frac{\cos\left(k(x-x_w)\right)}{\sin\left(k(L-x_w)\right)}e^{j\omega_f t}+ \tag{6.50}$$

$$j\frac{Bc_0\left(\frac{r}{\rho_0c_0}-j\frac{\omega_f M-\frac{k_s}{\omega_f}}{\rho_0c_0}\right)\frac{\cos(k(L-x))}{\sin^2(k(L-x_w))}e^{j(\omega_f t+\Phi)}}{\sqrt{\left[\left(\frac{r}{\rho_0c_0}\right)^2+\left(\frac{\omega_f M-\frac{k_s}{\omega_f}}{\rho_0c_0}\right)^2\right]\left[\left(\frac{r}{\rho_0c_0}\right)^2+\left[\left(\frac{\omega_f M-\frac{k_s}{\omega_f}}{\rho_0c_0}\right)-\cot(k(L-x_w))\right]^2\right]}}$$

Let's call:

$$R = \frac{r}{\rho_0 c_0}, \quad E = \frac{\omega_f M - \frac{k_s}{\omega_f}}{\rho_0 c_0}, \quad W = E - \cot(k(L - x_w))$$

$$A^2 = \left[\left(\frac{r}{\rho_0 c_0}\right)^2 + (E - \cot(k(L - x_w)))^2\right] = \left[R^2 + W^2\right]$$

to simplify 6.50:

$$\varphi_t(x,t) = jBc_0 \frac{\cos\left(k(x - x_w)\right)}{\sin\left(k(L - x_w)\right)} e^{j\omega_f t} - \frac{Bc_0(R - jE)}{A\sqrt{(R^2 + E^2)}} \frac{\cos(k(L - x))}{\sin^2(k(L - x_w))} e^{j(\omega_f t + \gamma)} \tag{6.51}$$

At this point, the imaginary part of the pressure at the boundary will be extracted. In fact, the scenario involving a perfectly reflecting wall presents a sinusoidal forcing function at the boundary. Consequently, to facilitate comparison of the results, it becomes necessary to retain the imaginary part of the solution.

$$p(x_w,t) = Bc_0\rho_0 \frac{\sqrt{R^2 + E^2}}{A} \frac{\cos(\omega_f t + \gamma)}{\sin(k(L - x_w))} \tag{6.52}$$

Then, using $\varphi_t(x_w,t) = \frac{p(x_w,t)}{\rho_0}$, and calling $\chi = \frac{\sqrt{R^2+E^2}}{A}$ one gets the potential at the boundary:

$$\varphi_t(x_w,t) = \chi Bc_0 \frac{\cos(\omega_f t + \gamma)}{\sin(k(L - x_w))} \tag{6.53}$$

With this in mind, it is possible to evaluate the radiation pressure by using the King's formula:

$$p_{rad} = \rho_0 \varphi_t + \frac{\rho_0^2 \varphi_t^2}{2c_0^2}$$

As a first step, one neglects the kinetic part of the pressure that will be take into account later on in this section. The time average of the simple harmonic functions is always zero, so one has to consider only the quadratic term for the time derivative potential.

$$\overline{p}_{rad} = \frac{1}{T}\int_0^T \frac{\rho_0^2}{2c_0^2}\left(\frac{\chi Bc_0}{\sin(k(L - x_w))}\right)^2 \cos^2(\omega_f t + \gamma)dt = \frac{\rho B^2 \chi^2}{4\sin^2(He)} = \chi^2 \overline{p_{rad}}_{rig} \tag{6.54}$$

Where $He = k(L - x_w)$ and $\chi^2 = \frac{R^2+E^2}{A^2}$. Therefore, in the limit of high impedance one recovers the case of perfectly rigid panel, indeed:

$$\lim_{R,E,A\to\infty} \chi^2 = 1$$

Now, in order to pass to the non-system and to apply the perturbation method as in 6.2 one has to recover the solution in velocity potential. Then the application of perturbation method will be straightforward due to the symmetry between particle velocity and velocity potential. Since:

$$\varphi_t(x,t) = jBc_0 \frac{\cos\left(k(x - x_w)\right)}{\sin\left(k(L - x_w)\right)} e^{j\omega_f t} - \frac{Bc_0(R - jE)}{A\sqrt{(R^2 + E^2)}} \frac{\cos(k(L - x))}{\sin^2(K(L - x_w))} e^{j(\omega_f t + \gamma)}$$

I can simplify the denominator of the second term calling $C = \sin^2(k(L - x_w))\sqrt{R^2 + E^2}A$. Now the solution looks like:

$$\varphi_t(x,t) = jBc_0\frac{\cos\left(k(x-x_w)\right)}{\sin\left(k(L-x_w)\right)}e^{j\omega_f t} - \frac{Bc_0(R-jE)}{C}\cos(k(L-x))e^{j(\omega_f t+\gamma)}$$

If one performs the time integration, the solution in terms of potential will be:

$$\varphi(x,t) = \frac{Bc_0}{\omega_f}\frac{\cos\left(k(x-x_w)\right)}{\sin\left(k(L-x_w)\right)}e^{j\omega_f t} + j\frac{Bc_0(R-jE)}{\omega_f C}\cos(k(L-x))e^{j(\omega_f t+\gamma)}$$

And for the case of sinusoidal excitation, the result is:

$$\varphi(x,t) = \frac{Bc_0}{\omega_f}\frac{\cos\left(k(x-x_w)\right)}{\sin\left(k(L-x_w)\right)}\sin(\omega_f t) + \frac{Bc_0R}{\omega_f C}\cos(k(L-x))\cos(\omega_f t+\gamma) + \frac{Bc_0E}{\omega_f C}\cos(k(L-x))\sin(\omega_f t+\gamma) \tag{6.55}$$

6.3.2 Non-linear Solution

In this case as well, it is necessary to find the second-order solution, as done previously, by introducing a parameter ε and directly applying the perturbation method.

$$\begin{cases} \varphi_{tt} - \varphi_{xx}(c_0^2 - \varphi_x^2) = 2\varphi_x\varphi_{xt} \\ \varphi_x(x_w,t) = \frac{p(x_w,t)}{r+j\left(\omega_f M - \frac{k_s}{\omega_f}\right)} \\ \varphi_x(L,t) = -A_p(t) \\ \varphi(x,0) = 0, \quad \varphi_t(x,0) = 0 \end{cases} \tag{6.56}$$

Indeed, the problem is completely analogous to the previous one for a fixed wall and can also be divided into one part referring to the solution of order ε and another with a solution of order ε^2. In this case, it is preferable to divide the solution this way to simplify the calculations:

$$\varphi(x,t) = \varphi_0(x,t) + \varphi_1(x,t)$$

Where $\varphi_0(x,t)$ is of order ε and φ is of order ε^2.

Order ε

Without resorting to dimensionless variables, the first-order system is illustrated directly, with its solution equivalent to that shown above in 6.55. The system appears as:

$$\begin{cases} \varphi_{0_{tt}} = c_0^2\varphi_{0_{xx}} \\ \varphi_{0_x}(x_w,t) = \frac{p(x_w,t)}{r+j\left(\omega_f M - \frac{k_s}{\omega_f}\right)} \\ \varphi_{0_x}(L,t) = -A(t) \\ \varphi_0(x,0) = 0, \quad \varphi_{0_t}(x,0) = 0 \end{cases} \tag{6.57}$$

The only difference with respect to 6.42 is the change of sign at the boundary since by definition $\nabla\varphi = -u$. Considering the symmetry of the solutions, one has:

$$\varphi_0(x,t) = \frac{Bc_0}{\omega_f}\frac{\cos\left(k(x-x_w)\right)}{\sin\left(k(L-x_w)\right)}\sin(\omega_f t)+\frac{Bc_0R}{\omega_f C}\cos(k(L-x))\cos(\omega_f t+\gamma)+\frac{Bc_0E}{\omega_f C}\cos(k(L-x))\sin(\omega_f t+\gamma)$$

Now, let's use this result to evaluate the solution at second order.

Order ε^2

Since the application of the method is straightforward, one proceed by directly calculating the solution for the variable φ_1.

$$\begin{cases} \varphi_{1_{tt}} - \varphi_{1_{xx}}(c_0^2 - \varphi_{0_x}^2) = 2\varphi_{0_x}\varphi_{1_{xt}} \\ \varphi_{1_x}(x_w,t) = 0 \\ \varphi_{1_x}(L,t) = 0 \\ \varphi_1(x,0) = 0, \quad \varphi_{1_t}(x,0) = 0 \end{cases} \tag{6.58}$$

Now, let's evaluate the derivatives present on the nonlinear wave equation inhomogeneous term:

$$\varphi_{0_x}(x,t) = -B\frac{\sin\left(k(x-x_w)\right)}{\sin\left(k(L-x_w)\right)}\sin(\omega_f t)+\frac{BR}{C}\cos(k(L-x))\cos(\omega_f t+\gamma)+\frac{BE}{C}\sin(k(L-x))\sin(\omega_f t+\gamma) \tag{6.59}$$

$$\varphi_{0_{xt}}(x,t) = -B\omega_f\frac{\sin\left(k(x-x_w)\right)}{\sin\left(k(L-x_w)\right)}\cos(\omega_f t)-\frac{B\omega_f R}{C}\cos(k(L-x))\sin(\omega_f t+\gamma)+\frac{B\omega_f E}{C}\sin(k(L-x))\cos(\omega_f t+\gamma) \tag{6.60}$$

Then, after some mathematical manipulations and after using some trigonometric identities, one gets a simplified version of the forcing term:

$$\begin{aligned} 2\varphi_{0_x}\varphi_{0_{xt}} = {} & \frac{B^2\omega_f\sin^2\left(k(x-x_w)\right))}{\sin^2\left(k(L-x_w)\right)}\sin(2\omega_f t)+\frac{B^2\omega_f\left(E^2-R^2\right)\sin^2(k(L-x))}{\sin^4(k(L-x_w))[R^2+E^2][R^2+W^2]}\sin(2\omega_f t+2\gamma) \\ & -\frac{2B^2\omega_f\sin(k(x-x_w))\sin(k(L-x))}{\sin^3(k(L-x_w))\sqrt{[R^2+E^2][R^2+W^2]}}\left[R\cos(2\omega_f t+\gamma)+E\sin(2\omega_f+\gamma)\right] \\ & +2B^2\omega_f\frac{ER\sin^2(k(L-x))}{\sin^4(k(L-x_w))[R^2+E^2][R^2+W^2]}\cos(2\omega_f t+2\gamma) \end{aligned} \tag{6.61}$$

By substituting this forcing function into the system of partial differential equation looks, then it looks like to the general form treated in [92] and in 6.2 where 6.23 is the general solution. In this case $\Phi(x,t) = 2\varphi_{0_x}\varphi_{0_{xt}}$ and $G(x,\xi,t)$ is the Green's function for the wave equation in case of reflecting boundary conditions [93]:

$$G(x,\xi,t) = \frac{t}{L-x_w} + \frac{2}{c_0\pi}\sum_{n=1}^{\infty}\frac{1}{n}\cos\left(\frac{n\pi(x-x_w)}{L-x_w}\right)\cos\left(\frac{n\pi(\xi-x_w)}{L-x_w}\right)\sin\left(\frac{n\pi c_0 t}{L-x_w}\right) \tag{6.62}$$

by using the same notation, functions $g_1(t)$, $g_2(t)$, $f_0(x)$, and $f_1(x)$ are identically set to zero, simplifying the integration evaluation of 6.23 and resulting in:

$$\varphi_1(x,t) = \int_0^1\int_0^t \Phi(\xi,\tau)G(x,\xi,t-\tau)\,d\xi\,d\tau \tag{6.63}$$

Then by substituting the actual forcing function, one obtains:

$$\varphi_1(x,t) = \int_0^t \int_{x_w}^L \left[\frac{B^2\omega_f \sin^2\left(k(x-x_w)\right))}{\sin^2\left(k(L-x_w)\right)} \sin(2\omega_f t) + \frac{B^2\omega_f \left(E^2-R^2\right)\sin^2(k(L-x))}{\sin^4(k(L-x_w))[R^2+E^2][R^2+W^2]} \sin(2\omega_f t+2\gamma) \right.$$
$$- \frac{2B^2\omega_f \sin(k(x-x_w))\sin(k(L-x))}{\sin^3(k(L-x_w))\sqrt{[R^2+E^2][R^2+W^2]}} \left[R\cos(2\omega_f t+\gamma) + E\sin(2\omega_f+\gamma)\right]$$
$$\left. +2B^2\omega_f \frac{ER\sin^2(k(L-x))}{\sin^4(k(L-x_w))[R^2+E^2][R^2+W^2]} \cos(2\omega_f t+2\gamma) \right] \left[\frac{t-\tau}{L-x_w}\right] d\xi\, d\tau \tag{6.64}$$

Even in this case, one neglects the contribution of the infinite sum as in the previous case. By solving the integration, four distinct contributions appear:

- $\varphi_{1_1}(x,t) = -\frac{B^2\left(\frac{\sin(2\omega_f t)}{2}-\omega_f t\right)\left(\omega_f x_w - L\omega_f + \frac{c_0}{2}\sin(2k(L-x_w))\right)}{2\omega_f^2(L-x_w)\left(\cos\left(\frac{2\omega_f(L-x_w)}{c_0}\right)-1\right)}$
- $\varphi_{1_2}(x,t) = -\frac{B^2\omega_f(E^2-R^2)\left(2\omega_f x_w - 2L\omega_f + c_0\sin(2k(L-x_w))\right)\left(\sin(2\gamma)-\sin(2\gamma+2\omega_f t)+2\omega_f t\cos(2\gamma)\right)}{16[R^2+E^2][R^2+W^2]\omega_f^3\sin^4(k(L-x_w))(L-x_w)}$
- $\varphi_{1_3}(x,t) = -\frac{2B^2\omega_f\left(c_0\sin(k(l_0-x_w))-l_0\omega_f\cos(k(l_0-x_w))+\omega_f x_w\cos(k(l_0-x_w))\right)}{8\omega_f^3\sin^3(k(l_0-x_w))(l_0-x_w)\sqrt{[R^2+E^2][R^2+E^2]}}\cdot$

  $\cdot\left(R\sin(2\omega_f t+\gamma) - R\sin(\gamma) + E\cos(2\omega_f t+\gamma) - E\cos(\gamma) - 2\omega_f Rt\cos(\gamma) + 2E\omega_f t\sin(\gamma)\right)$
- $\varphi_{1_4}(x,t) = \frac{2B^2 ER\omega_f\left(2\omega_f x_w - 2l_0\omega_f + c_0\sin(2k(l_0-x_w))\right)\left(\cos(2\gamma+2\omega_f t)-\cos(2\gamma)+2\omega_f t\sin(2\gamma)\right)}{16[R^2+E^2][R^2+W^2]\omega_f^3\sin^4(k(l_0-x_w))(l_0-x_w)})$

Then, taking the time derivative and performing the mean value of each, the following terms are obtained:

- $\langle\varphi_{1_{t_1}}\rangle = \frac{B^2}{4\sin^2(He)}\left(1-\frac{\sin(2He)}{2He}\right)$
- $\langle\varphi_{1_{t_2}}\rangle = \frac{B^2}{4\sin^2(He)}\left(1-\frac{\sin(2He)}{2He}\right)\left(\frac{(E^2-R^2)\cos(2\gamma)}{\sin^2(He)[R^2+E^2][R^2+W^2]}\right)$
- $\langle\varphi_{1_{t_3}}\rangle = \frac{B^2}{4\sin^2(He)}\left(\cos(He)-\frac{\sin(He)}{He}\right)\left(\frac{2E\cos(\gamma)-2R\sin(\gamma)}{\sin(He)\sqrt{[R^2+E^2][R^2+W^2]}}\right)$
- $\langle\varphi_{1_{t_4}}\rangle = -\frac{B^2}{4\sin^2(He)}\left(1-\frac{\sin(2He)}{2He}\right)\left(\frac{2ER\sin(2\gamma)}{\sin^2(He)[R^2+E^2][R^2+W^2]}\right)$

Where in this case, $He = \frac{\omega_f(L-x_w)}{c_0}$ is the local Helmholtz number. The sum of the 4 terms gives the mean value of the time derivative potential of the acoustic field:

$$\langle\varphi_{1_t}\rangle = \frac{B^2}{4\sin^2(He)}\left\{\left[1-\frac{\sin(2He)}{2He}\right]\left(1+\frac{E^2-R^2}{\sin^2(He)[R^2+E^2][R^2+W^2]}\cos(2\gamma)\right.\right.$$
$$\left.\left. -\frac{2ER\sin(2\gamma)}{\sin^2(He)[R^2+E^2][R^2+W^2]}\right) + \left(\cos(He)-\frac{\sin(He)}{He}\right)\left(\frac{2E\cos(\gamma)-2R\sin(\gamma)}{\sin(He)\sqrt{[R^2+E^2][R^2+W^2]}}\right)\right\}$$

In such a way, the total expression for the radiation pressure can be evaluated using the King's Formula:

$$p_{rad} = \rho_0\varphi_t + \frac{\rho_0^2\varphi_t^2}{2c_0^2}$$

To clarify, it is essential to analyze the order of magnitude between the two terms. On one hand, the zero-order solution is proportional to Bc_0, while the first-order solution is proportional to B^2. This leads to the conclusion that the first-order contribution can be neglected in the squared term of the radiation pressure. Conversely, $\langle \varphi_{1_t} \rangle$ significantly contributes to the linear part of the radiation pressure expression. Indeed, while the zero-order solution has a mean value of zero, the first-order solution does not, resulting in nearly twice the value of the radiation pressure when considering the linear acoustic field solution. By putting everything together, the final expression for the mean value of the radiation pressure is:

$$\langle p_{rad} \rangle = \frac{\rho_0 B^2}{4\sin^2(He)} \left\{ \chi^2 + \left[1 - \frac{\sin(2He)}{2He} \right] \left(1 + \frac{E^2 - R^2}{\sin^2(He)[R^2+E^2][R^2+W^2]} \cos(2\gamma) \right. \right.$$
$$\left. \left. - \frac{2ER\sin(2\gamma)}{\sin^2(He)[R^2+E^2][R^2+W^2]} \right) + \left(\cos(He) - \frac{\sin(He)}{He} \right) \left(\frac{2E\cos(\gamma) - 2R\sin(\gamma)}{\sin(He)\sqrt{[R^2+E^2][R^2+W^2]}} \right) \right\} \tag{6.65}$$

The ratio between the fully non-linear acoustic field solution and the linear field solution using the same expression for the radiation pressure is:

$$\eta = \frac{\overline{p}_{rad_{imp}}}{\overline{p}_{rad_{lin}}} = \left\{ \chi^2 + \left[1 - \frac{\sin(2He)}{2He} \right] \left(1 + \frac{E^2 - R^2}{\sin^2(He)[R^2+E^2][R^2+W^2]} \cos(2\gamma) \right. \right.$$
$$\left. \left. - \frac{2ER\sin(2\gamma)}{\sin^2(He)[R^2+E^2][R^2+W^2]} \right) + \left(\cos(He) - \frac{\sin(He)}{He} \right) \left(\frac{2E\cos(\gamma) - 2R\sin(\gamma)}{\sin(He)\sqrt{[R^2+E^2][R^2+W^2]}} \right) \right\} \tag{6.66}$$

In the limit of infinite impedance, the ratio is exactly equal to that found for a rigid panel:

$$\lim_{R,E,A \to \infty} \eta = 2 - \frac{\sin(2He)}{2He}$$

Kinetic Energy Contribution

So far, the classic radiation pressure expression without the kinetic energy term has been considered. But now, it is quite clear that the kinetic energy plays an important role since the wall is moving with a certain speed. That emerges from the left boundary condition that states exactly:

$$u(x_w, t) = \frac{p(x_w, t)}{Z_w} = -\varphi_x(x_w, t)$$

The condition is valid for one dimensional case, and it modifies the radiation pressure equation in the complete version:

$$p_{rad} = \rho_0 \varphi_t + \frac{\rho_0 \varphi_t^2}{2c_0^2} - \frac{\rho_0 \left| \varphi_x \right|^2}{2} \tag{6.67}$$

Therefore, from the boundary condition, one gets the exact formula for the gradient at the boundary. From 6.47 one gets the desired result:

$$|\varphi_x| = \frac{|p(x_w, t)|}{|Z_w|} = \frac{B}{\sin(He)A} = \frac{B}{\sin(He)\sqrt{R^2+W^2}}$$

Then, when elevating to the power of two, it becomes:

$$|\varphi_x|^2 = \frac{B^2}{\sin^2(He)A^2} = \frac{B^2}{\sin^2(He)(R^2+W^2)} \tag{6.68}$$

The phase, instead, is evaluated taking:

$$\Psi = \Phi - \arctan\left(\frac{\omega_f M - \frac{k_s}{\omega_f}}{r}\right) = \frac{\pi}{2} - \arctan\left(\frac{\left(\omega_f M - \frac{k_s}{\omega_f}\right)\sin(He) - \rho_0 c_0 \cos(He)}{r\sin(He)}\right)$$

Even in this case, one considers the imaginary part and then evaluating the mean value of this term, one gets a mean value that is proportional to the same expression already found. Indeed:

$$\frac{1}{T}\int_0^T \frac{\rho_0 |\varphi_x|^2}{2}\cos^2(\omega_f t + \Psi)dt = \frac{B^2\rho_0}{4\sin^2(He)(R^2+W^2)} \tag{6.69}$$

So, considering also the contribution given by the kinetic energy one gets the full expression of the radiation pressure in the case of moving wall:

$$\langle p_{rad}\rangle = \frac{\rho_0 B^2}{4\sin^2(He)}\left\{\chi^2 + \left[1 - \frac{\sin(2He)}{2He}\right]\left(1 + \frac{E^2-R^2}{\sin^2(He)[R^2+E^2][R^2+W^2]}\cos(2\gamma)\right.\right.$$

$$\left.\left. - \frac{2ER\sin(2\gamma)}{\sin^2(He)[R^2+E^2][R^2+W^2]}\right) + \left(\cos(He) - \frac{\sin(He)}{He}\right)\left(\frac{2E\cos(\gamma) - 2R\sin(\gamma)}{\sin(He)\sqrt{[R^2+E^2][R^2+W^2]}}\right) - \frac{1}{R^2+W^2}\right\} \tag{6.70}$$

In this analysis, only the first order solution was considered because of higher order of magnitude with respect to the second order solution for φ_x.

6.3.3 Numerical Results

Numerical Simulations were performed to validate the accuracy of the formula in presence of impedance and kinetic contribution of the moving wall. It is important to see how much the results differ from the case of perfectly rigid wall, indeed in the case of a moving wall/mass, the vibration of the latter may significantly modify the value of the radiation pressure leading to wrong interpretation of the result. From now on, attention should be paid on two different non-dimensional parameters. In this case, no effect of any stiffness was included to make the simulations consistent to a case of a free moving wall simply supported by the friction between pipe's walls and so no springs are present in the system. The formula is still valid once using $k_s = 0$.

Hence, knowing that $W = E - \cot(He) = \frac{\omega_f M}{c_0\rho_0} - \cot(He)$, one can express the first non-dimensional coefficient as a product of two important parameters related to the driving frequency and on the mass of the wall. Indeed, driven frequency could be written in terms of the first natural frequency of the closed pipe:

$$\omega_f = \alpha\omega_n = \frac{\alpha 2\pi c_0}{2L} = \frac{\alpha c_0 \pi}{L}$$

Hence, the first part of W can be rewritten as:

$$\frac{\omega_f M}{\rho_0 c_0} = \frac{\alpha c_0 \pi M}{L c_0 \rho_0} = \frac{\alpha \pi M}{L \rho_0} = \frac{\alpha \pi M}{m_a} = \frac{\alpha \pi \beta_w L_w}{L} = \alpha \beta \pi$$

Where that $m_a = L\rho_0$ is the mass of the fluid per unit surface and $M = \beta_w L_w \rho_0 = \beta \rho_0$ is the mass of the wall expressed as a multiple of the mass of the fluid. At this point, I can express the mass of the wall as a multiple of the mass of the fluid in the tube:

$$M = \beta m_a \tag{6.71}$$

Leading to a very simple and rigorous expression for W in terms of non-dimensional coefficients:

$$W = \alpha \beta \pi - \cot(He)$$

Therefore, each simulation is performed considering the values of α and β to make comparison between rigid and impedance case. Obviously, the bigger the β is, the closer to the rigid case the simulation gets. For each simulation, the ratio between the piston stroke and the tube length was assumed equal to 0.005%, the resulting pressure is expressed in dB and also the relative error between the expressions is shown. Three different frequency cases are presented just to show the goodness of the analytical formula with respect of the numerical simulations. In this case, the numerical simulations were performed introducing the dynamic of the wall at the node $i = 1$.

$$\begin{cases} u(x_w, t) = A_w(t), & (Moving\ Wall) \\ u(L, t) = A_p(t), & (Moving\ Piston) \end{cases} \tag{6.72}$$

Where $A_p(t)$ represents the velocity of the piston at the right-hand side of the cylinder and $A_w(t)$ is the actual velocity of the wall subjected to the acoustic field.
This case needs conservation of momentum on both ends, leading to this set of boundary conditions:

$$\begin{cases} P_x(0, t) = -\rho \dot{u}(x_w, t) & (Moving\ Wall) \\ P_x(L, t) = -\rho \dot{u}(L, t) & (Moving\ Piston) \end{cases} \tag{6.73}$$

Where $\dot{u}(L, t)$ is always provided analytically because of prescribed motion of the piston while $\dot{u}(x_w, t)$ is evaluated step by step using the information from the previous step to compute the unknown velocity of the wall.
By simply applying the same relationships found at the moving wall ($x = L$) the new following conditions are defined for each time step j at the moving boundary ($x = x_w$):

$$\begin{cases} u_0 = -u_2 + 2u(x_w, t) \\ p_0 = p_2 - 2h\rho \dot{u}(x_w, t) \end{cases}$$

Figures 6.5,6.6 and 6.7 show the three different pressure lines on the wall trend depending on the value of β.

- The green line represents the pressure obtained by Eq. 6.70;
- The red line is the pressure evaluated by the numerical simulations using the momentum conservation equation as approximation of $\dot{u}(x_w, t)$ at the boundary conditions at the moving boundary;

$\alpha = 1.2$

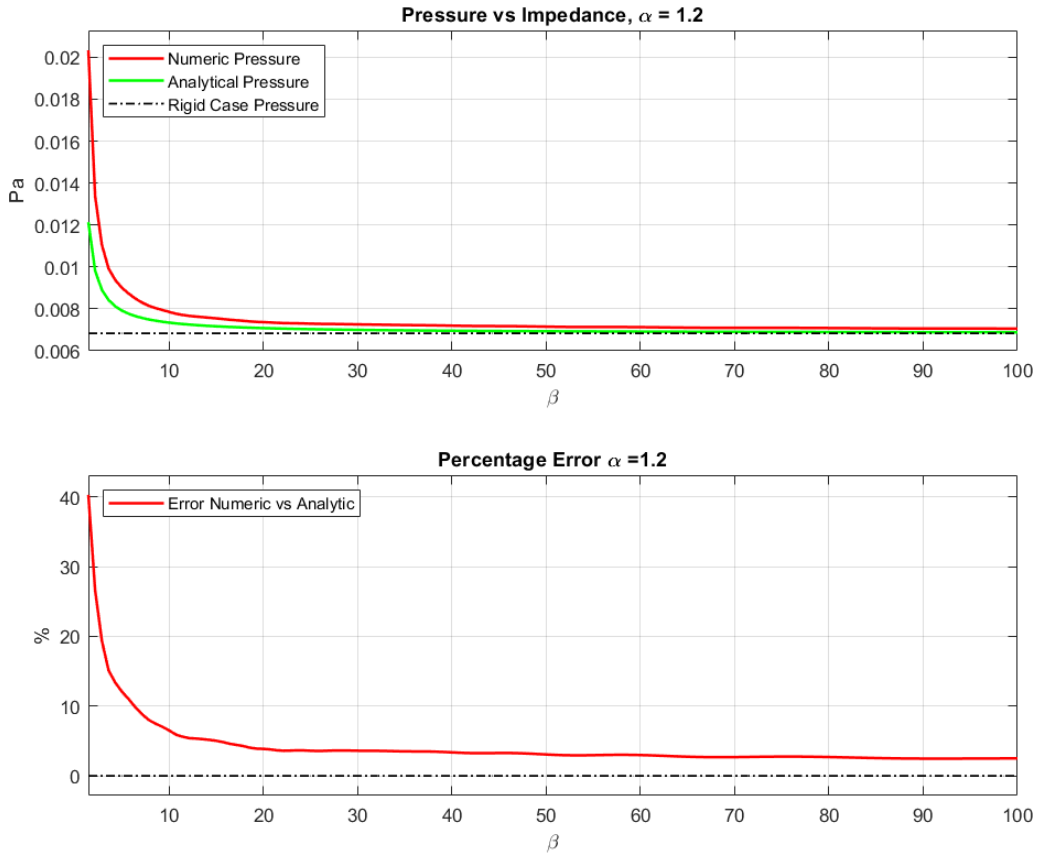

Figure 6.5. Radiation Pressure vs Impedance, $\alpha = 1.2$

Figure 6.5 shows that the red line is very close to the green one leading to a very good approximation of the formula. This is due to the fact that $\dot{u}(x_w, t)$ is a quantity evaluated with information coming from the previous time step and it may lead to some errors (under 5% for $\beta > 10$). The stability of the results are also due to the distance of the driven frequency with respect to resonance ones.

$\alpha = 1.3$

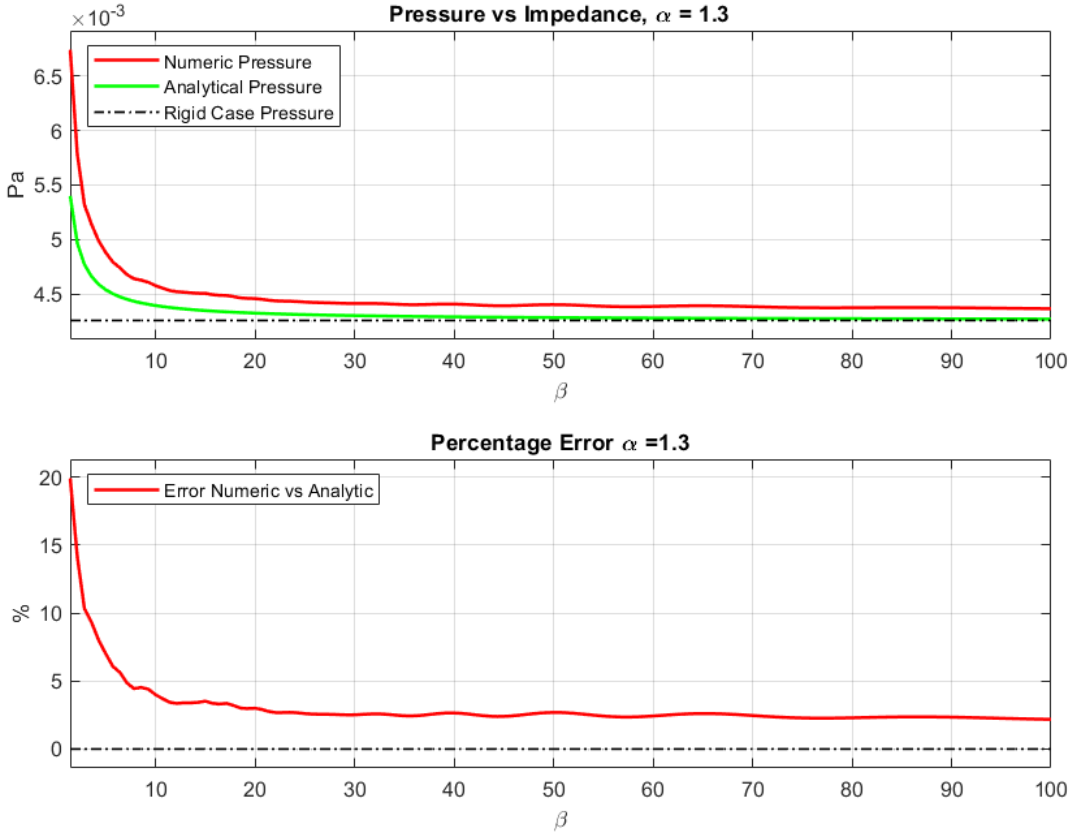

Figure 6.6. Radiation Pressure vs Impedance, $\alpha = 1.3$

Figure 6.6 shows the same results of the previous one but with a different driving frequency. In this case as well, the red curve closely approaches the green one, further reducing the error between the numerical results and those derived analytically.

$\alpha = 1.7$

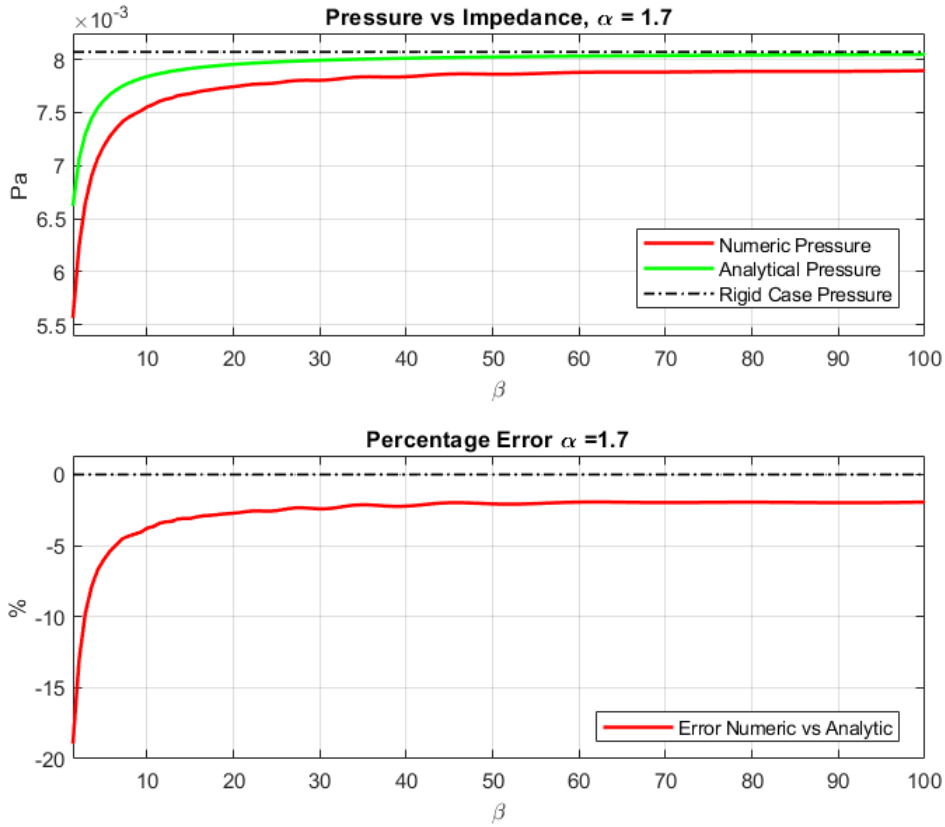

Figure 6.7. Radiation Pressure vs Impedance, $\alpha = 1.7$

The same trend is also observed in figure 6.7, confirming the validity of the expression derived in equation 6.70 even when extending the frequency range. Specifically, it can be seen that as the anti-resonance frequency is surpassed, the behavior of the curves is inverted, a phenomenon reflected both in the numerical simulations and in the analytical results.

$\alpha = 2.2, 2.3, 2.8$

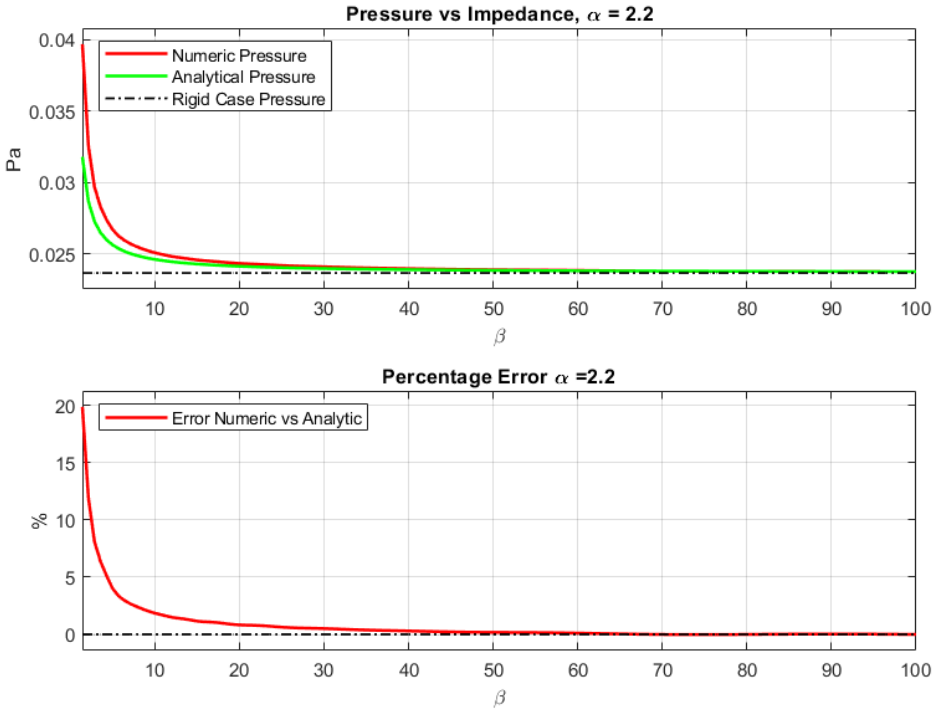

Figure 6.8. Radiation Pressure vs Impedance, $\alpha = 2.2$

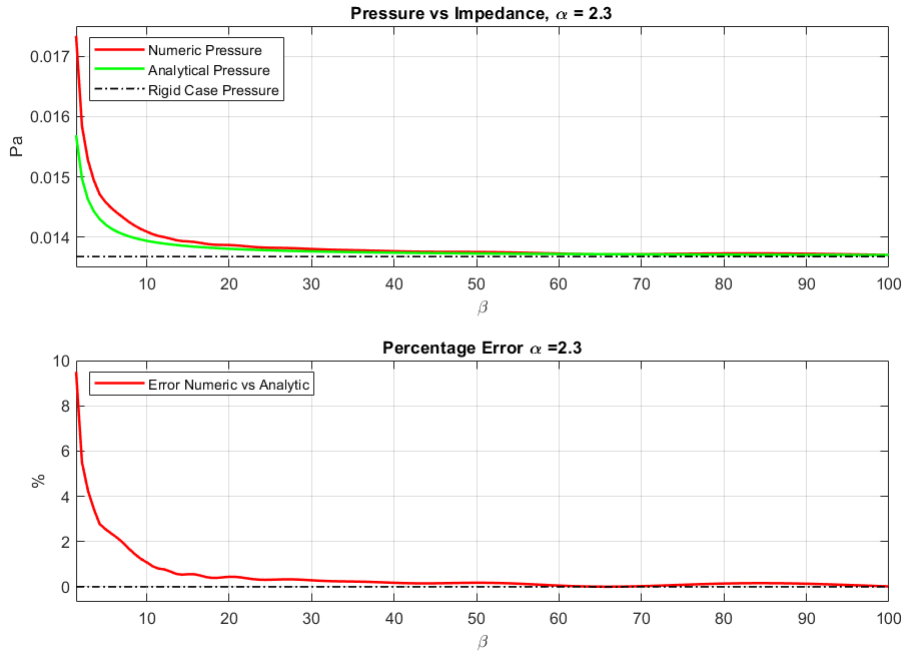

Figure 6.9. Radiation Pressure vs Impedance, $\alpha = 2.3$

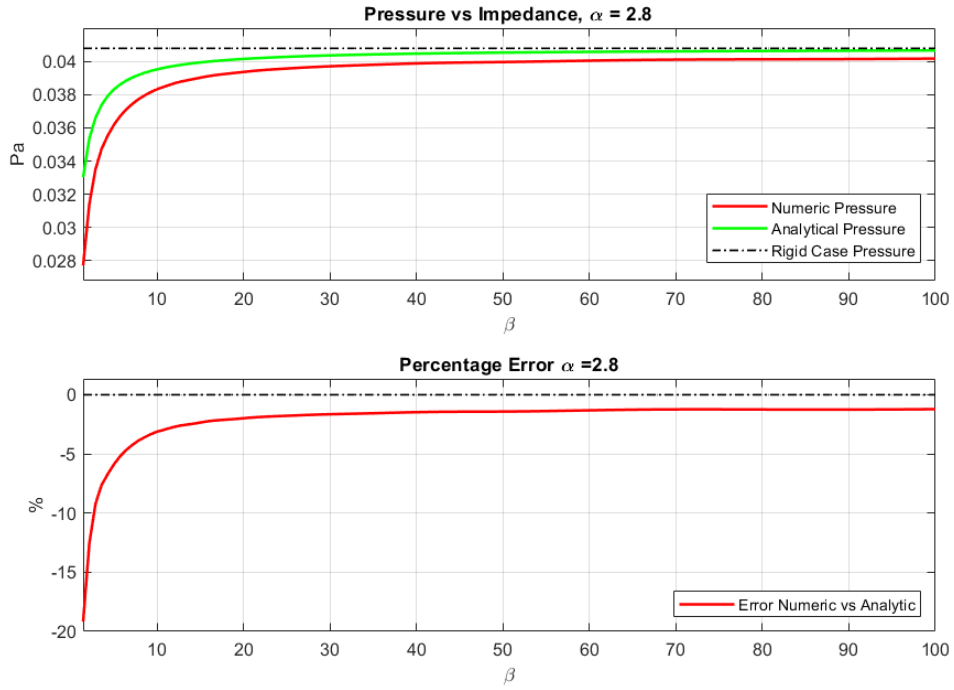

Figure 6.10. Radiation Pressure vs Impedance, $\alpha = 2.8$

Additional cases are presented here for illustrative purposes to demonstrate the accuracy of equation 6.70 and to confirm the slope inversion occurring at the midpoint of the resonance interval.

Chapter 7

Model Predictive Control For One Dimensional Problem

The problem of controlling a body subjected to an acoustic field has historically been analyzed and simulated using finite element methods or other numerical approaches [38, 102]. In particular, attention to these types of problems has always been focused on the field of acoustic levitation. In this case, the aspect of acoustic levitation is marginal; the important and novel component is the description of an average pressure acting on the body through an analytical law directly linked to the geometry of the mechanical system and the type of boundary condition expressed. This approach allows for the direct formulation of a control law on the system that can modify parameters in real time and achieve local control of the object's position.
In this study, following numerous efforts to simplify the problem starting from the complete general equations for an acoustic field in an inviscid medium, a nonlinear model predictive control (NMPC) algorithm was used for the analytical equations.

7.1 Description of the Model

The considered system is one-dimensional and involves a generic wall with mechanical impedance as described in section 6.3, subjected to two opposing acoustic fields generated by the movement of two pistons. The structure is straightforward and well-documented in the literature; however, the innovative aspect lies in the expression and application of these equations to address a control problem.
Specifically, the mechanical system is confined within a closed environment, with boundaries represented by two movable walls on either side, ideally modeled as two pistons. Each piston can be controlled independently and serves as the primary mechanism for generating acoustic waves within the tube. A mass-bearing body is positioned midway between the two walls, allowing it to slide within the tube; contact is modeled through a friction coefficient between the walls and the body.

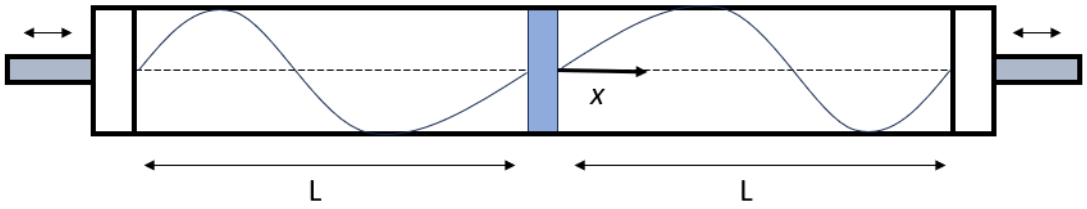

Figure 7.1. System Model

As previously mentioned, the primary objective is to use an analytical law to control the time-averaged position of an object subjected to an acoustic field within a finite domain. The system can be simply described using Newton's laws of dynamics, where the total driving force is represented as the difference between the two net pressures acting on the wall. By setting a positive reference system towards the right, as shown in figure 7.1, the following equation is obtained:

$$M\dot{v} + rv = F(t) = S(P_{+}(t) - P_{-}(t))$$

In linear acoustic, M is the mass of the moving wall and $r = r_{fr} + 2\rho_0 c_0$ is the damping coefficient composed by the friction between the body and the tube (r_{fr}) and the classic acoustic loading term ($2\rho_0 c_0$) that arises from the radiated and reflected waves produced by the motion of the barrier [103]. In this case, no stiffness is present.

In general, within the realm of linear dynamics, a body subjected to a driving force is constrained to move in a manner similar to that of the force itself. In the laws of linear acoustics, the acoustic field consists only of purely sinusoidal waveforms, whose time-averaged components are always zero, so in principle no drift effect is expected. However, as deeply analysed in Chapter 6, the real acoustic field exhibits nonlinear components, which are responsible for a non-zero time-averaged effect on the quantities involved. At the end, the total pressure acting on the wall consists of several sinusoidal components with integer multiples of the driving frequency, which will cause the body to oscillate around its actual position, and a component with a non-zero time average that contribute to the body drift.

As pointed out and analyzed by Mohazzabi and Greenebaum, there is still the possibility of obtaining drift with purely sinusoidal driving forces depending on the phase [104]. However, the presence of friction in real applications negates this effect, so the net component of radiation pressure remains essential for moving the body after a transient, which at this stage is considered negligible.

As a first approximation, the general pressure on the wall can be divided into two components: one due to the sinusoidal components and one due to the net component since:

$$P(t) = P_{osc}(t) + P_{rad}(t)$$

For this reason, the general motion can be separated in:

$$v_{tot}(t) = v_{osc}(t) + v_{dc}(t)$$

And since:

$$P_{osc} \gg P_{rad}$$

Then:

$$v_{osc} \gg v_{dc},$$

As a result, the general equation of motion can thus be rewritten as follows:

$$M\dot{v}_{osc} + M\dot{v}_c + rv_{osc} + rv_{dc} = S\left[P_{osc_+}(t) - P_{osc_-}(t) + P_{dc_+}(t) - P_{dc_-}(t)\right]$$

This study aims to highlight the net effects that occur over the period of the driving force and to use a real-time control algorithm to manipulate the position of a body. Therefore, if the time average of the quantities involved is performed over a characteristic period T, a zero mean is always obtained for the oscillatory components, while the mean for the net components is non-zero. In this way, it is possible to directly use the equation 6.70 for the net radiation pressure over the period.

$$M\dot{v}_c + rv_{dc} = S\left[P_{dc_+}(t) - P_{dc_-}(t)\right] \tag{7.1}$$

Equation 7.1 is the time-dependent equation of the average displacement values of the wall associated with the net difference of the driving forces and it will be use in the NMPC prediction model's dynamic. The driving forces are represented by the net pressures on the wall and are directly functions of the geometry, position, and rotational frequency of the piston. Recalling equation 6.70, this expression can be rewritten by explicitly stating the control variable. In this case, the control variable will be the oscillation frequencies of the two pistons.

$$\overline{P(\omega)}_{dc} = \frac{\rho_0 B^2}{4\sin^2(He(\omega))}\cdot$$

$$\cdot\left\{\chi(\omega)^2 + \left[1 - \frac{\sin(2He(\omega))}{2He(\omega)}\right]\left(1 + \frac{E(\omega)^2 - R^2}{\sin^2(He(\omega))[R^2 + E(\omega)^2][R^2 + W(\omega)^2]}\cos(2\gamma) - \right.\right.$$

$$\left. - \frac{2E(\omega)R\sin(2\gamma)}{\sin^2(He(\omega))[R^2 + E(\omega)^2][R^2 + W(\omega)^2]}\right) - \frac{1}{R^2 + W(\omega)^2} +$$

$$\left.\left(\cos(He(\omega)) - \frac{\sin(He(\omega))}{He(\omega)}\right)\left(\frac{2E\cos(\gamma) - 2R\sin(\gamma)}{\sin(He(\omega))\sqrt{[R^2 + E(\omega)^2][R^2 + W(\omega)^2]}}\right)\right\} \tag{7.2}$$

To enhance the rigor of the analysis, the physical parameters of the problem will be rewritten using the dimensionless parameters introduced in Section 6.3. This approach not only simplifies the mathematical treatment but also facilitates the comparison of results across different scales and conditions and decreases the computational time of the implemented controller. In order to more easily introduce the control parameters, one defines:

$$\begin{cases} B = L_p\omega = \zeta L\omega \\ \omega = \alpha\omega_n = \alpha\frac{c_0\pi}{L} \\ M = \beta_w L_w m_a = \beta\rho_0 \\ He_- = \frac{\omega_1}{c_0}(L - x_w(t)) = \alpha_1\pi\left(1 - \frac{x_w(t)}{L}\right) \\ He_+ = \frac{\omega_2}{c_0}(L + x_w(t)) = \alpha_2\pi\left(1 + \frac{x_w(t)}{L}\right) \end{cases} \tag{7.3}$$

Where He_- and He_+ represent the local Helmholtz number for the acoustic field on the right and left sides of the body, respectively. The sign change of x_w is due to the inversion of the boundary conditions for a perturbation coming from the left. Assuming a unit surface, the equation of predicted dynamics becomes:

$$\overline{a}_{dc} + \frac{r_{fr}}{\beta m_a}\overline{v}_{dc} = \frac{1}{\beta m_a}(\overline{P}_{dc_+}(\alpha_2) - \overline{P}_{dc_-}(\alpha_1))$$

Where the driving force on the right is directly linked to the control parameter (α_1), while that on the left is linked to (α_2). In this way, the general net force on the wall is written as:

$$\overline{P(\alpha)}_{dc} = \frac{\rho_0\zeta^2\alpha^2 c_0^2\pi^2}{4\sin^2(He(\alpha))}\cdot$$

$$\cdot\left\{\chi(\alpha)^2 + \left[1 - \frac{\sin(2He(\alpha))}{2He(\alpha)}\right]\left(1 + \frac{E(\alpha)^2 - R^2}{\sin^2(He(\alpha))[R^2 + E(\alpha)^2][R^2 + W(\alpha)^2]}\cos(2\gamma) - \right.\right.$$

$$\left. - \frac{2E(\alpha)R\sin(2\gamma)}{\sin^2(He(\alpha))[R^2 + E(\alpha)^2][R^2 + W(\alpha)^2]}\right) - \frac{1}{R^2 + W(\alpha)^2} +$$

$$\left.\left(\cos(He(\alpha)) - \frac{\sin(He(\alpha))}{He(\alpha)}\right)\left(\frac{2E(\alpha)\cos(\gamma) - 2R\sin(\gamma)}{\sin(He(\alpha))\sqrt{[R^2 + E(\alpha)^2][R^2 + W(\alpha)^2]}}\right)\right\} \tag{7.4}$$

It is evident that the general pressure on the wall is highly nonlinearly dependent on both the position of the wall and the frequency of the piston. This necessitates the use of a highly sophisticated control tool capable of managing the nonlinearity of the driving force and the geometric constraints of the system under analysis. Indeed, the control algorithm must ensure that the wall remains within the cylinder, meaning its position cannot exceed the boundaries defined by the boundary conditions. The same consideration applies to the piston frequencies, which must remain away from resonance values. This is because the accuracy of the mathematical model used may be compromised due to the lack of viscosity in the system, in addition the general tendency to avoid resonant phenomena during the real use of a device must be followed. For this reason, the range between resonance frequencies has been initially excluded, limiting the search for an optimal solution between the first and second resonance frequencies of the system. To prevent the control algorithm from selecting values close to resonances, a margin of approximately 5% above and below the interval extremes has been taken.

7.1.1 MPC: a short introduction

There are various control algorithms that can be used to solve problems of this kind. However, as can be seen from equation 7.4, the presence of high non-linearity in the expression of the force has effectively excluded the possibility of choosing controls of a simpler nature such as those based on PID, Sliding Mode or Lyapunov methods. So, among the most well-known and effective, nonlinear model predictive control (NMPC) was chosen.

To begin with, let's start describing Linear Model Predictive Control (MPC) and its capabilities. MPC is an advanced and sophisticated method which is used to control a process while satisfying a certain number of constraints. The fundamental benefit of MPC is that it enables timeslot optimization while taking future timeslots into consideration. In contrast to a linear-quadratic regulator (LQR), this is accomplished by optimizing a finite time horizon, but only implementing the current timeslot before optimizing once again, repeatedly. MPC is also capable of foreseeing future events and taking appropriate control measures, a feature not present in commonly used PID controllers [105, 106]. Basically, MPC is an optimal control technique where the calculated control actions are used to minimize a cost function for a constrained dynamical system over a finite and "receding" horizon. An MPC controller receives or estimates the current state of the plant at each time step. Next, it calculates the sequence of control actions that minimizes the cost over the horizon by solving a constrained optimization problem that relies on an internal plant model and depends on the current system state. Latly, the controller only applies the first computed control action to the plant, ignoring the subsequent ones and the entire procedure is repeated in the following time steps. MPC can be equivalent to LQR control when the cost function is quadratic, the plant is linear and the horizon tends to infinity. [107].

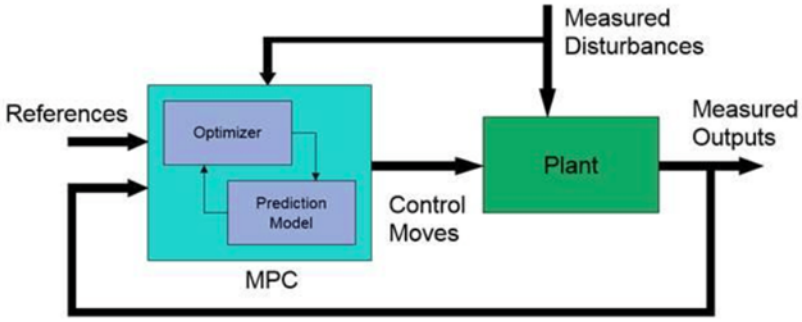

Figure 7.2. MPC Control Loop Representation

Dynamic models are typically employed to simulate both complex and simple dynamical systems. Simple systems are frequently well controlled by generic PID controllers, therefore there is typically no need for the added complexity of the MPC control algorithm to give more acceptable results. High-order dynamics and substantial time delays are two common dynamic characteristics that are challenging for PID controllers. MPC uses the current plant measurements, the current dynamic state of the process, the MPC models, and the process variable

targets and limits to calculate future changes in the dependent variables. These adjustments are calculated to respect constraints on both the independent and dependent variables and keep the dependent variables around their target. The MPC normally repeats the calculation when the subsequent change is required, after sending out the first change for each independent variable to be applied. While many real processes are not linear, they can often be considered approximately linear over a small operating range. When linear models are not sufficiently accurate to represent the real process nonlinearities, several approaches can be used. To reduce nonlinearity, the process variables may occasionally be changed before and/or after the linear MPC model, otherwise a nonlinear MPC (NMPC), which employs a nonlinear model directly in the control application, may be used in the process.

Receding Horizon philosophy

MPC is based on iterative, finite-horizon optimization of a plant model. At time t the current plant state is sampled and there is the computation of a cost minimizing control strategy for a relatively short time horizon in the future $[t; t+T]$. The control method is only used in its initial stage, which means only the first step of the control strategy is implemented, after which the plant state is sampled once again and the computations are repeated beginning with the new current state, producing a new control and new predicted state path. Because the prediction horizon is always moving forward, MPC is also known as "receding horizon control". Although this strategy is not ideal, in practice it has produced excellent outcomes.

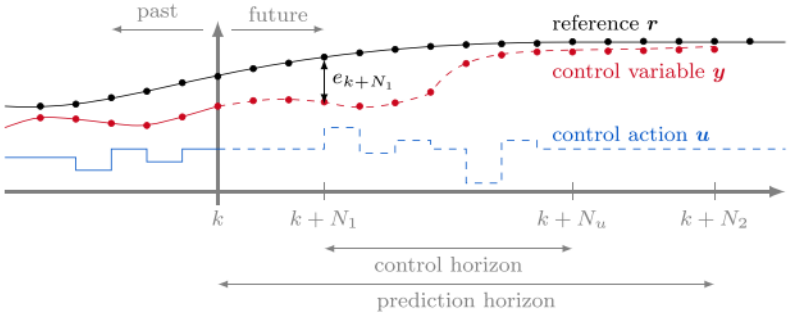

Figure 7.3. MPC Algorithm Representation

As shown in the figure 7.3, the MPC determines an output u by solving a constrained optimization problem. It is one of the few control methods that directly considers constraints. Usually, the cost function is formulated in such a way that the system output y tracks a given reference r for a horizon N_2. The system only uses the first value of the optimized output trajectory. Each time, this prediction and optimization are repeated. A short-term (predictive) optimization essentially leads to optimality over a long period of time. This is expected to be true since the error of a proximal forecast is considered to be smaller than that of a distant prediction. The primary distinction between this methodology and traditional control methods, which rely on precomputed control principles, is the combination of prediction and optimization. To accu-

rately represent the impact of a change in the manipulated variable u on the control variable y, the prediction horizon N_2 must be long enough.

Principles and Design of MPC

MPC is a multivariable control algorithm which uses:

- An internal dynamic model of the process;
- A cost function J over the receding horizon;
- An optimization algorithm which minimizes the cost function J through the use of a control input

An example of a quadratic cost function for the optimization is:

$$J = \sum_{i=1}^{N} w_{x_i}(r_i - x_i)^2 + \sum_{i=1}^{N} w_{u_i}\Delta u_i^2 \tag{7.5}$$

Where:

- $x_i = i^{th}$ controlled variable;
- $r_i = i^{th}$ reference variable;
- $u_i = i^{th}$ manipulated variable;
- w_{x_i} weighting coefficient reflecting the relative importance of x_i;
- w_{u_i} weighting coefficient penalizing relative big changes in u_i;

Considering the simplest case (traditional or linear MPC), in which both plant and constraints are linear and the cost function is quadratic, the MPC is characterized by these steps [108].
Specify Plant: Describe the internal plant model the MPC controller use to forecast plant behaviour over the prediction horizon.
Define signal types: For MPC design purposes, plant signals are typically divided by many input and output types. In the plant object defined in the previous phase, it is normally possible to use coding functions which are able to declare whether each plant output is measured or unmeasured as well as whether each plant input is a controlled variable (i.e., a control input) or a measured or unmeasured disturbance.
Create MPC object: After providing the signal types in the plant object, the next step is to create an MPC object and to specify the object's controller parameters such as the sample time, prediction and control horizons, cost function weights, constraints and disturbances. The most important parameters that are needed to be selected are:

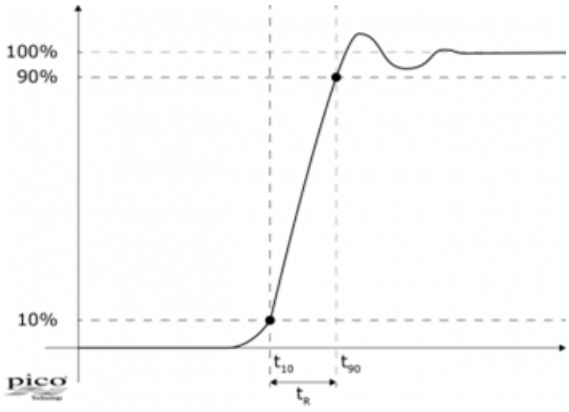

Figure 7.4. Rise Time Representation

- Sample time: a reasonable starting guess can be to set the controller sample time so that 10 to 20 samples cover the rise time of the plant. Rise time is defined as the amount of time taken for a signal to cross from a predetermined low value to a specified high value; essentially it is the time it takes for a signal to increase from 10% to 90% of its ultimate value. In both analog and digital systems, the rise time is a critical characteristic;

- Prediction horizon: the quantity of upcoming samples that the controller will attempt to minimize the cost. It should be long enough to capture the transient response and cover the significant dynamics of the system and to increase both performance and computational requirements. 10 to 20 samples typically make up a prediction horizon. The figure 7.5

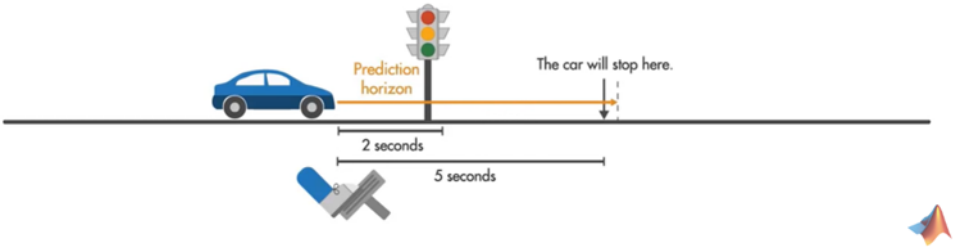

Figure 7.5. Prediction Horizon Representation

perfectly represents the importance of the prediction horizon, which is the number of predicted future time steps and shows how far the controller predicts into the future: assuming that the car is going at 50mph, it will take it 5 seconds to stop once the brake pedal is pressed; if the prediction horizon is 2 seconds, by the time the traffic lights are seen, it will be too late to apply the brakes; the car will be able to stop only after passing the traffic lights. So, the prediction horizon can't be too short, but it has to be chosen in order to cover the significant dynamic of the system;

- Control horizon: the number of free control moves that the controller does to minimize the cost over the prediction horizon. Each control move can be thought of as a free variable

that needs to be computed by the optimizer. As well as for the prediction horizon, the longer the control horizon, the better the performance and computational requirements. Typically, it is possible to set the control horizon to $10 - 20\%$ of the prediction horizon;

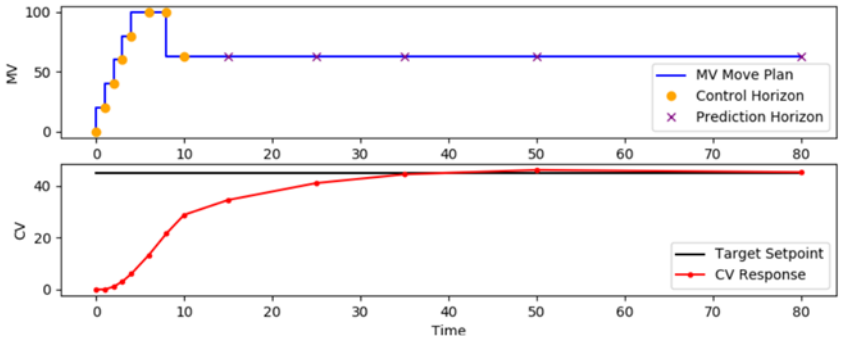

Figure 7.6. Control Horizon Representation

- Constraints: they represent the physical limits of the problem; generally, it is recommended to set the input constraints as "hard", which means they can't be violated in the optimization, while the output constraints as "soft";
- Weights: by altering the cost function tuning weights, it is possible to set the controller's performance objectives. Greater output weights typically result in aggressive reference tracking, whereas larger weights on the manipulated variable rates enable smoother control moves that increase robustness;
- Disturbance and noise models: they can affect the plant.

Simulate closed loop: after the creation of the MPC controller, the performance of it has to be evaluated by simulating it in the closed loop with the specified plant; this operation can be done through MATLAB, Simulink or the MPC Designer app.
Refine design: after a starting evaluation of the closed loop, refine the design is necessary by adjusting the controller parameters and making different simulation scenarios.
Speed up execution and deploy controller: In order to both optimize the design for future simulations and to satisfy the more stringent computing needs of embedded applications, it is necessary to seek for ways to speed up the execution once the simulation performance of the controller design is quite satisfactory.
There are many ways to increase and improve the performances of the MPC controller: for example, by increasing the sample time, because if it is too small not only there is the reduction of the available computation time for the controller but also there is the necessity to use a larger prediction horizon to cover the system response in a more computationally expensive optimization problem to be solved at each time step; by decreasing prediction and control horizons; by varying parameters only when needed; by limit the maximum number of iterations

that the controller is able to use to solve the quadratic optimization problem; by tuning the solver and its options.

Nonlinear MPC

Nonlinear model predictive control, or NMPC, is a variant of MPC which is characterized by the use of nonlinear system models in the prediction; in fact, differently from the model predictive control, it is able to treat the nonlinear dynamics and constraints directly and explicitly, as opposed to using linear approximations. Like the linear MPC, NMPC requires the iterative solution of optimal control problems on a finite prediction horizon. The difference is that in the linear MPC these problems are convex while in the NMPC the situation is not the same. This affects both the NMPC stability theory and numerical solution.

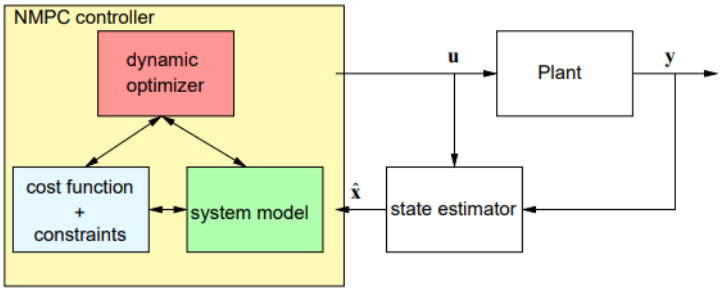

Figure 7.7. NMPC Block Scheme

The basic NMPC scheme works in this way:

- Obtain measurements/estimates of the states of the system;
- Compute an optimal input signal by minimizing a given cost function over a certain prediction horizon in the future using a model of the system;
- Implement the first part of the optimal input signal until new measurements/estimates of the state are available;
- Continue with the first point.

Whether a limited horizon NMPC technique actually results in the closed-stability loop's is undoubtedly one of the fundamental questions in NMPC. The main issue with a finite prediction and control horizon, as said, is because there is typically a difference between the predicted open and the resulting closed-loop behaviour. The ideal NMPC method would be one that achieves closed-loop stability regardless of the cost functional's performance parameters and, if possible, approximates the infinite horizon NMPC scheme as good as possible. A NMPC approach with "guaranteed stability" is one that guarantees closed-loop stability regardless of the selection of the performance parameters.

7.1.2 Case Studies

The simulations aim to demonstrate that it is possible to implement a simple control strategy to move an object along one dimension. The control strategy involves the use of NMPC (Nonlinear Model Predictive Control) with the system's predicted dynamics expressed by equation 7.1 and a quadratic function related to the error with respect to the state and the square of the input as described in equation 7.6.

$$J = \sum_{i=1}^{N} w_{x_i}(r_i - x_i)^2 + \sum_{i=1}^{N} w_{u_i}\left(\Delta P_i(+)^2 + \Delta P_i(-)^2\right) \tag{7.6}$$

The scenarios studied were chosen to verify how the control algorithm responded to different desired trajectory of the object. The goal is to ensure that the same strategy could work in different cases and to observe the different dynamics of various objects when subjected to externally controlled acoustic fields.
To avoid exceeding the range of validity of the system's physical model together with the approximation of the moving wall pressure equation 7.4, limits were imposed on the geometry and the piston's frequency. Specifically:

- $-L < x < L$
- $1 + \delta < \alpha_i < 3 - \delta$

The first constraint represents a true geometric limitation, physically bounded by the pistons, while the second is more related to control logic to avoid selecting oscillation frequency values near the resonance extremes of the system. As a consequence, the control algorithm will autonomously choose to bypass the resonance frequencies, as they would otherwise significantly increase the pressure value, preventing the minimization of the cost function 7.6. The value of δ, based on the numerical results obtained in 6.2, was set to 0.075.
It was decided to set the piston frequency up to the second resonance to observe how the algorithm behaves when transitioning from one interval to another. Of course, this can be extended to any desired frequency. The cases analyzed are shown in Table 7.1:

Table 7.1. Table: Cases 1-3

Case #	Reference Signal	β
1	Step Function	10
2	Sine Function	10
3	Ramp	10

As can be seen, three classic reference signals and a value of the relative density of the object with respect to that of air were chosen to test the control algorithm. Indeed, referring to equation

6.71, a value of $\beta = 10$ has been used to represents an object with a relative low density. For each case, the piston stroke was set to a value of $u_p = 0.015\%L$ with a simulation time of $T = 45s$. All simulations were conducted using the same type of controller to demonstrate the different dynamics of the body subjected to the acoustic field as a function of its mass density. The actual computational time resulted always less than one third of the real time of simulation, leading the chance to use it also for real time applications.

Step Function

The input signal given as a reference is a double step, first increasing and then decreasing, to return it to the exact starting point.
As can be easily inferred, the step response illustrated in figure 7.8 highlights a clear capability of the controller performance in cases of light-weighted bodies. NMPC satisfies always the constraints and the implemented cost function and the body reaction seems to be good without significant effort. The upper figure presents a comparison between the light body position and velocity (in blue) against the reference trajectory, which is represented by the dashed black line. Conversely, the lower figure displays the physical variables of positive and negative pressure and the control variables (i.e. the pistons' frequency).
In detail, the red curves represent the variables in the field on the right of the object, which induce a displacement in the negative direction relative to the reference system established in figure 7.1, while the blu ones depict quantities related to the left side, contributing to a positive displacement.
The radiation pressure reaches relative low peak values; however, the input variables manage to compensate for the inertia of the mass involved. As it can be clearly seen, the input values are always within the interval $1 < \alpha < 3$. The overall imposed displacement is approximately 1 cm in this very first case.
An important consideration must be made concerning velocities of the boundary. Figure 7.8b shows the velocity trend over time and one can see that the maximum value is around $0.06\,\frac{m}{s}$ that is negligible compared to the speed of sound $c_0 = 343\,\frac{m}{s}$. This validates the use of the Uniform Doppler Approximation introduced in Section 6.3, leading to expected low errors with respect to the actual solution in a real application.

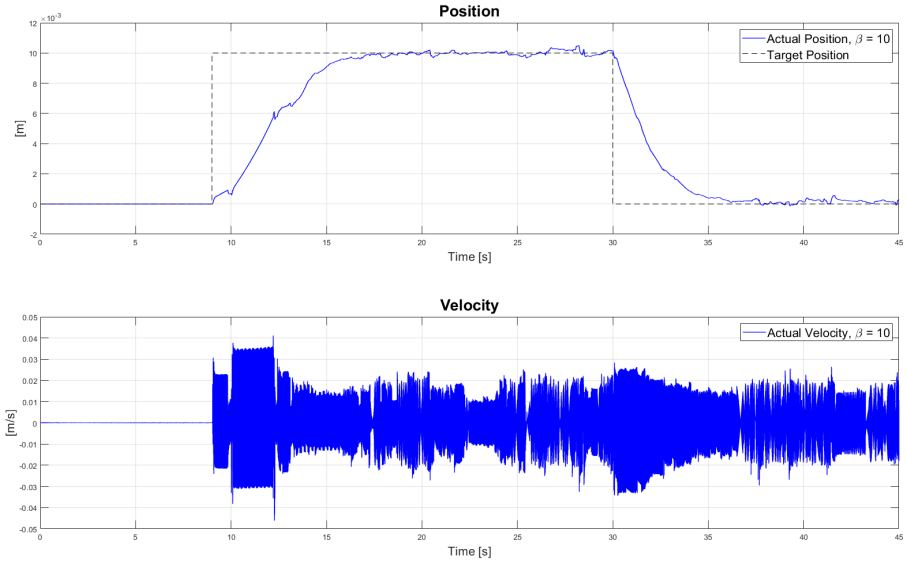

(a) Position and Velocity

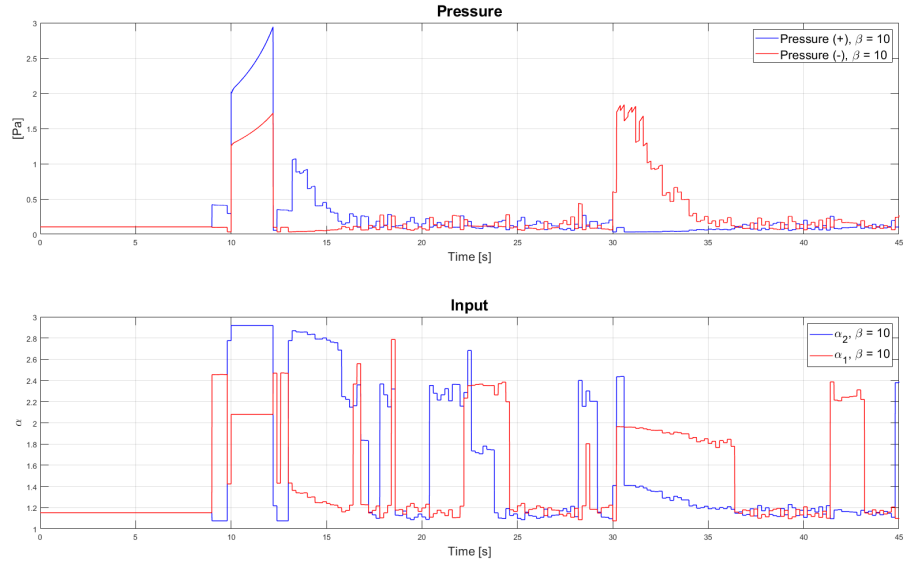

(b) Pressure and Control Frequency

Figure 7.8. Reference step Function

Sine Function

In this second case, the input signal given as a reference is a simple sinusoid with maximum values of 5 mm, chosen to verify how both control variables can be combined to achieve harmonic motion. The blue colored line and the black dashed one in figure 7.9 follow the same convention as the previous case.

This simulation is particularly interesting as it demonstrates how the controller, despite using

the same cost function, is still able to manage a different scenario. This is because, to follow the designated trajectory, the controller is not seeking maximum performance, as happens in figure 7.8, and therefore has more flexibility among the range of values for input α_i. In fact, in the second image, the control variables for the light body case do not immediately seek maximum pressure and remain within the first resonance frequency interval. The control variables exceed the first natural frequency in search of a greater net pressure, demonstrating the ability to adapt and seek the optimal solution in every circumstance.

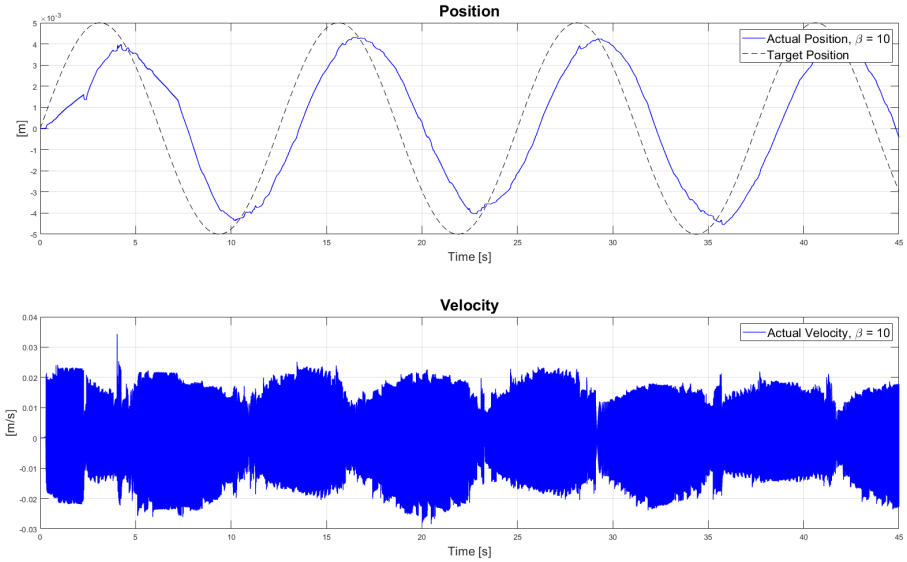

(a) Position and Velocity

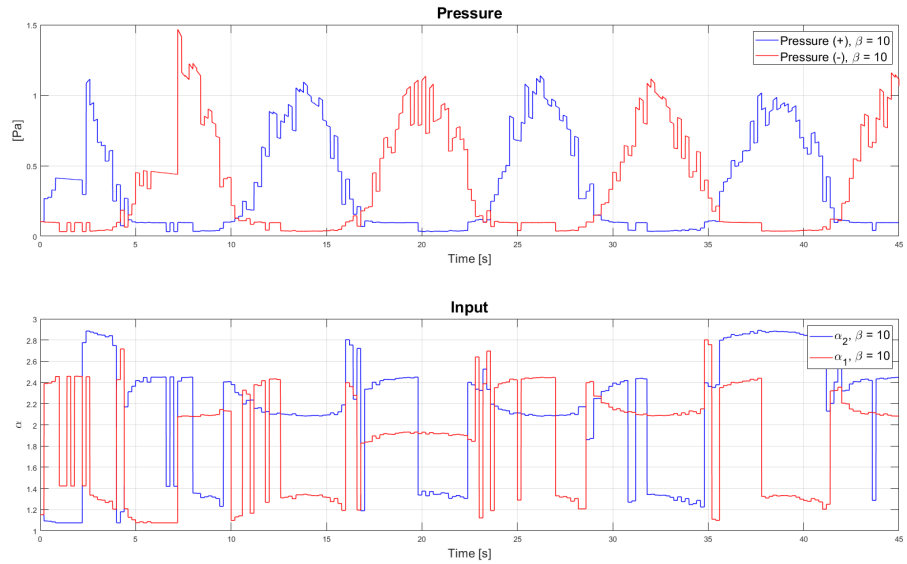

(b) Pressure and Control Frequency

Figure 7.9. Reference Sine Function

Ramp

In the last case under analysis, the input signal is a linear ramp. This is mathematically equivalent to imposing a constant velocity on the body and is a very useful reference to observe how the controller adjusts the frequency to compensate for the object's movement and maintain a constant zero phase.

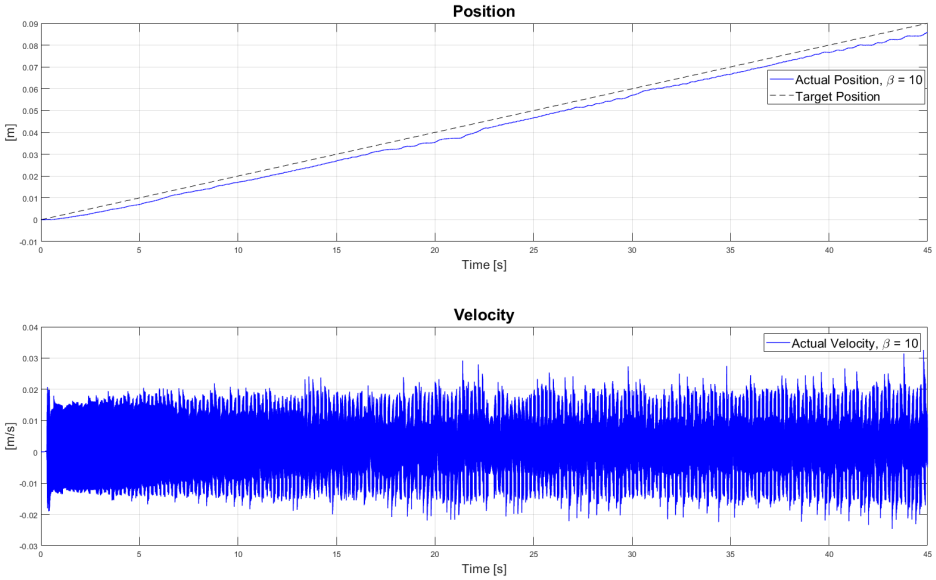

(a) Position and Velocity

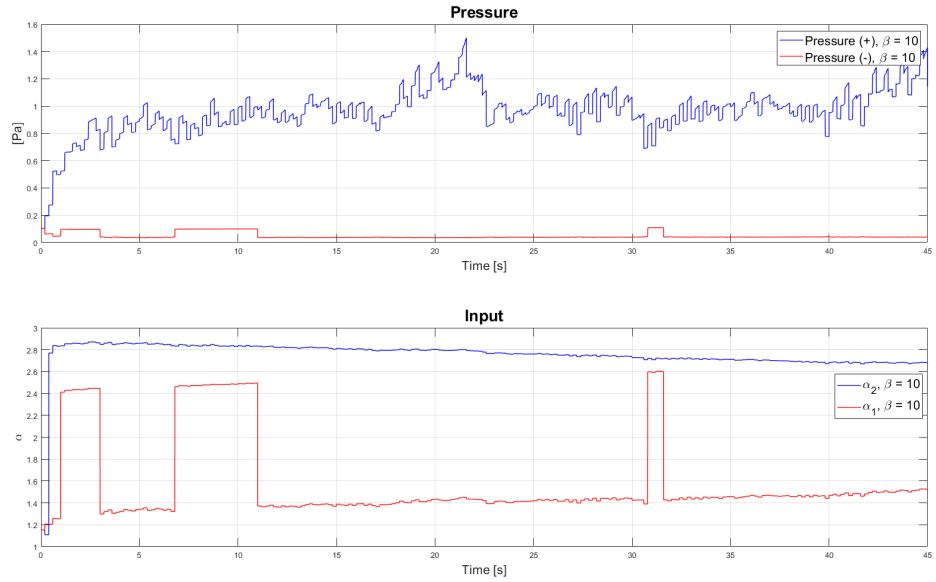

(b) Pressure and Control Frequency

Figure 7.10. Reference Linear Function

As in the sinusoidal reference case, the controller manages this scenarios very well. The theoretical aspect of modulating the frequency to follow the object's position is here quite evident even in case of small displacement. With this in mind, the following simulation (figure 7.11) was conducted in the case of a light body, where following the ramp signal is more challenging. As a result, it is possible to monitor a bigger frequency shift effect over time to ensure that the pressure on the body surface remains as constant as possible.

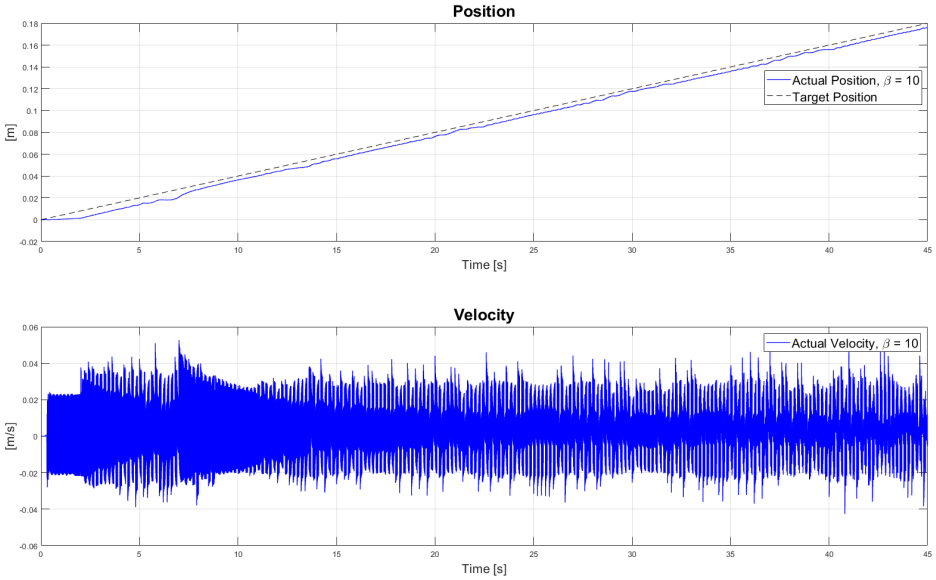

(a) Position and Velocity

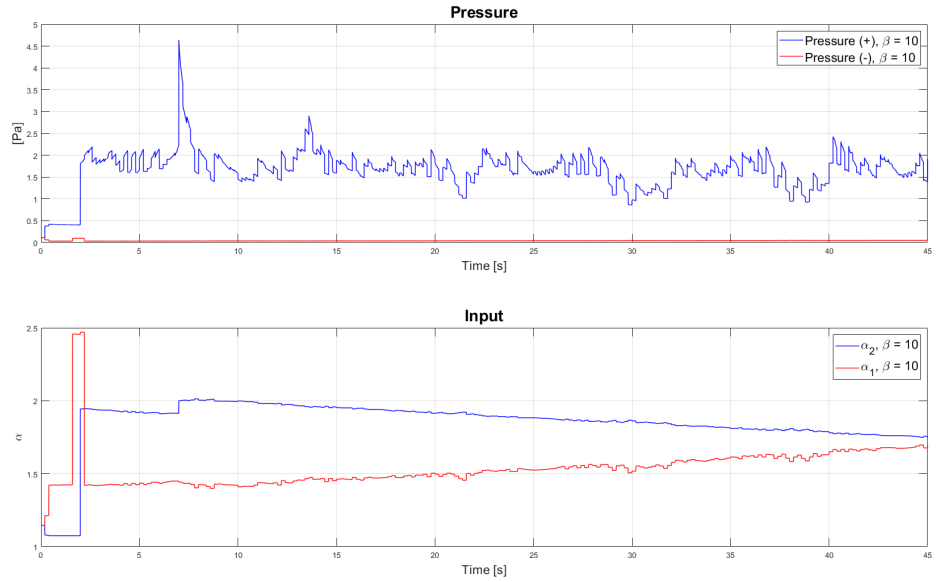

(b) Pressure and Control Frequency

Figure 7.11. Reference Linear Function 2

Figure 7.11 shows a ramp with approximately twice the slope, meaning a velocity twice as fast is imposed 7.10 for the same body. As shown in figure 7.11b, the control action starts with an approximate value of $\alpha = 2$ and ends with a value around $\alpha = 1.75$. Even in this case, the manipulated variable is adjusted linearly in time to follow the body. It demonstrates that to achieve continuous and constant velocity control over time, the frequency of the incident field must be continuously adjusted.

Chapter 8

Conclusions and further developments

The study of the nature of radiation pressure and the control of an object using acoustic beams has revealed significant aspects within the realm of nonlinear acoustics. Despite being a topic that has been extensively explored for over a century, the complexity of the phenomenon renders it both fascinating and challenging to manage. It is sufficient to consider how minor deviations in assumptions, resolutions, or the introduction of approximations can alter the final outcome, thereby maintaining an aura of mystery that keeps acoustic radiation pressure as one of the most uncertain scientific-engineering fields.

Nevertheless, numerous experiments have been conducted on acoustic levitation and the control of lightweight objects through acoustic waves, demonstrating the potential of this phenomena. However, a clear and definitive theory explaining these occurrences remains a subject of debate; contributions to a simple one-dimensional problem can serve as a foundation for three-dimensional extensions to more complex issues. Throughout this thesis, the fundamental aspects encompassing radiation pressure have been addressed, spanning from its origins to the most recent engineering applications, with an analysis of the phenomenon starting from its very initial definition.

Chapter 1 introduces the foundational concepts underlying the phenomenon of acoustic radiation pressures, emphasizing its importance in the interaction between sound waves and material bodies. The discussion begins with a historical perspective, tracing the initial studies, started by Lord Rayleigh, that revealed how sound waves could exert forces on objects. Key historical milestones and theoretical breakthroughs that have shaped the field are outlined, highlighting the contributions of pioneers in acoustics. The narrative then transitions to the nonlinear nature of acoustic phenomena, which surpasses the scope of traditional linear theories. This nonlinear behavior is central to understanding how acoustic radiation pressure generates a net force on immersed objects, enabling applications such as contactless manipulation and precise control of micro-objects described in detail in Chapter 2.

While Chapter 3 highlights the traditional differential approach to the field of nonlinear acoustic, leading to the well-known equations of Kuznetsov and Thompson's for inviscid fluid, Chapter 4 introduces a new perspective in the physics and mathematics of the problem. Unlike the historically accepted differential approach used by many, the variational method increases the level of accuracy and rigor necessary for addressing such problems, and it can be extensively applied to various situations and hypotheses (e.g. tridimensional motion, introduction of viscosity, parallelism with electromagnetic field, etc...). Indeed, there is potential to incorporate viscosity effects into the physical model by simply modifying the definition of Hamilton's Action, as well as introducing rotational motions by adjusting the kinetic energy and degrees of freedom within the system. The Hamiltonian principle well suited the aim of finding the force acting on a moving body immersed into an inviscid compressible fluid leading to a new general expression of the force expressed through the following integral over the moving body surface (4.21). Moreover, the latter can be specialized for any constitutive relationship $p(\rho)$ and it shows how the total energy density plays a crucial role in the radiation force expression. In the case of adiabatic reversible gas transformation, our results lead to (4.19). That is equivalent to Thompson's expression for the radiation pressure and showing the equivalence between the historical method and the proposed approach. A key result concerns the role of the total energy density, $\mathcal{E}$, which is represented by the Lagrangian density, $\mathcal{L}$, when applying an approximate second-order expansion of Bernoulli's (4.20). Then, a better clarification of the distinction between the scalar and tensorial forms, the formula based on the principle of momentum conservation was derived (4.28). In fact, in the limit of $S \to S_B$ the formula gives a trivial result since the momentum flux vanishes at the body surface; in addition, the the extra term $\rho\,(v \times v)$ is an unmotivated complication, just coming from the geek choice of considering another surface S, instead of S_B, to calculate the integral. Moreover, Chapter 4 highlights an important result concerning the nature of boundary conditions. Unlike the standard differential approach, which often overlooks boundary conditions, this study emphasizes their critical role. Here, the interaction between the acoustic field and the immersed body emerges directly from the variational principle. This approach provides a more rigorous mathematical framework, enabling the derivation of the nonlinear system of equations with greater precision and adherence to physical realities.

Chapter 5 delves into numerical methods for solving nonlinear systems related to the interaction between acoustic waves and bodies. It emphasizes the use of finite difference methods due to their versatility and simplicity, particularly for one-dimensional models. A new relationship for the derivatives of the potential was applied in simulations, with special care given to boundary conditions to maintain accuracy in the final results. Among the methods explored, the Rusanov method emerged as the most effective, striking the best balance between computational speed and accuracy. This approach highlighted differences among various radiation pressure models, setting the stage for subsequent chapters that aim to derive an approximated analytical relationship for radiation pressure to enable real-time control of moving objects. Indeed, the results obtained demonstrate the possibility of expressing a second-order quantity derived from

a system of partial differential equations as a semi-analytical equation applicable for control strategies. The achievement of an analytical equation, although approximated to the second order, may facilitate the use of much simpler real-time control strategies for manipulating objects at will. Moreover, regarding current numerical techniques and various simulation tools, the proposed equation represents a novelty compared to the one based on the Lagrangian.
Chapter 6 examines the perturbation method applied to two distinct scenarios: one with a fixed wall and the other with a moving wall. In the case of the fixed wall, a new formula has been developed to describe the acoustic potential and the radiation pressure in case of a rigid piston-tube problem, the same of Rayleigh at the beginning of XX century [6]. The equation leads to results that are significantly different compared to traditional models previously shown in Chapter 1 and extremely in accordance with the recent numerical simulations.
Concerning the moving wall problem, the study becomes more complex due to the dynamic interaction between the acoustic waves and the wall's motion. A first order impedance relationship has been derived to address the coupling between the wall's velocity and the acoustic field, leading to formulas that are not only innovative but, thanks to the good matching with numerical results, also open the door to practical applications in real-time control systems. The ability to model radiation pressure more accurately in dynamic conditions is a breakthrough, highlighting differences across various models and emphasizing the potential for finding an analytical expression. This lays the groundwork for controlling objects in motion with high precision, marking a significant step forward in both theoretical research and practical implementation.
Finally, Chapter 7 investigates the control component, as previously emphasized, and how it is linked to the demands and complexities of the physics of the problem. The presence of a forcing function directly associated with the nonlinearities of the medium renders the system significantly challenging to control using standard techniques. In this context, model predictive control (MPC), based on a simplified model and on the approximated radiation pressure expression, provides exceptional theoretical results that are also practically feasible to replicate. Concerning theoretical aspects, it is also demonstrated what is often hypothesized in such phenomena, namely a phase control by acting on the frequency variation in the control. Indeed, by manipulating the piston, the frequency of the waves on the controlled body is constantly changing to maximize the forcing component.
The next step, following this theoretical-numerical analysis, is undoubtedly the construction of a scaled model using loudspeakers within a closed structure (such as a Kundt's tube) to control the motion of objects inside it. Therefore, the experimental phase will be a fundamental aspect to validate the theory and numerical analysis presented in this study. The extension to multiple dimensions of the control volume will be the final step to complete the theoretical model initiated here, aiming to improve and provide a significant contribution to the analysis of acoustic radiation pressure, akin to the great works of the past.

List of Figures

Bibliography

[1] Robert Thomas Beyer. *Nonlinear acoustics*. US Government Printing Office, 1974.

[2] JH Poynting. Xxxix. radiation pressure. *The London, Edinburgh, and Dublin Philosophical Magazine and Journal of Science*, 9(52):393–406, 1905.

[3] FE Borgnis. Acoustic radiation pressure of plane compressional waves. *Reviews of Modern Physics*, 25(3):653, 1953.

[4] Peter Lebedew. The pressure of light on gases. *Astrophysical Journal, vol. 31, p. 385*, 31:385, 1910.

[5] Lord Rayleigh. Xxxiv. on the pressure of vibrations. *The London, Edinburgh, and Dublin Philosophical Magazine and Journal of Science*, 3(15):338–346, 1902.

[6] Lord Rayleigh. Xlii. on the momentum and pressure of gaseous vibrations, and on the connexion with the virial theorem. *The London, Edinburgh, and Dublin Philosophical Magazine and Journal of Science*, 10(57):364–374, 1905.

[7] Robert T Beyer. Radiation pressure—the history of a mislabeled tensor. *The Journal of the Acoustical Society of America*, 63(4):1025–1030, 1978.

[8] Louis Vessot King. On the acoustic radiation pressure on spheres. *Proceedings of the Royal Society of London. Series A-Mathematical and Physical Sciences*, 147(861):212–240, 1934.

[9] Qing Wang, Antoine Riaud, Jia Zhou, Zhixiong Gong, and Michael Baudoin. Acoustic radiation force on small spheres due to transient acoustic fields. *Physical Review Applied*, 15(4):044034, 2021.

[10] AA Doinikov. Acoustic radiation pressure on a rigid sphere in a viscous fluid. *Proceedings of the Royal Society of London. Series A: Mathematical and Physical Sciences*, 447(1931):447–466, 1994.

[11] Takahi Hasegawa and Katuya Yosioka. Acoustic-radiation force on a solid elastic sphere. *The Journal of the Acoustical Society of America*, 46(5B):1139–1143, 1969.

[12] Oleg A Sapozhnikov and Michael R Bailey. Radiation force of an arbitrary acoustic beam on an elastic sphere in a fluid. *The Journal of the Acoustical Society of America*, 133(2):661–676, 2013.

[13] Xucai Chen and Robert E Apfel. Radiation force on a spherical object in an axisymmetric wave field and its application to the calibration of high-frequency transducers. *The Journal of the Acoustical Society of America*, 99(2):713–724, 1996.

[14] Alexander A Doinikov. On the radiation pressure on small spheres. *The Journal of the Acoustical Society of America*, 100(2):1231–1233, 1996.

[15] Junru Wu, Gonghuan Du, Steven S Work, and David M Warshaw. Acoustic radiation pressure on a rigid cylinder: An analytical theory and experiments. *The Journal of the Acoustical Society of America*, 87(2):581–586, 1990.

[16] Wesley L Nyborg. Radiation pressure on a small rigid sphere. *The Journal of the Acoustical Society of America*, 42(5):947–952, 1967.

[17] Takahi Hasegawa, Tohru Kido, Chen Wei Min, Takeshi Iizuka, and Chihiro Matsuoka. Frequency dependence of the acoustic radiation pressure on a solid sphere in water. *Acoustical Science and Technology*, 22(4):273–282, 2001.

[18] Léon Brillouin. Sur les tensions de radiation. *Ann. phys.*, 4:528–586, 1925.

[19] K Beissner. Two concepts of acoustic radiation pressure. *The Journal of the Acoustical Society of America*, 79(5):1610–1612, 1986.

[20] Peter J Westervelt. The mean pressure and velocity in a plane acoustic wave in a gas. *The Journal of the Acoustical Society of America*, 22(3):319–327, 1950.

[21] Peter J Westervelt. The theory of steady forces caused by sound waves. *The Journal of the Acoustical Society of America*, 23(3):312–315, 1951.

[22] James A Rooney and Wesley L Nyborg. Acoustic radiation pressure in a traveling plane wave. *American Journal of Physics*, 40(12):1825–1830, 1972.

[23] Boa-Teh Chu and Robert E Apfel. Acoustic radiation pressure produced by a beam of sound. *The Journal of the Acoustical Society of America*, 72(6):1673–1687, 1982.

[24] CP Lee and TG Wang. Acoustic radiation pressure. *The Journal of the Acoustical Society of America*, 94(2):1099–1109, 1993.

[25] Takahi Hasegawa, Tohru Kido, Takeshi Iizuka, and Chihiro Matsuoka. A general theory of rayleigh and langevin radiation pressures. *Acoustical Science and Technology*, 21(3):145–152, 2000.

[26] Wesley L Nyborg and James A Rooney. Comments on "acoustic radiation pressure produced by a beam of sound"[j. acoust. soc. am. 7 2, 1673–1687 (1982)]. *The Journal of the Acoustical Society of America*, 75(1):263–264, 1984.

[27] Boa-Teh Chu and Robert E Apfel. Response to the comments of nyborg and rooney [j. acoust. soc. am. 7 5, 263–264 (1984)]. *The Journal of the Acoustical Society of America*, 75(3):1003–1004, 1984.

[28] Robert T Beyer. Radiation pressure in a sound wave. *American Journal of Physics*, 18(1):25–29, 1950.

[29] P.A. Thompson. *Compressible-fluid Dynamics*. Advanced engineering series. 1988.

[30] J.J Thompson J.H. Poynting. *A Textbook of Physics*. Charles Griffin Co, 1904.

[31] Karl Bücks and Hans Müller. Über einige beobachtungen an schwingenden piezoquarzen und ihrem schallfeld. *Zeitschrift für Physik*, 84:75–86, 1933.

[32] Erna MJ Herrey. Experimental studies on acoustic radiation pressure. *The Journal of the Acoustical Society of America*, 27(5):891–896, 1955.

[33] Isadore Rudnick. Measurements of the acoustic radiation pressure on a sphere in a standing wave field. *The Journal of The Acoustical Society of America*, 62(1):20–22, 1977.

[34] E Leung, N Jacobi, and T Wang. Acoustic radiation force on a rigid sphere in a resonance chamber. *The Journal of the Acoustical Society of America*, 70(6):1762–1767, 1981.

[35] Takahi Hasegawa and Katuya Yosioka. Acoustic radiation force on fused silica spheres, and intensity determination. *The Journal of the Acoustical Society of America*, 58(3):581–585, 1975.

[36] Takahi Hasegawa, Masayuki Ochi, and Kiichiro Matsuzawa. Acoustic radiation force on a solid elastic sphere in a spherical wave field. *The Journal of the Acoustical Society of America*, 69(4):937–942, 1981.

[37] LW Anson and RC Chivers. Frequency dependence of the acoustic radiation force function (y p) for spherical targets for a wide range of materials. *The Journal of the Acoustical Society of America*, 69(6):1618–1623, 1981.

[38] Marco AB Andrade, Nicolás Pérez, and Julio C Adamowski. Review of progress in acoustic levitation. *Brazilian Journal of Physics*, 48:190–213, 2018.

[39] Paul A Dayton, Karen E Morgan, Alexander L Klibanov, Gary Brandenburger, Kathryn R Nightingale, and Katherine W Ferrara. A preliminary evaluation of the effects of primary and secondary radiation forces on acoustic contrast agents. *IEEE transactions on ultrasonics, ferroelectrics, and frequency control*, 44(6):1264–1277, 1997.

[40] Mehmet Hakan Kandemir and Mehmet Çalışkan. Standing wave acoustic levitation on an annular plate. *Journal of Sound and Vibration*, 382:227–237, 2016.

[41] WJ Xie, CD Cao, YJ Lü, ZY Hong, and B Wei. Acoustic method for levitation of small living animals. *Applied Physics Letters*, 89(21), 2006.

[42] A. Kundt. Beobachtungen über schall und klangfiguren in luft. *Annalen der Physik*, 203:497–523, 1866.

[43] Marco AB Andrade, Nicolás Pérez, and Julio C Adamowski. Particle manipulation by a non-resonant acoustic levitator. *Applied physics letters*, 106(1), 2015.

[44] Masaya Takasaki, Daisuke Terada, Yasuhiro Kato, Yuji Ishino, and Takeshi Mizuno. Non-contact ultrasonic support of minute objects. *Physics Procedia*, 3(1):1059–1065, 2010.

[45] Su Zhao and Jörg Wallaschek. A standing wave acoustic levitation system for large planar objects. *Archive of Applied Mechanics*, 81:123–139, 2011.

[46] Marco AB Andrade, Anne L Bernassau, and Julio C Adamowski. Acoustic levitation of a large solid sphere. *Applied Physics Letters*, 109(4), 2016.

[47] Yoichi Ochiai, Takayuki Hoshi, and Jun Rekimoto. Three-dimensional mid-air acoustic manipulation by ultrasonic phased arrays. *PLOS ONE*, 9:1–5, 05 2014.

[48] M.M. Saffren D.D. Elleman J.C. Fletcher, T.G. Wang.

[49] Yoshiki Hashimoto, Yoshikazu Koike, and Sadayuki Ueha. Transporting objects without contact using flexural traveling waves. *Journal of the Acoustical Society of America*, 103(6):3230–3233, 1998.

[50] Marco AB Andrade, Asier Marzo, and Julio C Adamowski. Acoustic levitation in mid-air: Recent advances, challenges, and future perspectives. *Applied Physics Letters*, 116(25), 2020.

[51] Diego Baresch, Jean-Louis Thomas, and Régis Marchiano. Observation of a single-beam gradient force acoustical trap for elastic particles: acoustical tweezers. *Physical review letters*, 116(2):024301, 2016.

[52] Asier Marzo, Abanoub Ghobrial, L Cox, Mihai Caleap, Anthony Croxford, and BW Drinkwater. Realization of compact tractor beams using acoustic delay-lines. *Applied Physics Letters*, 110(1), 2017.

[53] Diego Baresch, Jean-Louis Thomas, and Régis Marchiano. Spherical vortex beams of high radial degree for enhanced single-beam tweezers. *Journal of Applied Physics*, 113(18), 2013.

[54] Asier Marzo, Sue Ann Seah, Bruce W Drinkwater, Deepak Ranjan Sahoo, Benjamin Long, and Sriram Subramanian. Holographic acoustic elements for manipulation of levitated objects. *Nature communications*, 6(1):8661, 2015.

[55] *Riemann Solvers and Numerical Methods for Fluid Dynamics: A Practical Introduction*. Berlin, Heidelberg: Springer Berlin Heidelberg: Imprint: Springer, 1999.

[56] Mads Peter Sørensen and Peter Leth Christiansen. Driven oscillating nonlinear acoustic waves. *Meccanica*, 58(6):1151–1161, 2023.

[57] Barbara Kaltenbacher and Vanja Nikolic. Parabolic approximation of quasilinear wave equations with applications in nonlinear acoustics. *SIAM Journal on Mathematical Analysis*, 54(2):1593–1622, 2022.

[58] Barbara Kaltenbacher. Mathematics of nonlinear acoustics. *Evolution Equations and Control Theory*, 4(4):447–491, 2015.

[59] George Keith Batchelor. *An introduction to fluid dynamics*. Cambridge university press, 2000.

[60] C Truesdell. Bernoulli's theorem for viscous compressible fluids. *Physical Review*, 77(4):535, 1950.

[61] Mikkel Settnes and Henrik Bruus. Forces acting on a small particle in an acoustical field in a viscous fluid. *Physical Review E—Statistical, Nonlinear, and Soft Matter Physics*, 85(1):016327, 2012.

[62] Jean-Louis Thomas, Régis Marchiano, and Diego Baresch. Acoustical and optical radiation pressure and the development of single beam acoustical tweezers. *Journal of Quantitative Spectroscopy and Radiative Transfer*, 195:55–65, 2017.

[63] Jonas T Karlsen and Henrik Bruus. Forces acting on a small particle in an acoustical field in a thermoviscous fluid. *Physical Review E*, 92(4):043010, 2015.

[64] Jan S Hesthaven. *Numerical methods for conservation laws: From analysis to algorithms*. SIAM, 2017.

[65] Randall J LeVeque and Randall J Leveque. *Numerical methods for conservation laws*, volume 214. Springer, 1992.

[66] Ivan Christov, CI Christov, and PM Jordan. Modeling weakly nonlinear acoustic wave propagation. *Quarterly Journal of Mechanics and Applied Mathematics*, 60(4):473–495, 2007.

[67] Ivan Christov, CI Christov, and PM Jordan. Cumulative nonlinear effects in acoustic wave propagation. *COMPUTER MODELING IN ENGINEERING AND SCIENCES*, 17(1):47, 2007.

[68] Ivan Christov, PM Jordan, and CI Christov. Nonlinear acoustic propagation in homentropic perfect gases: A numerical study. *Physics Letters A*, 353(4):273–280, 2006.

[69] Richard Courant, Kurt Friedrichs, and Hans Lewy. Über die partiellen differenzengleichungen der mathematischen physik. *Mathematische annalen*, 100(1):32–74, 1928.

[70] Jianwu Dang, Qingzhi Hou, and Futang Wang. A study of sound propagation in ducts with a moving wall. 2018.

[71] Sergio Pirozzoli. Numerical methods for high-speed flows. *Annual review of fluid mechanics*, 43(1):163–194, 2011.

[72] Gilbert Strang. Accurate partial difference methods: Ii. non-linear problems. *Numerische Mathematik*, 6(1):37–46, 1964.

[73] Randall J LeVeque. *Finite volume methods for hyperbolic problems*, volume 31. Cambridge university press, 2002.

[74] Justin Hudson, PK Sweby, and MJ Baines. *Numerical techniques for conservation laws with source terms*. PhD thesis, Citeseer, 1998.

[75] Peter D Lax. Weak solutions of nonlinear hyperbolic equations and their numerical computation. In *Selected Papers Volume I*, pages 198–232. Springer, 2005.

[76] Kurt O Friedrichs. Symmetric hyperbolic linear differential equations. *Communications on pure and applied Mathematics*, 7(2):345–392, 1954.

[77] T. J. Poinsot and S.K. Lelef. Boundary conditions for direct simulations of compressible viscous flows. *Journal of computational physics*, 101(1):104–129, 1992.

[78] A Alexeev and C Gutfinger. Resonance gas oscillations in closed tubes: Numerical study and experiments. *Physics of Fluids*, 15(11):3397–3408, 2003.

[79] Marianne Cuif Sjöstrand, Yves D'Angelo, and Eric Albin. No-slip wall acoustic boundary condition treatment in the incompressible limit. *Computers & Fluids*, 86:92–102, 2013.

[80] Jianwu Dang, Qingzhi Hou, and Futang Wang. A study of sound propagation in ducts with a moving wall. In *Euronoise*, 2018.

[81] Alina Chertock, Armando Coco, Alexander Kurganov, and Giovanni Russo. A second-order finite-difference method for compressible fluids in domains with moving boundaries. *Commun Comput Phys*, 23(1), 2018.

[82] George Adomian. *Nonlinear stochastic operator equations*. Academic press, 2014.

[83] Ji-Huan He. Homotopy perturbation technique. *Computer methods in applied mechanics and engineering*, 178(3-4):257–262, 1999.

[84] Syed Tauseef Mohyud-Din and Muhammad Aslam Noor. Homotopy perturbation method for solving partial differential equations. *Zeitschrift für Naturforschung A*, 64(3-4):157–170, 2009.

[85] Mukesh Kumar and Umesh. Recent development of adomian decomposition method for ordinary and partial differential equations. *International Journal of Applied and Computational Mathematics*, 8(2):81, 2022.

[86] Esmail Babolian, A Azizi, and Jamshid Saeidian. Some notes on using the homotopy perturbation method for solving time-dependent differential equations. *Mathematical and computer modelling*, 50(1-2):213–224, 2009.

[87] Jafar Biazar and H Ghazvini. Homotopy perturbation method for solving hyperbolic partial differential equations. *Computers & Mathematics with Applications*, 56(2):453–458, 2008.

[88] Nawal A Al-Zaid, Huda O Bakodah, and Abdelhalim Ebaid. Solving a class of partial differential equations with different types of boundary conditions by using a generalized inverse operator: Decomposition method. *Nonlinear Anal. Differ. Equ*, 6(1):25–41, 2018.

[89] Ali H Nayfeh. *Perturbation methods*. John Wiley & Sons, 2008.

[90] Ali H Nayfeh. A comparison of perturbation methods for nonlinear hyperbolic waves. In *Singular perturbations and asymptotics*, pages 223–276. Elsevier, 1980.

[91] Abdul-Majid Wazwaz. *Partial differential equations and solitary waves theory*. Springer Science & Business Media, 2010.

[92] Andrei D Polyanin. *Handbook of linear partial differential equations for engineers and scientists*. Chapman and hall/crc, 2001.

[93] Dean G Duffy. *Green's functions with applications*. Chapman and Hall/CRC, 2015.

[94] Norman Christopher Corbett. Initial moving-boundary value problems associated with the wave equation. 1991.

[95] Christian Dopper. Ueber das farbige licht der doppelsterne und einiger anderer gestirre des himmels. *Abhandlungen der k. Böhm*, 2:465–482, 1842.

[96] Albert Einstein et al. Zur elektrodynamik bewegter körper. *Annalen der physik*, 17(10):891–921, 1905.

[97] Nandor L Balazs. On the solution of the wave equation with moving boundaries. *Journal of Mathematical Analysis and Applications*, 3(3):472–484, 1961.

[98] Lakhdar Gaffour. Analytical method for solving the one-dimensional wave equation with moving boundary. *Progress In Electromagnetics Research*, 20:63–73, 1998.

[99] Dan Censor. The generalized doppler effect and applications. *Journal of the Franklin Institute*, 295(2):103–116, 1973.

[100] Dan Censor. Acoustical doppler effect analysis—is it a valid method? *The Journal of the Acoustical Society of America*, 83(4):1223–1230, 1988.

[101] Jeffery Cooper. Scattering of electromagnetic fields by a moving boundary: the one-dimensional case. *IEEE Transactions on Antennas and Propagation*, 28(6):791–795, 1980.

[102] Henrik Bruus. Acoustofluidics 7: The acoustic radiation force on small particles. *Lab on a Chip*, 12(6):1014–1021, 2012.

[103] Sestieri Aldo. Dispense del corso di controllo delle vibrazioni e del rumore. 2010.

[104] Pirooz Mohazzabi and Ben Greenebaum. Counterintuitive behaviour of a particle under the action of an oscillating force. *Physics Education*, 46(2):215, 2011.

[105] Alberto Isidori. *Nonlinear control systems: an introduction*. Springer, 1985.

[106] Hassan K. Khalil. *Nonlinear Control*. Pearson, 2015.

[107] Carlos E Garcia, David M Prett, and Manfred Morari. Model predictive control: Theory and practice—a survey. *Automatica*, 25(3):335–348, 1989.

[108] M. Morari A. Bemporad, N.L. Ricker. *Model Predictive Control Toolbox*. Mathworks, 2023.